Uniwersytet im. Adama Mickiewicza w Poznaniu
Adam Mickiewicz University in Poznań
Wydział Nauk Geograficznych i Geologicznych
Faculty of Geographic and Geological Sciences

Małgorzata Bronikowska

Numerical modeling of Pleistocene soft-sediment deformation structures in glacigenic sediments

Modelowanie numeryczne plejstoceńskich struktur deformacyjnych w osadach glacigenicznych

Praca doktorska pod kierunkiem
prof. dr hab. Małgorzaty Pisarskiej-Jamroży (promotorka)

PhD dissertation supervised by
Prof. PhD habil. Małgorzata Pisarska-Jamroży (Principal Advisor)

Poznań, 2022

Spis treści / Table of contents

Załączniki / Attachments:

Artykuł nr 1 (Paper no. 1): Bronikowska, M., Pisarska-Jamroży, M., Van Loon, A.J., 2021. First attempt to model numerically seismically-induced soft-sediment deformation structures – a comparison with field examples. *Geological Quarterly* 65, 60.

Artykuł nr 2 (Paper no. 2): Bronikowska, M., Pisarska-Jamroży, M., Van Loon, A.J., 2021. Dropstones deposition – results of numerical modelling of deformation structures, and implications for the reconstruction of the water depth in shallow lacustrine and marine successions. *Journal of Sedimentary Research* 91, 507-519.

Artykuł nr 3 (Paper no. 3): Pisarska-Jamroży, M., Van Loon, A.J., Bronikowska, M., 2018. Dumpstones and dropstones as records of overturning ice rafts in a Weichselian proglacial lake (Rügen Island, NE Germany). *Geological Quarterly* 62, 917-924.

Podziękowania

Jestem niezmiernie wdzięczna wszystkim osobom, które w mojej drodze naukowej stanowiły dla mnie autorytet oraz wsparcie, przekazując mi bezcenną wiedzę oraz pozwalając na poszukiwania własnej drogi. Szczególnie dziękuję mojej Promotorce Małgorzacie Pisarskiej-Jamroży, będącej dla mnie Mentorką, Przewodniczką po świecie geologii oraz niesamowitym wsparciem podczas poruszania się po krętych drogach nauki. Dziękuję także pozostałym członkom zespołu badawczego grantu GREBAL, w ramach którego powstała niniejsza dysertacja, za owocne dyskusje oraz dane obserwacyjne niezbędne do walidacji tworzonych przeze mnie modeli numerycznych. Pragnę również wyrazić ogromną wdzięczność Tomowi Van Loonowi, który zawsze służył mi dobrą radą i pomocą oraz, wraz z moją Promotorką, pokazał mi, w jaki sposób mówić prostym językiem o skomplikowanych zagadnieniach matematycznych i fizycznych. Na koniec, chciałabym podziękować moim przyjaciołom, rodzinie, koleżankom i kolegom z Instytutu Geologii UAM oraz wszystkim osobom, które towarzyszyły mi podczas trudów pracy naukowej nieustannie mnie wspierając.

Badania, przeprowadzone w ramach niniejszej dysertacji, finansowane były z dwóch grantów badawczych Narodowego Centrum Nauki: grantu OPUS „GREBAL" (kierownik: prof. Małgorzata Pisarska-Jamroży) nr 2015/19/B/ST10/00661 oraz grantu PRELUDIUM 18 (kierownik: mgr Małgorzata Bronikowska) nr 2019/33/N/ST10/00095.

Acknowledgements

I am extremely grateful to all the people who have guided and supported me along my scientific path, providing me with such invaluable knowledge and yet allowing me to find my own way. I am especially grateful to my Supervisor, Małgorzata Pisarska-Jamroży, who has been my mentor and guide to the world of Geology, and who has provided such wonderful support while navigating the winding paths of Science. I would also like to thank the other members of the GREBAL grant research team, in whose framework this dissertation was prepared, for fruitful discussions and the observational data needed to validate the numerical models I created. I would also like to express my deep gratitude to Tom Van Loon, for always providing good help and advice and, together with my Supervisor, showed me how to describe complex mathematical and physical problems in simple language. Finally, I would like to thank my friends, family and colleagues from the Institute of Geology of Adam Mickiewicz University, and all those who accompanied me during the hardships of my scientific work, and have provided such enduring support.

The research carried out as part of this dissertation was financed by two research grants from the National Science Centre: the OPUS "GREBAL" grant (head: Prof. Małgorzata Pisarska-Jamroży) No. 2015/19 / B / ST10 / 00661 and the PRELUDIUM 18 grant (head: Małgorzata Bronikowska, MA) No 2019/33 / N / ST10 / 00095.

Lista publikacji wchodzących w skład rozprawy / List of publications

Przedstawiona rozprawa doktorska składa się ze spójnego tematycznie zbioru **trzech recenzowanych artykułów naukowych** poprzedzonych wspólnym streszczeniem. Artykuły zostały opublikowane w czasopismach posiadających współczynnik wpływu (*Impact Factor, IF*). **Sumaryczny *IF* zbioru publikacji wynosi 6,024**. Łączna liczba cytowań publikacji w bazie *Web of Science* (WoS) wynosi 5 (stan: luty 2022 r.). **Indeks Hirscha** doktorantki wynosi **4 (WoS), sumaryczna ilość publikacji,** w których jest współautorem **- 13 (WoS) a sumaryczna ilość cytowań** (bez autocytowań) **- 45.**

This thesis consists of a set of **three peer-reviewed research papers** with an introductory summary section. The research papers were published in scientific journals with impact factor (IF). **The total IF of the collection of research papers is 6.024**. The current total number of citations in Web of Science (WoS) is 5. **Hirsch index** of PhD student is **4 (WoS), sum of research papers in WoS is 13**, and **sum of citation** (without self-citation) in WoS is **45.**

W skład rozprawy wchodzą następujące artykuły / The thesis consists of the following papers:

1. **Bronikowska, M.**, Pisarska-Jamroży, M., Van Loon, A.J., 2021a. First attempt to model numerically seismically-induced soft-sediment deformation structures – a comparison with field examples. *Geological Quarterly* 65, 60 (**IF= 1,35; 100 pkt.** wg wykazu czasopism naukowych MEN / 100 points on the list of scientific journals by Polish Ministry of Education and Science; 0 cytowań w WoS / 0 citations in WoS),

2. **Bronikowska, M.**, Pisarska-Jamroży, M., Van Loon, A.J., 2021b. Dropstones deposition – results of numerical modelling of deformation structures, and implications for the reconstruction of the water depth in shallow lacustrine and marine successions. *Journal of Sedimentary Research* 91, 507-519 (**IF= 3,324; 100 pkt.** wg wykazu czasopism naukowych MEN / 100 points on the list of scientific journals by Polish Ministry of Education and Science; 2 cytowania w WoS / 2 citations in WoS),

3. Pisarska-Jamroży, M., Van Loon, A.J., **Bronikowska, M.**, 2018. Dumpstones and dropstones as records of overturning ice rafts in a Weichselian proglacial lake (Rügen Island, NE Germany). *Geological Quarterly* 62, 917-924 (**IF= 1,35; 100 pkt.** wg wykazu czasopism naukowych MEN / 100 points on the list of scientific journals by Polish Ministry of Education and Science; 3 cytowania w WoS / 3 citations in WoS),

Streszczenie rozprawy doktorskiej mgr Małgorzaty Bronikowskiej

Modelowanie numeryczne plejstoceńskich struktur deformacyjnych
w osadach glacigenicznych

Numerical modeling of Pleistocene soft-sediment deformation structures in glacigenic sediments

1. WPROWADZENIE

Struktury deformacyjne w nieskonsolidowanych osadach (ang. *soft-sediment deformation structures*; SSDS) są przedmiotem badań geologów i geomorfologów od dawna i cały czas przyciągają ich uwagę (Dżułyński i Radomski, 1966; Anketell i in., 1970; Liszkowski, 1975; Dżułyński, 1996; Shanmugan, 2016). Mimo tego, wciąż nie istnieje spójna definicja obejmująca ponad sto pięćdziesiąt opisanych rodzajów SSDS, do których zalicza się każde zaburzenie pierwotnego kształtu, układu lub budowy wewnętrznej ławic w osadzie przed jego ostateczną lityfikacją (Gradziński i in., 1986). SSDS mogą powstać podczas zdarzeń o charakterze katastrofalnym (**wysokoenergetycznym**), jak osuwiska morskie (Odonne i in., 2011), tsunami (Matsumoto i in., 2008) czy trzęsienia ziemi (Moretti, 2000; Pisarska-Jamroży i in., 2019), a także w wyniku działania procesów **niskoenergetycznych**, jak opadanie kropli deszczu (Fichman i in., 2015) czy opadanie swobodne ziaren na dna zbiorników wodnych (Haarland i in., 1966; Menzies 2002; Pisarska-Jamroży i in., 2018). Niezależnie jednak od mechanizmu inicjującego procesy prowadzące do powstania SSDS, sam proces ich generowania oraz zależność pomiędzy cechami strukturalnymi SSDS a litologią osadów, w których występują, czy działających sił, wciąż pozostaje słabo rozpoznany.

Wysokoenergetyczne mechanizmy inicjujące powstanie SSDS. SSDS, których genezę można przypisać wysokoenergetycznym mechanizmom inicjującym, powstają w warunkach wysokiego ciśnienia i związane są z procesami uwodnienia oraz upłynnienia osadów (Allen, 1982), jak na przykład powstające na skutek trzęsienia ziemi – sejsmity (Rosetti i in., 1999; Owen i Moretti, 2011; Van Loon i in., 2020). Sejsmity są wewnętrznie zdeformowanymi ławicami, w których SSDS powstały w efekcie propagacji fali/fal sejsmicznych (Seilacher, 1969). Proces uwodnienia (ang. *fluidization*), nie wymagający udziału znacznej energii, związany jest z wypełnieniem wodą pustych porów w osadzie (Campbell, 2003). Uwodniony osad zyskuje plastyczność oraz znaczną lepkość, przez co może poruszać się pod wpływem

grawitacji, jak na przykład podczas spływów masowych (Allen, 1982). Proces upłynnienia (ang. *liquefaction*) osadów wymaga dostarczenia do układu znacznie większej energii, i jest obserwowany podczas tak katastrofalnych procesów, jak trzęsienia ziemi czy upadki meteorytów. Do upłynnienia dochodzi najczęściej w osadach wysyconych wodą (Campbell, 2003) i pozbawionych kohezyjności (Seed i Idriss, 1971), gdy wytrzymałość osadów zostanie znacznie zredukowana przez działanie ciśnienia wywołanego na przykład przejściem fal sejsmicznych. W efekcie działania tego ciśnienia, ziarna tracą kontakt między sobą, co pozwala im przemieszczać się w sposób płynny (Vaid i Thomas, 1995; Youd i Idriss, 2001).

Zarówno upłynnienie, jak i uwodnienie osadów mogą powodować poważne zniszczenia na obszarach zamieszkałych, w tym przede wszystkim odpowiadać za zniszczenia budynków mieszkalnych i innej infrastruktury. Z tego też powodu, badania tych procesów skupiały się głównie na znalezieniu kluczowych parametrów materiałowych osadów, przy których można spodziewać się uwodnienia i upłynnienia oraz na tworzeniu funkcji pozwalających przewidzieć ich wystąpienie (Andrus i Stoke, 1997; Rahman i Lo, 2014; Rahman i in., 2020). Istniejące modele skupiają się więc bardziej na przewidywaniu katastrof (i potencjału uwodnienia/upłynnienia osadów) niż na samym procesie, czy jego udziale w powstawaniu struktur deformacyjnych. Prawdopodobnie dlatego, nasza wiedza o wewnątrzławicowych strukturach deformacyjnych, powstających w efekcie trzęsień ziemi (=sejsmity), jest wciąż niewielka. Obserwacje wskazują, że sejsmity mogą powstawać podczas trzęsień ziemi o M>5 (Ambraseys, 1988) oraz, w znacznej większości, tworzą się do czterdziestu kilometrów od epicentrum (Galli, 2000). Na ogół sejsmity występują w dobrze wysortowanych, drobnoziarnistych osadach piaszczystych z niewielką zawartością mniejszych frakcji, na przykład w osadach jeziornych, morskich czy fluwialnych (Hoffmann i Reicherter, 2012; Van Loon i Pisarska-Jamroży, 2014; Pisarska-Jamroży, i in., 2018). Powszechnie przyjęte kryteria rozpoznania sejsmitów nie są ścisłe i obejmują: 1) poziomą rozciągłość zdeformowanych wewnętrznie ławic, 2) powtarzalność pionową występowania zdeformowanych ławic, 3) podobieństwo geometrii struktur deformacyjnych występujących w ławicach zdeformowanych wewnętrznie do tych obserwowanych podczas współczesnych trzęsień ziemi, 4) zmianę złożoności i częstości występowania SSDS wraz z odległością od epicentrum, 5) prawdopodobieństwo wystąpienia trzęsienia ziemi (np. bliskość aktywnego obecnie lub w przeszłości uskoku).

Wiele pytań, dotyczących powstawania struktur deformacyjnych indukowanych sejsmicznie wciąż jednak pozostaje bez odpowiedzi. Nieznany jest wpływ właściwości materiałowych

osadu na geometrię indukowanych sejsmicznie SSDS, czy udział parametrów fizycznych trzęsienia ziemi na rozkład przestrzenny SSDS w osadzie. Wypełnienie tej istotnej luki może przyczynić się do dokładniejszego rozpoznawania sejsmitów w stanie kopalnym, lepszego poznania ich parametrów i zasięgu oraz może pozwolić na wskazanie tych cech SSDS, które pomogą pomóc w ich identyfikacji.

Niskoenergetyczne mechanizmy inicjujące powstanie SSDS. SSDS, tworzące się pod wpływem dopływu niewielkiej energii, związane są na ogół z procesami opadania czy dryfowania, jak na przykład te, powstające podczas depozycji dropstonów (=klasty z napławiania; ang. *dropstones*). Są to pojedyncze ziarna o dowolnych średnicach, wyraźnie większych niż średnice ziaren otaczających je osadów (Haarland i in., 1996; Menzies, 2002). Obserwowane są na ogół w dobrze wysortowanych osadach jeziornych i morskich, zaś ich genezę wiąże się głównie (choć nie tylko; por. Pisarska-Jamroży i in., 2019) z wytapianiem ziaren z dryfujących kier czy gór lodowych (Hoffmann i Schrag, 2000). Nagromadzenie dropstonów zwane jest w literaturze jako IRD (ang. *ice-rafted debris, ice-rafted deposits*) czy dumpstony (ang. *dumpstones*). Występowanie dropstonów zostało opisane w licznych publikacjach (Thomas i Connell, 1985; Gilbert, 1990; Brodzikowski i Van Loon, 1991; Le Heron, 2015; Pisarska-Jamroży i in., 2018) a ich potencjał w rekonstrukcji jeziornych i morskich paleośrodowisk depozycyjnych jest istotny (Dowdeswell i in., 2000; Livingstone, 2015; Van Loon i in., 2019).

Mimo dobrego rozpoznania dropstonów oraz towarzyszących im struktur deformacyjnych, także w tym przypadku, wiele pytań wciąż pozostaje bez odpowiedzi. Czy istnieje to jaki związek, pomiędzy śladem pozostawionym w osadzie dna przez opadające dropstony, a głębokością jeziora/morza? Czy możliwa jest rekonstrukcja procesu depozycji dropstonów na podstawie obserwacji ich położenia przestrzennego i powstałych wokół niego struktur deformacyjnych oraz jakie są możliwości i ograniczenia takich rekonstrukcji?

Niniejsza rozprawa doktorska stanowi próbę stworzenia i zastosowania modeli numerycznych opisujących procesy powstawania dwóch rodzajów struktur deformacyjnych w plejstoceńskich osadach glacigenicznych oraz ich weryfikacji z obserwacjami terenowymi. Wybrane rodzaje struktur deformacyjnych to 1) SSDS występujące w sejsmitach, powstające na skutek propagacji fal sejsmicznych w osadach nieskonsolidowanych (**artykuł nr 1**: Bronikowska i in., 2021a) oraz 2) SSDS tworzące się w dnach zbiorników wodnych podczas depozycji dropstonów **(artykuł nr 3**: Pisarska-Jamroży i in., 2018; **artykuł nr 2**: Bronikowska i in., 2021b). Wybór ten podyktowany jest kilkoma

powodami. Po pierwsze, wybrane rodzaje SSDS zdają się mieć duże znaczenie w rekonstrukcji paleozdarzeń, a jednocześnie każdy z nich posiada znaczną reprezentację w literaturze i obserwacjach terenowych, co z kolei daje możliwość dobrej weryfikacji zastosowanych modeli numerycznych. Po drugie, stworzenie dwóch modeli obejmujących procesy zachodzące przy udziale wysokiej i niskiej energii, pozwala na zamknięcie klamrą warunków brzegowych dla powstawania struktur deformacyjnych.

Rozprawa doktorska składa się z zestawu trzech recenzowanych artykułów naukowych opublikowanych w czasopismach znajdujących się na liście *JCR*. **Pierwszy artykuł** opisuje zastosowanie modelu numerycznego w odtwarzaniu SSDS indukowanych sejsmicznie (występujących w sejsmitach) oraz weryfikuje wyniki modelu z obserwacjami terenowymi (Bronikowska i in., 2021a). **Drugi artykuł** przedstawia model numeryczny odnoszący się do depozycji dropstonów (Bronikowska i in., 2021b), dla którego preludium stanowiło opisanie depozycji dropstonów i dumpstonów w osadach plejstoceńskiego jeziora przylodowcowego na wyspie Rugia w NE Niemczech (**trzeci artykuł:** Pisarska-Jamroży i in., 2018).

Oba zaprezentowane modele (Bronikowska i in., 2021a, b) stanowią pierwsze na świecie opisy numeryczne tych dwóch procesów, mając jednocześnie potencjał do dalszego rozwoju, uszczegóławiania oraz dalszej weryfikacji. Autorka niniejszej rozprawy stworzyła, opisała, zweryfikowała, a także nadała potencjał predykcyjny dwóm nowym modelom numerycznym odnoszącym się do struktur deformacyjnych w plejstoceńskich osadach glacigenicznych. Jej wkład w powstanie **artykułów nr 1** oraz **2** jest wiodący i stanowi 85%. Zakres prac obejmował przeprowadzenie symulacji numerycznych, napisanie jednego z użytych programów (w języku C), opisanie uzyskanych wyników, odniesienie ich do obserwacji terenowych, wskazanie możliwych zastosowań, wskazanie błędów modeli oraz napisanie znacznej części tekstu artykułów. Współautorzy artykułów dostarczyli cennych danych terenowych, dzięki którym możliwa była weryfikacja modeli, napisali części artykułów odnoszące się do obserwacji terenowych a także znacząco pomogli w tworzeniu grafik oraz redagowaniu wszystkich części tekstu. W związku z tym, że specjalnością autorki niniejszej rozprawy jest modelowanie numeryczne, jej wkład w **artykuł nr 3** nie jest wiodący (20%) i polegał na udziale w badaniach terenowych i opracowywaniu wyników, a także na pisaniu i redagowaniu tekstu. Oświadczenia współautorów artykułów nr 1-3, włączonych w niniejszą dysertacje, znajdują się na końcu niniejszego streszczenia.

Hipotezy badawcze rozprawy doktorskiej

A. Model numeryczny powstawania indukowanych sejsmicznie SSDS, bazujący na dyskretnych odcinkach fali sejsmicznej oraz wywoływanych przez nią ciśnieniach pionowych, **jest w stanie odtworzyć artefaktyczne SSDS występujące w sejsmitach** (znane z obserwacji terenowych).

B. Powstawanie sejsmitów jest związane głównie z pionową składową prędkości fali sejsmicznej S, przez co wielkość, geometria oraz rozmieszczenie przestrzenne obserwowanych/ modelowanych SSDS zależeć będzie od prędkości tych fal, czyli odległości od epicentrum oraz magnitudy trzęsienia ziemi oraz od właściwości materiałowych osadu, w którym występują sejsmity..

C. Rekonstrukcja głębokości wody w paleozbiorniku na podstawie położenia dropstonów w osadzie jest możliwa jedynie przy użyciu dokładnych danych terenowych, przy czym rekonstrukcja ta będzie zawierać błędy odwrotnie proporcjonalne do liczby obserwowanych dropstonów w taki sposób, że większa ich liczba prowadzić będzie do coraz dokładniejszych rekonstrukcji.

D. Istnieje pewna granica głębokości wody, od której ziarno poruszać się będzie spadkiem swobodnym. W zbiornikach głębszych (powyżej tej głębokości granicznej), nie może być zrekonstruowana głębokości zbiornika.

E. Średnice, a co za tym idzie, masy dropstonów mają kluczowe znaczenie dla ewentualnej rekonstrukcji głębokości wody w zbiorniku. Im większa masa, tym większe prawdopodobieństwo, że ziarno osiągnie dno z prędkością pozwalającą zrekonstruować głębokość zbiornika.

Cele badawcze niniejszej rozprawy

A. Stworzenie modelu numerycznego powstawania struktur deformacyjnych związanych z aktywnością sejsmiczną, w tym: stworzenie metod pozwalających ominąć bariery numeryczne występujące powszechnie w tego typu symulacjach, walidacja modelu z obserwacjami terenowymi oraz wskazanie błędów modelu oraz jego zastosowań.

B. Stworzenie modelu numerycznego depozycji dropstonów w zbiornikach wodnych, w tym dobór odpowiednich metod numerycznych, weryfikacja modelu z obserwacjami terenowymi oraz wskazanie potencjału predykcyjnego modelu.

2. METODY BADAWCZE

Metody sedymentologiczne. Metody sedymentologiczne (analiza uziarnienia, litofacjalna, pomiary orientacji dłuższych osi ziaren), które zostały zastosowane w niniejszej dysertacji posłużyły m.in. do weryfikacji modeli numerycznych. W przypadku SSDS indukowanych sejsmicznie wyniki obserwacji terenowych zaprezentowano w **artykule nr 1**, natomiast w przypadku SSDS towarzyszących depozycji dropstonów – w **artykule nr 3** oraz **nr 2**.

Metody numeryczne. Metody numeryczne zastosowane w niniejszej rozprawie doktorskiej podzielono na dwa podrozdziały dotyczące (1) **modelu powstawania struktur deformacyjnych indukowanych sejsmicznie** w osadach nieskonsolidowanych (**artykuł nr 1**) oraz (2) **modelu depozycji dropstonów** w zbiornikach wodnych w osadach nieskonsolidowanych (**artykuł nr 2**). Mimo, że oba modele numeryczne mają wiele cech wspólnych, jak na przykład wykorzystanie programu iSALE2D w celu wykonania symulacji i obliczeń a także użycie podobnych cech materiałowych dla artefaktycznych osadów numerycznych, zachodzą między nimi znaczące różnice. Modele odtwarzają procesy zachodzące przy udziale (1) wysokiej i (2) niskiej energii, cechują się innymi błędami numerycznymi, ich kryteria walidacji są odmienne a także różnią się typami wykonanych symulacji. W przypadku opisu numerycznego depozycji dropstonów, autorka niniejszej dysertacji, napisała program w języku C, całkujący numerycznie ruch ziaren w wodzie.

- ***Model rozwoju struktur deformacyjnych indukowanych aktywnością sejsmiczną.***

Modelowanie numeryczne SSDS, powstających pod wpływem propagacji fal sejsmicznych, jest skomplikowane koncepcyjnie z wielu powodów, które można podzielić na dwie zasadnicze grupy: problemy obliczeniowe oraz problemy obserwacyjne.

Problemy związane z obliczeniami

A. Znaczna odległość występowania sejsmitów od epicentrum trzęsienia ziemi (Galli, 2000) powoduje, że pełne symulacje wysokiej rozdzielczości, pozwalającej na śledzenie propagacji fal sejsmicznych oraz rozpoznanie pojawiających się SSDS (rozdzielczość rzędu kilku centymetrów), musiałyby być prowadzone na siatce obliczeniowej złożonej z setek tysięcy oczek. Czas kalkulacji dla takiego modelu oraz ilość produkowanych przez niego danych liczbowych stanowczo wykracza poza możliwości najszybszych komputerów.

B. Dotychczasowe modele numeryczne, odnoszące się do propagacji fal sejsmicznych w osadach, wykorzystują metody niepozwalające na obserwację sejsmitów. Modele te bazują na równaniu fali w niezaburzonym ośrodku (Peng i Wang, 2019, Li i in., 2020), co wyklucza pojawienie się SSDS, lub upraszczają symulacje w taki sposób, że ośrodek wraca do pierwotnego stanu zaraz po przejściu czoła fali, co uniemożliwia śledzenie zaburzeń (Jefeeris i Been, 2015; Boulanger i Ziotopoulou, 2017). Modele te, mimo że dobrze przewidują makroskopowe skutki trzęsień ziemi, nie nadają się do modelowania sejsmitów.

C. Dotychczasowe modele skupiają się przede wszystkim na potencjale upłynnienia (Seed i Idriss, 1971; Vaid i Thomas, 1995; Andrus i Stoke, 1997; Youd i Idriss, 2001; Rahman i Lo, 2014; Rahman i in., 2020). Ich wyniki, mimo że są niezwykle cenne dla bezpieczeństwa na obszarach aktywnych sejsmicznie, nie zawierają informacji o powstających w wyniku uwodnienia i upłynnienia SSDS.

Problemy obserwacyjne utrudniające stworzenie i walidację modelu

A. Trudność w zlokalizowaniu epicentrum trzęsienia ziemi w przypadku dawnych zdarzeń, przez co zazwyczaj niemożliwe jest wskazanie punktu startowego symulacji.

B. Procesy postdepozycyjne mogą znacząco wpłynąć na zmianę geometrii oraz rozciągłości przestrzennej sejsmitów.

C. W przypadku dawnych zdarzeń sejsmicznych, właściwości osadów, w których powstawały SSDS mogą być jedynie szacowane. Model numeryczny odnoszący się do powstawania sejsmitów wymaga prowadzenia wielu symulacji próbnych w celu dopasowania wartości liczbowych dla konkretnych cech materiałowych osadów.

Wszystkie te ograniczenia sprawiają, że mimo dużego zainteresowania SSDS indukowanymi sejsmicznie nie powstał do tej pory model numeryczny opisujący ich powstanie.

Założenia i ograniczenia metodologiczne modelu

Ze względu na wymienione wcześniej trudności obliczeniowe oraz obserwacyjne, założenia oraz ograniczenia stworzonego modelu numerycznego powstawania sejsmitów zawierają wiele punktów, które należy mieć na uwadze przy korzystaniu z proponowanego rozwiązania.

A. Właściwości osadów, w tym wartość naprężenia ścinającego, a także prędkość wertykalna fali sejsmicznej S (odpowiedzialnej za ciśnienie powodujące uwodnienie i upłynnienie) są znane i stanowią dane wejściowe dla symulacji. Symulowany materiał odpowiada suchemu i mokremu piaskowi, zaś wartość prędkości skierowanej w dół waha się

pomiędzy 1,6 i 2,6 ms^{-1}. Przedział ten obejmuje typowe prędkości wertykalne fal sejsmicznych typu S w odległości kilkunastu/kilkudziesięciu kilometrów od epicentrum. Założenie to jest z pewnością prawomocne na pewnych odcinkach drogi pokonywanej przez propagującą falę, niezależnie od położenia epicentrum trzęsienia ziemi. Przyjęcie znanych wartości parametrów, mających wpływ na geometrię oraz rozmieszczenie przestrzenne SSDS, pozwoliło uniknąć problemów związanych z niewiadomym położeniem epicentrum czy magnitudą trzęsienia ziemi. Pozwoliło też wyeliminować problem dużej siatki obliczeniowej i błędów numerycznych wynikających ze skomplikowania modelu.

B. Ławice osadów są jednorodne (tj. masywne), występują naprzemiennie i różnią się jedynie gęstością oraz wartością naprężeń ścinających, przy czym różnice te są niewielkie. Założenie różnic pomiędzy osadami w ławicach jest konieczne dla zaistnienia dyspersji fali i powstania SSDS.

C. Porowatość osadu w prowadzonych symulacjach wynosi odpowiednio 15, 20 i 25%, co odpowiada zakresowi porowatości w piaszczystych i piaszczysto-mułowych osadach.

D. Prędkość wertykalna fali sejsmicznej S jest stała na niewielkim odcinku drogi (rzędu dziesiętnych części metrów), co pozwala na modelowanie dwuwymiarowe oraz uniknięcie konieczności obliczeń prędkości fali na całej jej długości, obciążonych dużymi błędami numerycznymi. Takie założenie jest również konieczne w celu uniknięcia problemu znacznej odległości sejsmitów od epicentrum i eliminuje niezwykle skomplikowane numerycznie symulacje propagacji fali w nieskonsolidowanym podłożu.

Ograniczenia metodologiczne dla zastosowania modelu

Ograniczenia modelu wynikają z braku rozwiązań numerycznych oraz z przyjętych założeń.

A. Brak możliwości symulacji powstawania SSDS związanych z częściową separacją wody. Wynika to z architektury użytego oprogramowania, które pozwala na symulacje zachowania nawodnionego osadu pod wpływem wysokiego ciśnienia jedynie poprzez „dodanie wody" do analitycznego równania stanu używanego jako model osadów. W związku z tym, ilość wody w symulacji pozostaje stała od początku do końca. Ograniczenie to nie jest znaczącą wadą proponowanego rozwiązania, bowiem woda zawsze niesie ze sobą osad, stając się gęstą zawiesiną, której dynamikę można porównać do dynamiki uwodnionego piasku.

B. Niewielka rozciągłość wertykalna modelu (rzędu metrów) wynikająca z przyjęcia stałej prędkości wertykalnej fali sejsmicznej typu S na jej krótkim odcinku. Ograniczenie to można ominąć przez przeprowadzenie wielu symulacji dla prędkości niewiele różniących się od

siebie, a następnie ich wertykalne złożenie. Fale sejsmiczne podczas propagacji w nieskonsolidowanym osadzie wraz z odległością od epicentrum ulegają spowolnieniu, przez co ich prędkość maleje w kierunku przeciwnym do epicentrum.

C. Symulowane ławice zawierają artefaktyczny masywny (jednorodny) osad drobnoziarnisty tj. piaszczyste czy piaszczysto-pylaste przez co nie dochodzi do dyspersji fali sejsmicznej wewnątrz ławic a jedynie na granicach, zróżnicowanych gęstościowo, ławic. W związku z tym, proponowane rozwiązanie nie nadaje się do osadów zawierających wyraźnie większe ziarna czy ziarna znacznie zróżnicowane pod względem frakcji (np. żwir piaszczysty).

D. W modelu nie uwzględniono odprężeń osadu po przejściu fal sejsmicznych, dlatego uzyskane wyniki dotyczące kompakcji osadu powinny być traktowane ostrożnie (por. Fig. 1 i 2 w **artykule nr 1**).

Przeprowadzone symulacje

Symulacje, wykonane w ramach prezentowanego modelu numerycznego, prowadzone były w wirtualnych tubach o głębokości 12 metrów oraz szerokości równej 0,6 metra. Tuby zostały wypełnione materiałem o właściwościach suchego i nawodnionego piasku, w którym zawartość wody wynosiła 25%. W modelu wykorzystano trzy wartości porowatości osadu: 15, 20 oraz 25% oraz przyjęto wartości prędkości wertykalnej fali sejsmicznej typu S między 1,6 a 2,6 ms^{-1}. Rozdzielczość symulacji dobrana została jako optymalna zarówno dla szybkości obliczeń, generowanych błędów numerycznych oraz dokładności modelu i wynosiła 3 centymetry. Jako początek symulacji obrano moment, w którym ciśnienie związane z propagującą falą zaczyna przenikać w głąb osadu, zaś jako koniec eksperymentu numerycznego uznano pierwsze odbicie fali od dna wirtualnej tuby. Zakończenie symulacji w tym momencie podyktowane było dwoma głównymi powodami. Pierwszy z nich, to brak rzeczywistego odpowiednika odbicia fali sejsmicznej na określonej głębokości, bowiem w rzeczywistych trzęsieniach ziemi, ciśnienie jest dystrybuowane w kierunku pionowym tak długo, aż fala nie ulegnie całkowitemu wygaszeniu czy dyspersji. Drugi powód to olbrzymie błędy numeryczne powstające podczas odbicia ciśnienia od wirtualnych ścian tuby. Podobne, choć mniejsze błędy, można zauważyć w wynikach modelu (por. Fig. 1 w **artykule nr 1**).

Do symulacji użyto oprogramowania iSALE2D (Wünnemann i in., 2006). Wybór ten podyktowany był architekturą programu pozwalającą na symulacje propagacji fali o prędkości przekraczającej prędkość dźwięku, w wąskich wirtualnych tubach. ISALE2D umożliwia

obliczenia wysokiej rozdzielczości, rzędu kilku centymetrów, koniecznej w modelowaniu SSDS. Program iSALE2D, bazujący na algorytmie hydro-kodowym (Amsden i in., 2006), wykorzystuje wirtualną siatkę wypełnioną materiałem (=osadem), na której węzłach obliczane są prędkości, położenia oraz inne zmienne charakteryzujące osad znajdujący się w otoczonych węzłami oczkach siatki. Takie rozwiązania są powszechnie stosowane do symulacji zachowań płynów oraz zachowujących się jak płyny substancji, ponieważ pozwalają one na poznanie cząstkowych zachowań osadu, nie traktując go jako jedną masę (jak na przykład podczas dwuwymiarowego całkowania numerycznego). ISALE2D bazuje na równaniach Naviera-Stokesa adresujących zasadę zachowania pędu w dynamicznym płynie oraz zawiera modele elastyczności, plastyczności i wytrzymałości wraz z równaniami stanu dla większości materiałów występujących powszechnie na ziemi (Collins i Wünnemann, 2004; Wünnemann i in. 2006). Program ten, stworzony pierwotnie do symulacji zderzeń obiektów kosmicznych z planetami (co niezmiennie stanowi jego najczęstsze wykorzystanie), został wielokrotnie zwalidowany z danymi obserwacyjnymi (Bronikowska i in., 2017), eksperymentalnymi (Davison i in., 2011) oraz innymi hydro-kodami (Pierazzo i in., 2008), co sprawia, że wykonane za jego pomocą symulacje należy traktować jako wiarygodne.

- **Model depozycji dropstonów i rozwoju struktur deformacyjnych wokół dropstonów**

Założenia metodologiczne

A. Kulisty kształt deponowanego dropstonu. Założenie to znacznie uprościło i przyspieszyło prowadzone symulacje i nie miało znaczącego wpływu na otrzymane wyniki.

B. Zawężenie działających sił do oporu ośrodka, siły wyporu oraz grawitacji, bez uwzględnienia pływów, falowania i innych czynników mogących nadać prędkość horyzontalną ziarna. Założenie to wynika przede wszystkim z zaniedbywalnego wpływu tych czynników na pionowe ciśnienie (wywołane prędkością wertykalną) wywierane na osady dna, a co za tym idzie, na powstające SSDS. **Uwzględnienie tych sił wiązać by się mogło z wprowadzeniem do modelu kolejnych niewiadomych, co uczyniłoby model zarówno bardziej skomplikowanym, jak też mniej dokładnym.**

C. Punktem startowym modelu jest powierzchnia zbiornika wodnego, zaś początkowa wartość prędkości ziarna wynosi 0 m/s.

D. Użycie ziaren kwarcowych jako materiału dna najlepiej oddaje mechaniczne zachowanie osadów jeziornych/morskich.

E. Założenie stałej temperatury oraz gęstości wody (do 10 metrów). Różnice temperatur i gęstości wody dla najgłębszych symulowanych zbiorników są niewielkie (stanowią ułamek procenta) i mogą być pominięte bez wpływu na otrzymane wyniki.

Ograniczenia modelu (wynikają głównie z zastosowanych założeń)

A. Model nie jest przystosowany do symulacji depozycji dropstonów w głębokich jeziorach/morzach, w których prędkość opadania ziarna przechodzi w spadek swobodny, co sprawia, że błędy numeryczne oraz te, wynikające z braku uwzględnienia prądów i pływów, rosną wraz z głębokością wody.

B. Model pozwala rekonstruować głębokość zbiornika z pewnymi błędami, jednak tylko w sytuacji, gdy dane obserwacyjne dotyczą przynajmniej trzech ziaren wraz z ich pierwotną głębokością zakopania w osadzie. Wynika to z konieczności wyznaczenia funkcji właściwości materiałowych osadów dna (por. Fig. 4 **w artykule nr 2**), pozwalającej na określenie jaka część energii zostanie zaabsorbowana przez osad, a jaka wytworzy deformacje w dnie.

Stworzony model depozycji dropstonów składa się z dwóch części. Pierwszą z nich stanowi całkowanie numeryczne równań ruchu w gęstym ośrodku, odpowiadający sytuacji opadania ziarna w wodzie. Drugą część stanowią symulacje reakcji osadów dna na, obliczoną w pierwszej części, prędkość ziarna. Z uwagi na mnogość sił działających jednocześnie w naturalnym środowisku, jego częściowe nieuporządkowanie oraz niewiadomą dotyczącą wszystkich procesów, modele numeryczne są w stanie jedynie oddawać sytuacje uproszczone, lub idealne.

Prędkości uderzenia dropstonu w osady dna

W celu obliczenia prędkości uderzenia dropstonu w osady dna napisano program w języku C, wykonujący całkowanie numeryczne Newtonowskich równań ruchu w gęstym ośrodku. Założono, że działające siły to: siła oporu ośrodka (F_d), siła wyporu (F_b) oraz grawitacja (F_g). W związku z tym, biorąc pod uwagę drugą zasadę dynamiki Newtona oraz zerową prędkość początkową, przyspieszenie ziarna w wodzie można opisać jako:

$$a = \frac{F_d + F_b + F_g}{m},$$

gdzie $F_{d,\,b,\,g}$ to wymienione wcześniej siły, przy czym:

$$F_d = -v_z \cdot v_{tot} \cdot \rho_w \cdot s_c \cdot C_D \,,\; F_b = \frac{\rho_w \cdot g \cdot m}{\rho_c},\; F_g = -mg$$

gdzie: v_z to prędkość wertykalna ziarna, v_{tot} jego prędkość całkowita, ρ_w oraz ρ_c oznaczają odpowiednio gęstość wody oraz opadającego dropstonu, s_c to powierzchnia ziarna (sfery o określonym promieniu, C_D jest stałym współczynnikiem tarcia, g oznacza stałą grawitacji, przy czym jej ujemna wartość wynika z wertykalnego skierowania w dół, natomiast m to masa ziarna, obliczaną za pomocą wzoru na masę kuli o określonym promieniu (r) i gęstości (ρ):

$$m = \frac{4}{3}\pi r^3 \rho.$$

Przekształcając powyższe wzory, wyprowadzono następujące całki ruchu:

$$\frac{\partial s_y}{\partial t} = v_y, \frac{\partial v_y}{\partial t} = a_y = -g - \frac{v_v \cdot v_{tot} \cdot \rho_w \cdot C_s \cdot D_c + \frac{\rho_w \cdot g \cdot m}{\rho_c}}{m},$$

oznaczające, że pochodną drogi pionowej po czasie jest prędkość wertykalna, natomiast pochodną prędkości po czasie jest opisane wcześniej przyspieszenie (co stanowi podstawowe prawa fizyki Newtonowskiej). Powyższe równania przecałkowano numerycznie wykorzystując napisany w języku C program oraz standardowy integrator numeryczny rkf45 (Shampine i Watts, 1976), bazujący na metodzie Runge-Kutta-Fehlberg z krokiem czasowym równym 0,1 sekundy. Taki krok czasowy uznano za najbardziej optymalny pod względem zarówno szybkości obliczeń, jak i błędów numerycznych wynoszących około 1%. Obliczenia przeprowadzono dla głębokości od 2 do 25 metrów.

Po przecałkowaniu numerycznym drogi i prędkości ziarna w wodzie, uzyskano prędkość końcową deponowanego w osadzie dropstona. Prędkość ta została następnie użyta jako zmienna wejściowa do symulacji „odpowiedzi osadu" na ciśnienie wywołane energią opadającego ziarna.

Reakcja osadów dna na ciśnienie wywołane prędkością końcową ziarna

Aby zbadać reakcję osadów dna na ciśnienie wywołane spadkiem ziarna, użyto programu iSALE2D (Wünnemann i in., 2006). Dane wejściowe, potrzebne do symulacji przy użyciu iSALE'a, to prędkość oraz średnica ziarna, a także właściwości materiałowe podłoża i litologiczne dropstonu. Jak wspomniano, prędkości wejściowe dla prowadzonych symulacji obliczone zostały w pierwszym kroku, natomiast przyjęte średnice wynosiły między 0,1 a 1,4 metra. Gęstość ziarna ustalono jako wartość typową dla granitu, zaś tabela zawierająca wykaz wartości użytych w modelu materiału podłoża znajduje się w załączonym **artykule nr 2**.

W ramach symulacji próbnych ustalono rozdzielczość modelu, wynoszącą 20 CPPR (ang. *cells per projectile radius*), co oznacza, że na odcinku równym promieniowi ziarna znajdowało się 20 oczek siatki. Taka rozdzielczość nie generowała znaczących błędów numerycznych oraz mieściła się w rozsądnym czasie trwania obliczeń (por. Fig. 1 **w artykule nr 2**). Następnie przeprowadzono serię symulacji dla każdej średnicy ziarna oraz głębokości wody z przyjętych przedziałów.

3. ZARYS TREŚCI ARTYKUŁÓW

Artykuł nr 1: **Bronikowska, M.**, Pisarska-Jamroży, M., Van Loon, A.J., 2021. First attempt to model numerically seismically-induced soft-sediment deformation structures – a comparison with field examples. *Geological Quarterly* 65, 60.

W pierwszym artykule, wchodzącym w skład niniejszej rozprawy doktorskiej, zaprezentowano wstępny model numeryczny powstawania struktur deformacyjnych indukowanych sejsmicznie wraz z jego walidacją z obserwacjami terenowymi. Artykuł ten skupia się głównie na nowej metodzie symulacji procesu formowania się sejsmitów oraz możliwościach nowego podejścia metodologicznego. W związku z tym, w artykule odniesiono się do dotychczasowego stanu badań numerycznych adresujących procesy odpowiedzialne za powstawanie indukowanych sejsmicznie SSDS, a także wskazano na złożoność problemu i dotychczasowy brak dostępnych rozwiązań. Następnie, zaproponowano nowe podejście, polegające na użyciu w hydro-kodowych symulacjach składowej wertykalnej fali sejsmicznej typu S. W artykule zaprezentowano wyniki dla prędkości wertykalnej wynoszącej między 1,6 a 2,6 ms^{-1} oraz osadów o porowatościach odpowiednio 15, 20 oraz 25%. Otrzymane w modelu artefaktyczne SSDS porównano z obserwowanymi w terenie SSDS, wskazując że są one niemal identyczne, jak w sejsmitach. Na końcu, wyciągnięto odpowiednie wnioski dotyczące wpływu poszczególnych parametrów modelu na geometrię powstałych SSDS.

Artykuł nr 2: **Bronikowska, M.**, Pisarska-Jamroży, M., Van Loon, A.J., 2021. Dropstones deposition – results of numerical modelling of deformation structures, and implications for the reconstruction of the water depth in shallow lacustrine and marine successions. *Journal of Sedimentary Research* 91, 507-519.

W drugim z artykułów przedstawiono pierwszy na świecie model numeryczny opisujący

proces depozycji dropstonów w zbiornikach wodnych oraz możliwości zastosowania modelu w rekonstrukcjach głębokości zbiorników wodnych. Zaprezentowano możliwe scenariusze depozycji ziaren o średnicach między 0,2 a 1 metr w osadach o różnych parametrach materiałowych, odpowiadających niskiej, średniej oraz wysokiej wytrzymałości. Symulowane głębokości wody wynosiły odpowiednio 2, 3, 4, 5 oraz 10 metrów. Otrzymane wyniki porównano z danymi terenowymi, co zapewniło walidację modelu, a także pozwoliło na wskazanie jego potencjału predykcyjnego. Na koniec, przedstawiono wyniki oraz wnioski zawierające zarówno opis procesu depozycji dropstonów w osadach płytkich zbiorników wodnych, jak i algorytm postępowania w wykorzystaniu modelu w interpretacji danych terenowych.

Artykuł nr 3: Pisarska-Jamroży, M., Van Loon, A.J., **Bronikowska, M.**, 2018. Dumpstones and dropstones as records of overturning ice rafts in a Weichselian proglacial lake (Rügen Island, NE Germany). *Geological Quarterly* 62, 917-924.

W trzecim artykule, wchodzącym w skład niniejszej dysertacji, dokonano obserwacji i opisu sedymentologicznego dropstonów (oraz dumpstonów) znajdujących się w plejstoceńskich osadach glacigenicznych na wyspie Rugia w NE Niemczech. Odtworzono, opisano i zinterpretowano widoczną sukcesję osadów (por. Fig 2 w **artykule nr 3**), z uwzględnieniem paleośrodowiska oraz zachodzących w nim procesów, szczególnie podczas depozycji dropstonów.

4. WYNIKI

W odniesieniu do wymienionych, w pierwszej części streszczenia, **celów** niniejszej rozprawy doktorskiej, jej **wynikami** są dwa **nowe modele numeryczne związane z powstawaniem struktur deformacyjnych w plejstoceńskich osadach glacigenicznych**.

Model **powstawania struktur deformacyjnych wywołanych aktywnością sejsmiczną** jest pierwszą na świecie próbą opisu numerycznego powstawania SSDS w sejsmitach. Stanowi on nie tyle kompletny model, ile wskazanie na możliwe rozwiązania problemów pojawiających się w symulacjach odnoszących się do warunków powstawania sejsmitów. Posiada on znaczny potencjał do dalszego rozwoju, a także pomaga w zrozumieniu mechanizmów odpowiedzialnych za geometrię oraz rozmieszczenie przestrzenne struktur deformacyjnych

indukowanych sejsmicznie. Pomimo znacznych uproszczeń, wielu założeń i ograniczeń modelu, jego zastosowanie umożliwiło wyciągnięcie wniosków dotyczących wpływu badanych parametrów, jak prędkość wertykalna fali sejsmicznej typu S i porowatość osadu, na powstające pod wpływem aktywności sejsmicznej SSDS. Model został także sprawdzony poprzez porównanie otrzymanych wyników symulacji z obserwowanymi w terenie SSDS występującymi w sejsmitach. Cel pierwszy pracy doktorskiej, jakim było stworzenie nowego modelu numerycznego, został osiągnięty. Szczegółowe wyniki odnoszące się do potencjału predykcyjnego modelu oraz jego zastosowań opisane zostały w **artykule nr 1**, natomiast płynące z modelu wnioski znajdują się w kolejnej części niniejszego streszczenia.

Model **powstawania struktur deformacyjnych związanych z depozycją dropstonów**, którego stworzenie stanowiło drugi cel niniejszej dysertacji, stanowi pełny opis procesu opadania ziaren w kolumnie wody oraz „odpowiedzi" osadów dna na ciśnienie wywołane uderzeniem ziarna. Jak wspomniano, w rozdziale dotyczącym metod, model ten, jak każdy opis numeryczny, posiada swoje założenia oraz ograniczenia. Co ważne, z uwagi na samą charakterystykę fizyczną zjawiska opadania ziaren w gęstym ośrodku, rekonstrukcja głębokości wody w jeziorach/morzach może być jedynie stosowana dla płytkich zbiorników wodnych. Wynika to z założeń modelu, w którym nie uwzględnia się prądów dennych, mogących znacznie wpływać na proces depozycji dropstonów, a także z istnienia głębokości granicznej, poniżej której ziarna wytracają całą swoją prędkość i opadają spadkiem swobodnym („tracąc" tym samym informacje o przebytej drodze). Stworzony model posiada potencjał predykcyjny opisany szerzej w **artykule nr 2**, pozwala na wyciągnięcie wniosków dotyczących obserwowanych SSDS, związanych z depozycją dropstonów oraz, w niektórych przypadkach, na rekonstrukcję głębokości zbiornika wodnego. Porównanie wyników symulacji numerycznych z obserwacjami terenowymi (**artykuł nr 3**) wskazuje, że pomimo użytych uproszczeń i założeń, jest on dokładny i wiarygodny.

5. WNIOSKI

Stworzone modele numeryczne można w prosty sposób odnieść do obserwowanych struktur deformacyjnych oraz na ich podstawie wyciągnąć wnioski dotyczące procesów ich powstawania.

Wnioski z symulacji i modelu numerycznego procesu powstawania SSDS związanych z aktywnością sejsmiczną:

1. W efekcie zastosowania uproszczenia, polegającego na użyciu w symulacjach wertykalnej składowej fali sejsmicznej typu S, otrzymano artefaktyczne SSDS niezwykle podobne do obserwowanych w sejsmitach. Na tej podstawie, można przypuszczać, że fala sejsmiczna typu S, a dokładniej wywoływane przez nią ciśnienie skierowane w dół, jest główną siłą odpowiedzialną za powstawanie SSDS związanych z aktywnością sejsmiczną.

2. Przeprowadzone symulacje wykazały silną zależność pomiędzy porowatością osadu, a geometrią i wielkością SSDS. Wzrost porowatości osadu powoduje wzrost wielkości SSDS oraz bardziej przypadkowe ich rozmieszczenie w ławicach.

3. Wyniki modelu pokazują, że zastosowanie różnych prędkości fal sejsmicznych typu S (w przedziale 1,6-2,6 km/s) ma **mniejszy wpływ na zróżnicowanie geometrii powstających SSDS, niż właściwości materiałowe osadu**. Wartość prędkości jest natomiast **istotna dla głębokości występowania SSDS w osadach**. Biorąc pod uwagę fakt, że podczas trzęsienia ziemi, prędkość rozchodzenia się fal sejsmicznych maleje wraz ze wzrostem odległości od epicentrum, wynik ten może znaleźć zastosowanie przy rekonstrukcji kierunku rozchodzenia się fal.

4. Z uwagi na silny związek głębokości występowania sejsmitów z prędkością pionową fali sejsmicznej typu S, ich obserwowane położenie przestrzenne może być powiązane z maksimami oraz minimami rozchodzących się fal. Wniosek ten wymaga dalszego zbadania.

5. Otrzymane wyniki są zgodne z dotychczasowymi obserwacjami terenowymi oraz badaniami struktur deformacyjnych wywołanych aktywnością sejsmiczną.

Wnioski z modelu numerycznego opisującego proces powstawania struktur deformacyjnych związanych z depozycją dropstonów w dnie zbiorników wodnych:

1. Czynnikiem mającym największy wpływ na powstające podczas depozycji dropstonów struktury deformacyjne są właściwości osadów, w których deponowane są dropstony. Przed przystąpieniem do rekonstrukcji głębokości wody w paleozbiorniku, należy wyznaczyć funkcję odpowiadającą wpływowi osadów na głębokość zakopania dropstonów (por. Fig. 4 w **artykule nr 2**). Funkcja ta może być wyznaczona przez pomiar zakopania przynajmniej trzech dropstonów.

2. Istnieje głębokość graniczna zbiorników wodnych, dla której ziarna, po wytraceniu prędkości, opadają spadkiem swobodnym. Głębokość ta zależy od średnicy ziaren i jest tym

mniejsza im mniejsza jest średnica opadających ziaren. Istnienie tej granicy wynika bezpośrednio z dynamiki Newtonowskiej i sprawia, że głębokość może być zrekonstruowana jedynie dla płytkich zbiorników wodnych.

3. Pozostawione przez dropstony „ślady" w osadzie dna silnie zależą od ich średnicy, przy czym zależność ta wynika nie tylko z ich masy, ale również z większej prędkości opadania dużych dropstonów. Obserwacja SSDS, powstałych w osadach dna zbiorników wodnych, po depozycji dropstonów, może pomóc w rekonstrukcjach scenariuszy ich depozycji.

Spis literatury

Allen, J.R.L., 1982. Sedimentary structures: their character and physical basis. Developments in Sedimentology, 30B.

Ambraseys, N., 1988. Engineering seismology. Earthquake Engineering and Structural Dynamics 17, 1-105.

Amsden, A., Ruppel, H., Hirt, C., 1980. SALE: A simplified ALE computer program for fluid flow at all speeds. Los Almos National Laboratories Report, LA-8095.

Andrus, R.D., Stoke K.H., 1997. Liquefaction resistance based on shear wave velocity. National Center for Earthquake Engineering Research (Salt Lake City) Report, 0022.

Anketell J.M., Cegła J., Dżułyński S., 1970. On the deformational structures in systems with reversed density gradients. Rocznik Polskiego Towarzystwa Geologicznego 40, 3-30.

Boulanger, R., Ziotopoulou, K., 2017. PM4 sand version 3.1: a sand plasticity model for earthquake engineering applications. Report UC Davis Center for Geotechnical Modeling Report, UCD/CGM-17/01.

Brodzikowski, K., Van Loon, A.J., 1991. Glacigenic Sediments: Amsterdam, Elsevier, Developments in Sedimentology 49, 664 p.

Bronikowska, M., Artemieva, N. A., Wünnemann, K., 2017. Reconstruction of the Morasko meteoroid impact – Insight from numerical modeling. Meteoritics & Planetary Science 1-18.

Campbell, C.S., 2003. Liquefaction and Fluidization. In: Middleton, G.V. (Ed.), Encyclopedia of sediments and sedimentary rocks. Kluwer Academic Publishers, Dordrecht, 412–413.

Collins, G.S., Melosh, H.J., Ivanov, B.A., 2004. Modeling damage and deformation in impact simulations. Meteoritics & Planetary Science 39, 217-231.

Davison, T.M., Collins, G.S., Elbeshausen, D., Wünnemann, K., Kearley, A., 2011. Numerical modeling of oblique hypervelocity impacts on strong ductile targets. Meteoritics & Planetary Science 46, 1510-1524.

Dowdeswell, J.A., Whittington, R.J., Jennings, A.E., Andrews, J.T., Mackensen, A., Marienfeld, P., 2000. An origin for laminated glacimarine sediments through sea-ice build-up and suppressed iceberg rafting: Sedimentology 47, 557-576.

Dżułyński, S., 1996. Erosional and deformational structures in single sedimentary beds: A genetic commentary. Rocznik Polskiego Towarzystwa Geologicznego 66, 101-189.

Dżułyński, S., Radomski, A., 1966. Experiments on bedding disturbances produced by the impact of heavy suspensions upon horizontal sedimentary layers. Bulletin de l 'Academie Polonaise des Sciences, Serie des Sciences Geologiques et Geographiques 14, 227-230.

Fichman, M.E., Crespi, J.M., Getty, P.R., Bush, A.M., 2015. Retrodeformation of Carboniferous trace fossils from the Narragansett Basin, U.S.A., using raindrop imprints and bedding-cleavage intersection lineation as strain markers. Palaios 30, 574-588.

Galli, P., 2000. New empirical relationships between magnitude and distance for liquefaction. Tectonophysics 324, 169-187.

Gilbert, R., 1990. Rafting in glacimarine environments: Geological Society of London Special Publication 53, 105-120.

Gradziński R., Kostecka A., Radomski A., Unrug R., 1986. Zarys sedymentologii. Wydawnictwo Geologiczne, Warszawa.

Haarland, W.B., Herod, K.N., Krinsley, D.H., 1966. The definition and identification of tills and tillites. Earth-Science Reviews 2, 225-256.

Hoffmann, P.F., Schrag, D.P., 2000. Snowball Earth. Scientific American 282, 68-75.

Hoffmann, G., Reicherter, K., 2012. Soft-sediment deformation of Late Pleistocene sediments along the south west ern coast of the Baltic Sea (NE Germany). International Journal of Earth Sciences 101, 351-363
Jeffeeris, M., Been, K., 2015. Soil Liquefaction – a Critical State Approach. CRC Press.
Le Heron, D.P., 2015. The significance of ice-rafted debris in Sturtian glacial successions. Sedimentary Geology 322, 19-33.
Li, C., Liu, J., Sun, Y., 2020. Optimal third-order sympletic integration modeling of seismic acoustic wave propagation. Bulletin of the Seismological Society of America 110, 754-762.
Liszkowski J., 1975. Geologiczne modele rozwoju filtracyjnych deformacji gruntów w Polsce. Materiały Konferencyjne: Aktualne problemy geologii inżynierskiej IAEG, Warszawa, 133-151.
Livingstone, S.J., Piotrowski, J.A., Bateman, M.D., Ely, J.C., 2015. Discriminating between subglacial and proglacial lake sediments: an example from the Danischer Wohld Peninsula, northern Germany. Quaternary Science Reviews 112, 86-108.
Matsumoto, D.H., Naruse, S., Fujino, A., Surphawajruksakul, T., Jarupongsakul, N., Sakakura, M., Murayama, M., 2008. Truncated flame structures within a deposit of the Indian Ocean tsunami: Evidence of synsedimentary deformation, Sedimentology, 55, 1559–1570.
Menzies, J., 2002. Modern and Past Glacial Environments: Elsevier, 576 p.
Moretti, M., 2000. Soft-sediment deformation structures interpreted as seismites in middle-late Pleistocene aeolian deposits (Apulian foreland, southern Italy). Sedimentary Geology 135, 167-179.
Odonne, F., Callot, P., Debroas, E.-J., Sempere, T. Hoareau, G., Maillard, A., 2011. Soft-sediment deformation from submarine sliding: Favourable conditions and triggering mechanisms in examples from the Eocene Sobrarbe delta (Ainsa, Spanish Pyrenees) and the mid-Cretaceous Ayabacas Formation (Andes of Peru). Sedimentary Geology 235, 234-248.
Owen, G., Moretti, M., 2011. Identifying triggers for liquefaction-induced soft-sediment deformation in sands. Sedimentary Geology 235, 141-147.
Peng, P., Wang, L., 2019. 3DMRT: a computer package for 3D model-based seismic wave propagation. Seismological Research Letters 90, 2039-2045.
Pierazzo, E., Artemieva, N., Asphaug, N., Baldwin, E., Cazamias, E.C., Coker, R., Collins, G.S., Crawford, D.A., Davison, T., Elbeshauen, D., Holsapple, K.A., Housen, K.R., Korycansky, D.G., Wünnemann, K., 2008. Validation of numerical codes for impact and explosion cratering: Impacts on strengthless and metal targets. Meteoritics & Planetary Science 43, 1917-1938.
Pisarska-Jamroży, M., Belzyt, S., Bitinas, A., Jusienå, A., Woronko, B., 2019. Seismic shocks, periglacial conditions and glacitectonics as causes of the deformation of a Pleistocene meandering river succession in central Lithuania. Baltica 32, 63-77.
Pisarska-Jamroży, M., Belzyt, S., Börner, A., Hoffmann, G., Hüneke, H., Kenzler, M., Obst, K., Rother, H., Van Loon, A.J., 2018. Evidence from seismites for glacioisostatically induced crustal faulting in front of an advancing land-ice mass Rügen Island, SW Baltic Sea). Tectonophysics 745, 338-348.
Rahman, M., Asce, M., Nguyen, H.B.K., Fourie, A.B., Kuhn, M.R., 2020. Critical state soil mechanics for cyclic liquefaction and postliquefaction behaviour: DEM study. Journal of Geotechnical and Geoenvironmental Engineering 147, 04020166.
Rahman, M., Lo, S., 2014. Undrained behaviour of sand-fines mixtures and their state parameters. Journal of Geotechnical and Geoenvironmental Engineering 140, 04014036.
Rossetti, D.F., 1999. Soft-sediment deformation structures in late Albian to Cenomanian deposits, Sao Luis Basin, northern Brasil: evidence for palaeoseismicity. Sedimentology 46, 1065-1081.
Seed, H.B., Idris, I.M., 1971. Simplified procedure for evaluating soil liquefaction potential. Journal of Soil Mechanics and Foundations Division 97, 1249-1273.
Seilacher, A., 1969. Fault-graded beds interpreted as seismites. Sedimentology 13, 15-159.
Shampine, L.F., Watts, H.A., 1976. Practical solution of ordinary differential equations by Runge-Kutta methods. [Writing a high-quality code; description of RKF45, in FORTRAN for CDC 6600 computer]. United States: N. p., 1976. Web.
Shanmugam, G., 2016. The seismite problem. Journal of Palaeogeography 5, 318-362.
Thomas, G.S., Connell, R.J., 1985. Iceberg drop, dump, and grounding structures from Pleistocene glaciolacustrine sediments. Journal of Sedimentary Petrology 55, 243-249.
Vaid, Y.P., Thomas, J., 1995. Liquefaction and postliquefaction behavior of sand. Journal of Geotechnical Engineering 121, 1321-1337.
Van Loon, A.J., Pisarska-Jamroży, M., 2014. Sedimentological evidence of Pleistocene earthquakes in NW Poland induced by glacioisostatic rebound. Sedimentary Geology 300, 1-10.
Van Loon, A.J., Pisarska-Jamroży, M., Woronko, B., 2020. Sedimentological distinction in glacigenic sediments between load casts induced by periglacial processes from those induced by seismic shocks. Geological Quarterly 64, 626-640.

Van Loon, A.J., Soms, J., Nartiss, M., Krievans, M., Pisarska-Jamroży, M., 2019. Sedimentological traces of ice-raft grounding in a Weichselian glacial lake near Dukuli (NE Latvia). Baltica 32, 170-181.
Wünnemann, K., Colling, G.S., Melosh, H., 2006. A strain-based porosity model for use in hydrocode simulations of impacts and implications for transient crater growth in porous target. Icarus 180, 514-527.
Youd, T.L., Idriss, I.M., 2001. Liquefaction resistance of soil: summary report from the 1996 NCEER and 1998 NCEER/NFS work - shop on evaluation of liquefaction resistance of soil. Journal of Geotechnical and Geoenvironmental Engineering 127, 1275-1285.

Summary of the PhD thesis by Małgorzata Bronikowska

Numerical modeling of Pleistocene soft-sediment deformation structures in glacigenic sediments

Modelowanie numeryczne plejstoceńskich struktur deformacyjnych w osadach glacigenicznych

1. INTRODUCTION

Soft-sediment deformation structures (SSDS) have been an enduring subject of research by geologists and geomorphologists and a constant source of fascination (Dżułyński and Radomski, 1966; Anketell et al., 1970; Liszkowski, 1975; Dżułyński, 1996; Shanmugan, 2016). Nevertheless, although 150 types of SSDS have been described, no coherent definition exists to account for the variations in original shape, arrangement or internal structure of the disturbance in sediments before their final litification (Gradziński et al., 1986). SSDS can arise during catastrophic (high-energy) events, such as sea landslides (Odonne et al., 2011), tsunami (Matsumoto et al., 2008) or earthquakes (Moretti, 2000; Pisarska-Jamroży et al., 2019), and as a result of low-energy processes, such as rainfall (Fichman et al., 2015) or the free fall of grains on the bottom of water reservoirs (Haarland et al., 1966; Menzies 2002; Pisarska-Jamroży et al., 2018). Regardless of the mechanism initiating the processes leading to the formation of SSDS, the very process of their generation and the relationship between the structural features of the SSDS and the lithology of the sediments in which they occur, or the forces acting on them, remain poorly understood.

High-energy mechanisms initiating the emergence of SSDS. SSDS which are believed to be initiated by high-energy mechanisms, arise under the conditions of high pressure, and their formation is associated with the processes of fluidization and liquefaction of sediments (Allen, 1982), for example seismites generated during the earthquakes (Rosetti et al., 1999; Owen and Moretti, 2011; Van Loon et al., 2020). Seismites are internally-deformed layer containing SSDS generated by the propagation of seismic waves (Seilacher, 1969). The fluidization process, which doesn't require high energy, can be linked with the fulfilling the

empty sediments pores by the water. The resulting fluidized sediments becomes plastic and highly viscous, which allows it to move under the influence of gravity, as observed during landslides (Allen, 1982).

In contrast, sediment liquefaction requires the supply of much more energy to the system, and is observed during such catastrophic processes as earthquakes and meteorite impacts. Liquefaction occurs most often in sediments saturated with water (Campbell, 2003) and those that lack cohesiveness (Seed and Idriss, 1971); it is observed when the strength of the sediments is significantly reduced by the pressure caused by, for example, the passage of seismic waves. The pressure causes the grains to lose contact with each other, and thus to move smoothly (Vaid and Thomas, 1995; Youd and Idriss, 2001).

Both the liquefaction and fluidization of sediments can cause serious damage to residential areas, particularly the destruction of residential buildings and other infrastructure. For this reason, studies of these processes have focused mainly on identifying the key material parameters predisposing the sediment to fluidization and liquefaction, and on creating functions that predict their occurrence (Andrus and Stoke, 1997; Rahman and Lo, 2014; Rahman et al., 2020). The existing models therefore focus more on the prediction of disasters (and the potential for sediment fluidization / liquefaction) than on the nature of the process itself or its participation in the formation of deformation structures. As such, our knowledge of seismites remains relatively poor. Previous observations indicate that they can occur during earthquakes with a magnitude of M> 5 (Ambraseys, 1988) and generally within forty kilometres from the epicentre (Galli, 2000). In general, SSDS induced by seismicity occur in well-sorted, fine-grained sandy sediments with a small content of smaller fractions, for example in lacustrine, marine or fluvial sediments (Hoffmann and Reicherter, 2012; Van Loon and Pisarska-Jamrożу, 2014; Pisarska-Jamrożу, et al., 2018).

The commonly-accepted criteria for identifying seismites are not strict. They include: 1) horizontal continuity of internally-deformed layers, 2) vertical repeatability of the occurrence of deformed layer, 3) similarity between the geometry of the deformation structures present in internally-deformed layer and those observed during modern earthquakes, 4) change in complexity and frequency of SSDS with distance from the epicentre, 5) probability of earthquake occurrence (e.g. proximity to a current or past active fault).

Many questions regarding the formation of SSDS remain unanswered. The influence of the material properties of the sediment on the geometry of seismically-induced SSDS, or the role of the physical parameters of an earthquake on the spatial distribution of SSDS in the

sediment is unknown. Filling this significant knowledge gap may foster a more accurate recognition of paleo seismites, a better understanding of their parameters and extent, and may characterise SSDS features that can be used in their identification.

Low-energy mechanisms initiating the emergence of SSDS. SSDS formed under the influence of low energy input are generally associated with sinking or drifting processes, such as those formed during the deposition of dropstones, i.e. individual grains that are clearly larger than those forming the surrounding sediments (Haarland et al., 1996; Menzies, 2002). They are generally observed in well-sorted lacustrine and marine sediments, and their origin is mainly (but not only; cf. Pisarska-Jamroży et al., 2019) associated with the melting of grains from drifting icebergs (Hoffmann and Schrag, 2000). The accumulation of dropstones is referred to in the literature as IRD (ice-rafted debris, ice-rafted deposits) or dumpstones. The occurrence of dropstones has been described in numerous publications (Thomas and Connell, 1985; Gilbert, 1990; Brodzikowski and Van Loon, 1991; Le Heron, 2015; Pisarska-Jamroży et al., 2018) and they are believed to have significant potential in the reconstruction of lacustrine and marine deposition palaeoenvironments (Dowdeswell et al., 2000; Livingstone, 2015; Van Loon et al., 2019).

Although dropstones and their accompanying deformation structures are relatively well understood, many questions still remain unanswered. For example, does any relationship exist between the footprint of the falling dropstones in the bottom sediment and the depth of the lake / sea? Is it possible to reconstruct the deposition process of a dropstone on the basis of its spatial position and the deformation structures formed around it; in addition, what are the possibilities and limitations of such reconstructions?

This doctoral dissertation attempts to create and apply numerical models describing the processes of formation of two types of deformation structures in Pleistocene glacigenic sediments, and verify the results with field observations. These types of deformation structures are 1) SSDS occurring in seismitees, resulting from the propagation of seismic waves in unconsolidated sediments (paper no.1: Bronikowska et al., 2021a) and 2) SSDS formed in the bottom sediments during the deposition of dropstones (paper no. 3: Pisarska-Jamroży et al., 2018; paper no. 2: Bronikowska et al., 2021b). This choice is dictated by several reasons. Firstly, these types of SSDS seem to play an important role in the reconstruction of palaeoenvironments, and both are well represented in the literature and field observations, which in turn allows for a good verification of the numerical models. Secondly, the creation of two models, i.e. involving high and low-energy processes, allows the closure

of the boundary conditions for the formation of deformation structures.

The doctoral dissertation consists of a set of three peer-reviewed scientific papers published in journals on the JCR list. The first paper describes the use of a numerical model in the reconstruction of seismically-induced SSDS (occurring in seismitees) and verifies the model results with field observations (Bronikowska et al., 2021a). The second paper presents a numerical model relating to the deposition of dropstones (Bronikowska et al., 2021b); the third paper is a description of the deposition of dropstones and dumpstones in the sediments of a Pleistocene glacial lake on the island of Rügen in NE Germany (third paper: Pisarska-Jamroży et al., 2018).

Both presented models (Bronikowska et al., 2021a, b) are the first numerical descriptions of these two processes, and offer potential for further development, detailing and further verification. The author of this dissertation created, described, verified and also gave the predictive potential of two new numerical models relating to deformation structures in Pleistocene glacigenous sediments. She was the lead author for **papers no. 1** and **2**, and her contribution accounts for 85%. The scope of the work included performing numerical simulations, writing one of the programs used for the model (in C, language), describing the obtained results, relating them to field observations, indicating possible applications, indicating model errors and writing a significant part of the text of the papers. The co-authors of the papers provided valuable field data that made it possible to verify the models, wrote parts of the papers relating to field observations, and significantly helped in creating graphics and editing all parts of the text. As the author of this dissertation specializes in numerical modelling, she did not play a leading role in **paper no. 3** (20%); her role consisted of participation in field research and elaboration of results, as well as in writing and editing the text. The statements of the co-authors of papers no. 1-3, included in this dissertation, can be found at the end of this dissertation summary.

The Research Hypothesis of the Doctoral Dissertation

Research hypotheses of the doctoral dissertation

A. The numerical model of seismically-induced SSDS formation, based on discrete sections of a seismic wave and the vertical pressures they cause, **is able to reproduce the artificial SSDS occurring in seismites** (known from field observations).

B. Seismites formation is mainly related to the vertical component of the S wave velocity; therefore, the size, geometry and spatial distribution of the observed / modelled

SSDS will depend on the velocity of these waves, i.e. the distance from the epicentre and the magnitude of the earthquake, and on the material properties of the sediment in which the seismites occur.

C. Accurate field data is needed to reconstruct the water depth in the palaeoreservoir based on the location of the dropstones in the sediments; as this reconstruction will contain errors inversely proportional to the number of dropstones observed, higher numbers of dropstones will allow more accurate reconstructions.

D. Below a certain depth of water, a grain will fall freely. Is not possible to reconstruct the water depth deeper than this limit.

E. The diameters, and thus the masses of the dropstones, are of key importance when reconstructing the water depth in the water reservoirs. Heavier grains are more likely to reach the bottom with a velocity allowing the reconstruction of the paleo water depth.

Research objectives of this dissertation

A. The first aim is to create a numerical model of the formation of deformation structures induced by seismicity. This process includes creating methods to bypass the numerical barriers commonly found in this type of simulations, validating the models against the field observations, and identifying the errors and applications associated with the model.

B. A second aim is to create a numerical model of dropstone deposition in lacustrine and marine sediments, including the selection of appropriate numerical methods, verification of the model with field observations and an indication of the predictive potential of the model.

2. RESEARCH METHODS

Sedimentology methods. The studies presented in frame of this dissertation employed various sedimentological methods (grain size and lithofacial analysis, measurements of the orientation of longer grain axes) to verify the numerical models. The results of field observations regarding seismically-induced SSDS are presented in **paper no. 1**, and those associated with SSDS accompanying dropstones deposition in **papers no. 3 and 2**.

Numerical methods The numerical methods used in this dissertation are divided into two sections, concerning (1) **the seismically-induced SSDS formation model** (**paper no. 1**) and

(2) **the dropstone deposition model** in bottom unconsolidated sediments (**paper no. 2**). Although both numerical models have many things in common, such as using iSALE2D to perform simulations and calculations, and employ similar material features for creating numerical artificial SSDS, they also have significant differences. The models reproduce the processes taking place with the participation of (1) high and (2) low energy; they demonstrate different numerical errors, use different validation criteria and require different types of simulations. To create a numerical description of dropstone deposition, the author of the dissertation wrote a program to numerically integrate the movement of grains in water in C language.

- ***A model of the development of deformation structures induced by seismic activity***

For many reasons, the numerical modelling of SSDS generated by the propagation of seismic waves is conceptually complicated; however, these reasons can be divided into two main groups: computational problems and observational problems.

Computational problems

A. The considerable distance of seismic occurrence from the epicentre of the earthquake (Galli, 2000) means that full high-resolution simulations, allowing for the tracking of seismic wave propagation and the recognition of emerging SSDS (resolution of several centimetres), would require a computational grid composed of hundreds of thousands of elements. The calculation time for such a model and the amount of numerical data it produces are far beyond the capabilities of the fastest computers.

B. The methods used by existing numerical models relating to the propagation of seismic waves in sediments do not allow for the observation of seismites. These models are based on functions describing a wave in an undisturbed medium (Peng and Wang, 2019, Li et al., 2020); this excludes the appearance of SSDS, or simplifies the simulations in such a way that the medium returns to its original state just after the wave front passes, which precludes the tracking of disturbences (Jefeeris and Been, 2015; Boulanger and Ziotopoulou, 2017). These models, although well suited for predicting the macroscopic effects of earthquakes, are not suitable for seismites modelling.

C. Existing models focus primarily on the liquefaction potential (Seed and Idriss, 1971; Vaid and Thomas, 1995; Andrus and Stoke, 1997; Youd and Idriss, 2001; Rahman and Lo, 2014; Rahman et al., 2020). Although their results are extremely valuable for ensuring safety

in seismically-active areas, they do not provide information about SSDS formed as a result of fluidization and liquefaction.

Observational problems complicating model creation and validation

A. It is often impossible to identify the starting point of the simulation due to the difficulties in pointing out of the epicentre of a past earthquake

B. In addition, post-deposition processes can significantly change the geometry and spatial extent of seismites.

C. Due to the fact, that in the case of past seismic events, the properties of the sediments where SSDS were formed can only be estimated. The numerical model for seismites generation requires many trial simulations to match the numerical values for the specific material characteristics of the sediments.

Due to all these limitations, despite the great interest in seismically-induced SSDS, no numerical models describing their formation currently exist.

Assumptions and methodological limitations of the model

Due to the mentioned computational and observational difficulties, the created numerical model of seismic formation is based on a number of assumptions and limitations that should be taken into account when using it.

A. The sediment properties, including the value of the shear stress, as well as the vertical velocity of the seismic S wave (responsible for the fluidization and liquefaction processes) must be known, as these are used as an input data for the simulation. The simulated material corresponds to dry and wet sand and the downward velocity value varies between 1.6 and 2.6 ms-1. This range covers the typical vertical velocities of S-type seismic waves at a distance of several / several dozen kilometres from the epicentre. This assumption is certainly valid on certain sections in the path of the propagating wave, regardless of the location of the epicentre of the earthquake. By this way, problems associated with epicentre location or earthquake magnitude were avoided by adopting known values of the parameters influencing the geometry and spatial distribution of the SSDS. This process also eliminated the need for a large computational grid and the numerical errors resulting from the complexity of the model.

B. The sediment layers are homogeneous (i.e. massive), alternate and differ only in density and shear stress, with these differences also being small. Differences between particular layers must be present to allow wave dispersion and the creation of SSDS.

C. The sediment porosity values used in the conducted simulations are 15, 20 and 25%, corresponding to the porosity range in sandy and sandy-silt sediments.

D. The vertical velocity of the S wave is constant over a short distance (i.e. tenths of metres); this allows two-dimensional modelling to be performed and avoids the need to calculate the speed of the wave along its entire length, which is burdened with large numerical errors. This assumption is also necessary to avoid the problem posed by the significant distance of the seismites from the epicentre and to eliminate the need for extremely complicated numerical simulations of wave propagation in unconsolidated medium.

Methodological limitations for the application of the model

The limitations of the model concern the lack of existing numerical solutions and its assumptions.

A. It is not possible to simulate the formation of SSDS related to partial water separation. This is due to the architecture of the software used, which simulates the behaviour of hydrated sediments under the high pressure only by "adding water" to the analytical equation of state used as the sediments (material) model. Therefore, in this case, the amount of water in the simulation remains constant from start to the end. This limitation is not a significant disadvantage to the proposed solution; as the water always carries sediment, acting as a thick suspension, its dynamics can be compared to those of hydrated sand.

B. A small vertical extension of the model (in the order of metres) resulting from the assumption that the S-type seismic wave maintains a constant vertical velocity over its short section. This limitation can be overcome by running many simulations for closely-related speeds, and then assembling them vertically. When seismic waves propagate in an unconsolidated sediment away from the epicentre, they slow down: their velocity decreases in the direction opposite to the epicentre.

C. The simulated sediments layer contain artificial massive (homogeneous) fine-grained sediment, i.e. sands or sandy-silt, which prevents seismic wave dispersion inside the layer, but only at their borders (due to the density differences). Therefore, the proposed solution is not suitable for sediments containing significantly larger grains or those which differ significantly in terms of fraction (e.g. sandy gravel).

D. The model does not take into account the relaxation of the sediment after the passage of seismic waves; therefore, the obtained results concerning the compaction of the sediment should be treated with caution (see Fig. 1 and 2 in paper no.1).

Performed simulations

The simulations performed within the presented numerical model were carried out in virtual tubes 12 metres deep and 0.6 metres wide. The tubes were filled with a material with the properties of dry and wet sand; the water content was 25%. Three values of sediment porosity were used in the model: 15, 20 and 25%, and the vertical velocity of the S wave ranged from 1.6 to 2.6 ms^{-1}. The resolution of the simulation was selected as 3 cm; this was optimal for the calculations speed, generated numerical errors and the accuracy of the model. The beginning of the simulation was defined as the moment when the pressure related to the propagating wave begins to penetrate deep into the sediment, and the end as when the first wave is reflected from the bottom of the virtual tube. This endpoint was chosen for two key reasons. The first reason is that in reality, there is no real equivalent to a reflection of a seismic wave at a certain depth, because in real earthquakes, the pressure is distributed vertically until the wave is completely extinct or dispersed. The second reason is that huge numerical errors occur when pressure is reflected from the virtual walls of the tube. Similar, although smaller, errors can be noticed in the model results (cf. Fig. 1, paper no. 1).

The simulation was performed using iSALE2D software (Wünnemann et al., 2006). This software was chosen because its architecture allows simulations of wave propagation faster than the speed of sound in narrow virtual tubes. ISALE2D is able to perform the high resolution computations, i.e. in the order of a few centimetres, necessary for SSDS modelling. The iSALE2D program, based on a hydro-code algorithm (Amsden et al., 2006), uses a virtual mesh filled with material (= sediment); velocities, positions and other variables characterizing the sediment are calculated on the nodes surrounded the mesh elements. Such solutions are commonly used to simulate the behaviour of fluids and the fluid-like substances because they allow the partial behaviour of a sediments to be determined without treating it as a single mass (such as during two-dimensional numerical integration). ISALE2D is based on Navier-Stokes equations concerning the principle of conservation of momentum in a dynamic fluid; it also includes models of the elasticity, plasticity and strength of most common materials on earth, together with their equations of state (Collins and Wünnemann, 2004; Wünnemann et al. 2006). This program was originally designed to simulate collisions of space objects with planets (which is invariably its most frequent use), has been repeatedly validated against observations (Bronikowska et al., 2017), laboratory experiments (Davison et al., 2011) and other hydro-codes. (Pierazzo et al., 2008), which means that the simulations performed with it should be treated as reliable.

- **Model of dropstone deposition and the development of deformation structures around dropstones**

Methodological assumptions

A. The deposited dropstone is a uniform sphere. This assumption significantly simplified and accelerated the simulations and had no significant impact on the obtained results.

B. Narrowing the number of acting forces to the resistance of the medium, buoyancy and gravity; eliminating tides, undulations and other factors that may supply the grain horizontal velocity. This assumption was made because the latter factors have a negligible effect on the vertical pressure placed on the bottom sediments as a result of vertical velocity and thus on the resulting SSDS. Taking these forces into account could entail the introduction of further unknowns into the model, increasing its complexity and reducing its accuracy.

C. The starting point of the model is the surface of the water reservoir, and the initial value of the grain velocity is 0 ms^{-1}.

D. The use of quartz grains as the bottom material best reflects the mechanical behaviour of lacustrine / marine sediments.

E. Assumption of constant temperature and water density up to 10 metres. The differences in temperature and water density for the deepest simulated reservoirs are small, constituting only a fraction of a percent, and hence can be ignored without affecting the obtained results.

Model limitations (mainly due to the assumptions used)

A. The model is not adapted to simulate the deposition of dropstones in deep lakes / seas; in such cases, the grain begins a free fall, and the numerical errors, and those resulting from the lack of consideration of currents and tides, increase with depth .

B. The model allows the depth of the reservoir to be reconstructed with some errors, but only if the observational data includes at least three grains, as well as their original burial depth in the sediment. This is necessitated by the need to identify the function of the material properties of the bottom sediments (see Fig. 4, paper no. 2), which is used to determine the proportion of the energy that will be absorbed by the sediment and thus generate deformations in the bottom.

The created dropstone deposition model consists of two parts. The first comprises the numerical integration of equations regarding motion in a dense medium; this corresponds to

the situation of a grain falling through water. The second part simulates the reaction of the bottom sediments to the grain impacting at the velocity calculated in the first part. Due to the multitude of forces acting simultaneously in the natural environment, its state of partial disorder and the unknowns regarding all processes, numerical models are only able to reflect simplified or ideal situations.

The velocity of the dropstone impacting the bottom sediments

In order to calculate the velocity of the dropstone hitting the bottom sediments, a program was written in C; its aim is to perform numerical integration of the Newtonian equations of motion in a dense medium. It was assumed that the acting forces comprised the resistance force of the medium (Fd), the buoyancy force (Fb) and the gravity (Fg). Therefore, based on Newton's second law of motion and assuming zero initial velocity, the acceleration of the grain in water can be described as:

$$a = \frac{F_d + F_b + F_g}{m},$$

where Fd, b, g are the forces given above, where:

$$F_d = -v_z \cdot v_{tot} \cdot \rho_w \cdot s_c \cdot C_D \, , F_b = \frac{\rho_w \cdot g \cdot m}{\rho_c}, F_g = -mg$$

where: v_z is the vertical velocity of the grain, v_{tot} its total velocity, ρ_w and ρ_c are the density of water and falling dropstone (respectively), s_c is the grain surface (spheres with a given radius), C_D is the constant coefficient of friction, g is the gravity constant (a negative value indicates a vertical orientation downward); m is the mass of the grain, calculated based on the formula for the mass of a sphere with a given radius (r) and density (ρ):

$$m = \frac{4}{3}\pi r^3 \rho.$$

By transforming the above formulas, the following integrals of motion were derived:

$$\frac{\partial s_y}{\partial t} = v_y, \frac{\partial v_y}{\partial t} = a_y = -g - \frac{v_v \cdot v_{tot} \cdot \rho_w \cdot C_s \cdot D_c + \frac{\rho_w \cdot g \cdot m}{\rho_c}}{m},$$

indicating that the derivative of the vertical path in time is the vertical velocity, while the derivative of the velocity in time is the acceleration described earlier (which is the basic law of Newtonian physics). The above equations were numerically integrated using the C program and the standard rkf45 numerical integrator (Shampine and Watts, 1976), based on the Runge-Kutta-Fehlberg method with a time step of 0.1 seconds. This time step was found offer optimal computational speed, with numerical errors of around 1%. The calculations were

made for the depth from 2 to 25 metres.

After numerical integration of the grain path and velocity in water, the final velocity of the impacting dropstone was obtained. This velocity was then used as an input variable to simulate the "sediments response" to the pressure caused by the energy of the falling grain.

The reaction of the bottom sediments to the pressure caused by final velocity of the grain

The reaction of the bottom sediments to the pressure caused by the impact of the falling grain was calculated using the iSALE2D program (Wünnemann et al., 2006) . The simulation with iSALE required the speed and diameter of the grain to be input, as well as the material properties of the substrate and the lithological properties of the dropstone. As mentioned, the input velocities for the simulations were calculated in the first step, with the assumed diameters being between 0.1 and 1.4 metres. The grain density was established as a typical value for granite; the table containing the values used in the model of the base material can be found in paper no. 2.

As part of the trial simulations, the model resolution was determined to be 20 CPPR (cells per projectile radius), i.e. the grain radius was equal to 20 mesh elements. This resolution did not generate significant numerical errors and was within a reasonable computation time (see Fig. 1, paper no. 2). Following this, a series of simulations was carried out for each grain diameter and water depth for the adopted intervals.

3 OUTLINE OF THE PAPERS

Paper no. 1: **Bronikowska, M.**, Pisarska-Jamroży, M., Van Loon, A.J., 2021. First attempt to model numerically seismically-induced soft-sediment deformation structures – a comparison with field examples. *Geological Quarterly* 65, 60.

The first paper included in this doctoral dissertation presents a preliminary numerical model of the formation of seismically-induced deformation structures along with its validation based on field observations. This paper mainly focuses on a new method for simulating the seismic formation process and the possibilities of a new methodological approach. It therefore refers to the current state of numerical research into the processes responsible for the formation of seismically-induced SSDS; it also highlights the complexity of the problem and the lack of available solutions.

Following this, a new approach was proposed, consisting in the use of the vertical component of an S wave in hydrocode simulations. The paper presents the results for a vertical velocities of between 1.6 and 2.6 ms-1 and sediments with porosity of 15, 20 and 25%. The artifacial SSDS obtained in the model were compared with those observed in the field; the findings indicate that they are almost identical to those present in seismites. Finally, appropriate conclusions were drawn regarding the influence of individual model parameters on the geometry of the resulting SSDS.

Paper no. 2: **Bronikowska, M.**, Pisarska-Jamroży, M., Van Loon, A.J., 2021. Dropstones deposition – results of numerical modelling of deformation structures, and implications for the reconstruction of the water depth in shallow lacustrine and marine successions. *Journal of Sedimentary Research* 91, 507-519.

The second paper presents a new numerical model, the first of its kind, describing the process of dropstone deposition in water bodies and its potential use in reconstructing the depth of these bodies. It presents various possible deposition scenarios of grains with diameters between 0.2 and 1 metre in sediments with different material parameters corresponding to low, medium and high strength. The simulated water depths were 2, 3, 4, 5 and 10 metres. The obtained results were compared with field data, which ensured the validation of the model, and gave an indication of its predictive potential. Finally, the results and conclusions are presented; these include a description of the dropstone deposition process in the sediments of shallow water reservoirs, and an algorithm for using the model in interpreting field data.

Paper no. 3: Pisarska-Jamroży, M., Van Loon, A.J., **Bronikowska, M.**, 2018. Dumpstones and dropstones as records of overturning ice rafts in a Weichselian proglacial lake (Rügen Island, NE Germany). *Geological Quarterly* 62, 917-924.

The third paper included in this dissertation presents observations and sedimentological descriptions of dropstones (and dumpstones) found in Pleistocene glacigenic sediments on the island of Rügen in NE Germany. The observed succession of sediments was reconstructed, described and interpreted (cf. Fig 2, paper no. 3) with regard to the palaeoenvironment and its processes, especially during dropstone deposition.

4 RESULTS

In line with the objectives of this doctoral dissertation, listed in the first part of the summary, the work resulted in **two new numerical models related to the formation of deformation structures in Pleistocene glacigenic sediments**.

The constructed model, concerning the **formation of deformation structures caused by seismic activity**, is the first numerical description of the formation of SSDS in seismites. However, it is not so much a complete model as an indication of possible solutions to problems arising in simulations relating to the conditions of seismic formation. It offers significant potential for further development and provides an insight into the mechanisms responsible for the geometry and spatial distribution of seismically-induced deformation structures. Despite its significant simplifications, and the many assumptions and limitations of the model, its application can be used to determine the influence of the tested parameters, such as the vertical velocity of the S wave and sediment porosity, on the SSDS formed under the influence of seismic activity. The model was also checked by comparing the obtained simulation results with the field observations of SSDS occurring in seismitees. The goal of the first doctoral work, which was to create a new numerical model, has been achieved. More detailed results regarding the predictive potential of the model and its applications are described in **paper no. 1**. The conclusions drawn from the model are presented in the next part of this summary.

The model created to represent the **formation of deformation structures related to the deposition of dropstones** provides a full description of the grain falling process in the water column and the bottom sediment "response" to a pressure caused by grain impact, thus it fulfils the second goal of this dissertation. As mentioned in the Methods, this model, like any numerical description, has its assumptions and limitations. One important limitation is that, due to the physical characteristics of the phenomenon of grains falling in a dense medium, the reconstruction of water depth can only be used for shallow water reservoirs. This is due to the assumptions of the model: it does not take into account bottom currents, which can significantly affect dropstone deposition, nor doe it account for the depth limit, below which the grains lose all their velocity and fall freely (thus "losing" information about the distance travelled). The created model has predictive potential, as described in more detail in paper no. 2. It also allows conclusions to be drawn about the nature of the SSDS associated with dropstone deposition and, in some cases, the depth of the water body. The numerical simulations were found to be accurate and reliable, despite its simplifications and

assumptions, as confirmed by comparison with field observations (**paper no. 3**).

5 CONCLUSIONS

The created numerical models can be easily related to the observed deformation structures, allowing conclusions to be drawn about the processes of their formation.

Conclusions from the simulation and numerical model of SSDS formation related to seismic activity:

1. By simplifying the model, i.e. by only using the vertical component of the S wave, an artifactual SSDS was obtained that was very similar to those observed in field seismites. Hence, it can be assumed that the S wave, and more specifically the downward pressure it causes, is the main force responsible for the generation of SSDS associated with seismic activity.

2. The simulations indicated a strong relationship between the porosity of the sediment and the geometry and size of the SSDS. Increased sediment porosity is positively associated with larger SSDS and a their more random distribution.

3. The model indicates that the velocity of the S waves (in the range of 1.6-2.6 kms^{-1}) has a smaller impact on the differentiation of the geometry of the generated SSDS than the material properties of the sediment. The velocity nevertheless has a significant influence on the depth of the occurrence of SSDS. Assuming that the velocity of propagation of seismic waves generated by an earthquake decreases with distance from the epicentre, this result can be used to reconstruct the direction of wave propagation.

4. Due to the strong relationship between the depth of the seismic occurrence and the vertical velocity of the S-type seismic wave, their observed spatial position may be related to the maxima and minima of propagating waves. This conclusion requires further investigation.

5. The obtained results are consistent with the field observations and studies of deformation structures caused by seismic activity to date.

Conclusions from the numerical model describing the process of formation of deformation structures related to the deposition of dropstones on the bottom sediments:

1. The properties of the sediments in which the dropstones are deposited appear to have the greatest impact on the deformation structures formed during dropstone deposition. Before attempting to reconstruct the water depth in a palaeolithic lakes, it is first necessary to determine the function corresponding to the influence of sediments on the depth of dropstone embedding (cf. Fig. 4, paper no. 2). This function can be determined by measuring the burial of at least three dropstones.

2. After entering a water body, grains first decelerate and then fall freely below a certain depth. This depth depends on the grain diameter, with smaller grains reaching a terminal velocity at a shallower depth. The existence of this boundary results directly from the Newtonian dynamics and means that the depth can only be reconstructed for shallow reservoirs.

3. The "traces" left by dropstones in the sediment of the bottom strongly depend on their diameter, and this dependence results not only from their mass, but and falling speed, which is greater for large dropstones. Observation of SSDS formed in the sediments of the bottom of water reservoirs after dropstone deposition, can be used to reconstruct their deposition scenarios.

References and bibliography

Allen, J.R.L., 1982. Sedimentary structures: their character and physical basis. Developments in Sedimentology, 30B.

Ambraseys, N., 1988. Engineering seismology. Earthquake Engineering and Structural Dynamics 17, 1-105.

Amsden, A., Ruppel, H., Hirt, C., 1980. SALE: A simplified ALE computer program for fluid flow at all speeds. Los Almos National Laboratories Report, LA-8095.

Andrus, R.D., Stoke K.H., 1997. Liquefaction resistance based on shear wave velocity. National Center for Earthquake Engineering Research (Salt Lake City) Report, 0022.

Anketell J.M., Cegła J., Dżułyński S., 1970. On the deformational structures in systems with reversed density gradients. Rocznik Polskiego Towarzystwa Geologicznego 40, 3-30.

Boulanger, R., Ziotopoulou, K., 2017. PM4 sand version 3.1: a sand plasticity model for earthquake engineering applications. Report UC Davis Center for Geotechnical Modeling Report, UCD/CGM-17/01.

Brodzikowski, K., Van Loon, A.J., 1991. Glacigenic Sediments: Amsterdam, Elsevier, Developments in Sedimentology 49, 664 p.

Bronikowska, M., Artemieva, N. A., Wünnemann, K., 2017. Reconstruction of the Morasko meteoroid impact – Insight from numerical modeling. Meteoritics & Planetary Science 1-18.

Campbell, C.S., 2003. Liquefaction and Fluidization. In: Middleton, G.V. (Ed.), Encyclopedia of sediments and sedimentary rocks. Kluwer Academic Publishers, Dordrecht, 412–413.

Collins, G.S., Melosh, H.J., Ivanov, B.A., 2004. Modeling damage and deformation in impact simulations. Meteoritics & Planetary Science 39, 217-231.

Davison, T.M., Collins, G.S., Elbeshausen, D., Wünnemann, K., Kearley, A., 2011. Numerical modeling of oblique hypervelocity impacts on strong ductile targets. Meteoritics & Planetary Science 46, 1510-1524.

Dowdeswell, J.A., Whittington, R.J., Jennings, A.E., Andrews, J.T., Mackensen, A., Marienfeld, P., 2000. An origin for laminated glacimarine sediments through sea-ice build-up and suppressed iceberg rafting: Sedimentology 47, 557-576.

Dżułyński, S., 1996. Erosional and deformational structures in single sedimentary beds: A genetic commentary. Rocznik Polskiego Towarzystwa Geologicznego 66, 101-189.

Dżułyński, S., Radomski, A., 1966. Experiments on bedding disturbances produced by the impact of heavy

suspensions upon horizontal sedimentary layers. Bulletin de l 'Academie Polonaise des Sciences, Serie des Sciences Geologiques et Geographiques 14, 227-230.
Fichman, M.E., Crespi, J.M., Getty, P.R., Bush, A.M., 2015. Retrodeformation of Carboniferous trace fossils from the Narragansett Basin, U.S.A., using raindrop imprints and bedding-cleavage intersection lineation as strain markers. Palaios 30, 574-588.
Galli, P., 2000. New empirical relationships between magnitude and distance for liquefaction. Tectonophysics 324, 169-187.
Gilbert, R., 1990. Rafting in glacimarine environments: Geological Society of London Special Publication 53, 105-120.
Gradziński R., Kostecka A., Radomski A., Unrug R., 1986. Zarys sedymentologii. Wydawnictwo Geologiczne, Warszawa.
Haarland, W.B., Herod, K.N., Krinsley, D.H., 1966. The definition and identification of tills and tillites. Earth-Science Reviews 2, 225-256.
Hoffmann, P.F., Schrag, D.P., 2000. Snowball Earth. Scientific American 282, 68-75.
Hoffmann, G., Reicherter, K., 2012. Soft-sediment deformation of Late Pleistocene sediments along the south west ern coast of the Baltic Sea (NE Germany). International Journal of Earth Sciences 101, 351-363
Jeffeeris, M., Been, K., 2015. Soil Liquefaction – a Critical State Approach. CRC Press.
Le Heron, D.P., 2015. The significance of ice-rafted debris in Sturtian glacial successions. Sedimentary Geology 322, 19-33.
Li, C., Liu, J., Sun, Y., 2020. Optimal third-order sympletic integration modeling of seismic acoustic wave propagation. Bulletin of the Seismological Society of America 110, 754-762.
Liszkowski J., 1975. Geologiczne modele rozwoju filtracyjnych deformacji gruntów w Polsce. Materiały Konferencyjne: Aktualne problemy geologii inżynierskiej IAEG, Warszawa, 133-151.
Livingstone, S.J., Piotrowski, J.A., Bateman, M.D., Ely, J.C., 2015. Discriminating between subglacial and proglacial lake sediments: an example from the Danischer Wohld Peninsula, northern Germany. Quaternary Science Reviews 112, 86-108.
Matsumoto, D.H., Naruse, S., Fujino, A., Surphawajruksakul, T., Jarupongsakul, N., Sakakura, M., Murayama, M., 2008. Truncated flame structures within a deposit of the Indian Ocean tsunami: Evidence of synsedimentary deformation, Sedimentology, 55, 1559–1570.
Menzies, J., 2002. Modern and Past Glacial Environments: Elsevier, 576 p.
Moretti, M., 2000. Soft-sediment deformation structures interpreted as seismites in middle-late Pleistocene aeolian deposits (Apulian foreland, southern Italy). Sedimentary Geology 135, 167-179.
Odonne, F., Callot, P., Debroas, E.-J., Sempere, T. Hoareau, G., Maillard, A., 2011. Soft-sediment deformation from submarine sliding: Favourable conditions and triggering mechanisms in examples from the Eocene Sobrarbe delta (Ainsa, Spanish Pyrenees) and the mid-Cretaceous Ayabacas Formation (Andes of Peru). Sedimentary Geology 235, 234-248.
Owen, G., Moretti, M., 2011. Identifying triggers for liquefaction-induced soft-sediment deformation in sands. Sedimentary Geology 235, 141-147.
Peng, P., Wang, L., 2019. 3DMRT: a computer package for 3D model-based seismic wave propagation. Seismological Research Letters 90, 2039-2045.
Pierazzo, E., Artemieva, N., Asphaug, N., Baldwin, E., Cazamias, E.C., Coker, R., Collins, G.S., Crawford, D.A., Davison, T., Elbeshauen, D., Holsapple, K.A., Housen, K.R., Korycansky, D.G., Wünnemann, K., 2008. Validation of numerical codes for impact and explosion cratering: Impacts on strengthless and metal targets. Meteoritics & Planetary Science 43, 1917-1938.
Pisarska-Jamroży, M., Belzyt, S., Bitinas, A., Jusienå, A., Woronko, B., 2019. Seismic shocks, periglacial conditions and glacitectonics as causes of the deformation of a Pleistocene meandering river succession in central Lithuania. Baltica 32, 63-77.
Pisarska-Jamroży, M., Belzyt, S., Börner, A., Hoffmann, G., Hüneke, H., Kenzler, M., Obst, K., Rother, H., Van Loon, A.J., 2018. Evidence from seismites for glacioisostatically induced crustal faulting in front of an advancing land-ice mass Rügen Island, SW Baltic Sea). Tectonophysics 745, 338-348.
Rahman, M., Asce, M., Nguyen, H.B.K., Fourie, A.B., Kuhn, M.R., 2020. Critical state soil mechanics for cyclic liquefaction and postliquefaction behaviour: DEM study. Journal of Geotechnical and Geoenvironmental Engineering 147, 04020166.
Rahman, M., Lo, S., 2014. Undrained behaviour of sand-fines mixtures and their state parameters. Journal of Geotechnical and Geoenvironmental Engineering 140, 04014036.
Rossetti, D.F., 1999. Soft-sediment deformation structures in late Albian to Cenomanian deposits, Sao Luis Basin, northern Brasil: evidence for palaeoseismicity. Sedimentology 46, 1065-1081.
Seed, H.B., Idris, I.M., 1971. Simplified procedure for evaluating soil liquefaction potential. Journal of Soil Mechanics and Foundations Division 97, 1249-1273.
Seilacher, A., 1969. Fault-graded beds interpreted as seismites. Sedimentology 13, 15-159.

Shampine, L.F., Watts, H.A., 1976. Practical solution of ordinary differential equations by Runge-Kutta methods. [Writing a high-quality code; description of RKF45, in FORTRAN for CDC 6600 computer]. United States: N. p., 1976. Web.

Shanmugam, G., 2016. The seismite problem. Journal of Palaeogeography 5, 318-362.

Thomas, G.S., Connell, R.J., 1985. Iceberg drop, dump, and grounding structures from Pleistocene glaciolacustrine sediments. Journal of Sedimentary Petrology 55, 243-249.

Vaid, Y.P., Thomas, J., 1995. Liquefaction and postliquefaction behavior of sand. Journal of Geotechnical Engineering 121, 1321-1337.

Van Loon, A.J., Pisarska-Jamroży, M., 2014. Sedimentological evidence of Pleistocene earthquakes in NW Poland induced by glacioisostatic rebound. Sedimentary Geology 300, 1-10.

Van Loon, A.J., Pisarska-Jamroży, M., Woronko, B., 2020. Sedimentological distinction in glacigenic sediments between load casts induced by periglacial processes from those induced by seismic shocks. Geological Quarterly 64, 626-640.

Van Loon, A.J., Soms, J., Nartiss, M., Krievans, M., Pisarska-Jamroży, M., 2019. Sedimentological traces of ice-raft grounding in a Weichselian glacial lake near Dukuli (NE Latvia). Baltica 32, 170-181.

Wünnemann, K., Colling, G.S., Melosh, H., 2006. A strain-based porosity model for use in hydrocode simulations of impacts and implications for transient crater growth in porous target. Icarus 180, 514-527.

Youd, T.L., Idriss, I.M., 2001. Liquefaction resistance of soil: summary report from the 1996 NCEER and 1998 NCEER/NFS work - shop on evaluation of liquefaction resistance of soil. Journal of Geotechnical and Geoenvironmental Engineering 127, 1275-1285.

Declaration of authors

Paper 1:

Bronikowska, M., Pisarska-Jamrożу, M., Van Loon, A.J. 2021. First attempt to model numerically seismically-induced soft-sediment deformation structures – a comparison with field examples. *Geological Quarterly* 65, 60.

I hereby declare that the contribution of Ms. Małgorzata Bronikowska can be estimated as **85%**. Ms. Małgorzata Bronikowska substantially contributed to the conception and design of the paper, prepared the draft and the final version of the manuscript (together with MPJ and TVL), and led the revision.

Names of Author(s)	Signature(s)	Date
Małgorzata Bronikowska		01.02.2022
Małgorzata Pisarska-Jamrożу		02.02.2022
A.J. (Tom) van Loon		02.02.2022

Declaration of authors

Paper 2:

Bronikowska, M., Pisarska-Jamroży, M., Van Loon, A.J., 2021. Dropstones deposition – results of numerical modelling of deformation structures, and implications for the reconstruction of the water depth in shallow lacustrine and marine successions. *Journal of Sedimentary Research* 91, 507-519.

I hereby declare that the contribution of Ms. Małgorzata Bronikowska can be estimated as **85%**. Ms. Małgorzata Bronikowska substantially contributed to the conception and design of the paper, prepared the draft and the final version of the manuscript (together with MPJ and TVL), and led the revision.

Names of Author(s)	Signature(s)	Date
Małgorzata Bronikowska		01.02.2022
Małgorzata Pisarska-Jamroży		02.02.2022
A.J. (Tom) van Loon		02.02.2022

Declaration of authors

Paper 3:

Pisarska-Jamroży, M., Van Loon, A.J., **Bronikowska, M.**, 2018. Dumpstones and dropstones as records of overturning ice rafts in a Weichselian proglacial lake (Rügen Island, NE Germany). *Geological Quarterly* 62, 917-924.

I hereby declare that the contribution of Ms. Małgorzata Bronikowska can be estimated as **20%**. Ms. Małgorzata Bronikowska participated in field work (site description and documentation, collection of samples; with co-authors), interpreted results, and participated in the interpretation and discussion of all results.

Names of Author(s)	Signature(s)	Date
Małgorzata Bronikowska		01.02.2022
Małgorzata Pisarska-Jamroży		02.02.2022
A.J. (Tom) van Loon		02.02.2022

Artykuł nr 1
Paper no. 1

Bronikowska, M., Pisarska-Jamroży, M., Van Loon, A.J.

First attempt to model numerically seismically-induced soft-sediment deformation structures – a comparison with field examples

Geological Quarterly 65, 60.

Geological Quarterly, 2021, 65: 60
DOI: http://dx.doi.org/10.7306/gq.1629

First attempt to model numerically seismically-induced soft-sediment deformation structures – a comparison with field examples

Małgorzata BRONIKOWSKA[1, *], Małgorzata PISARSKA-JAMROŻY[1] and A.J. (Tom) VAN LOON[2]

[1] Adam Mickiewicz University, Geological Institute, B. Krygowskiego 12, 61-680 Poznań, Poland

[2] Shandong University of Science and Technology, College of Earth Science and Engineering, Qingdao, China

Bronikowska, M., Małgorzata Pisarska-Jamroży, M., Van Loon, A.J. (Tom) 2021. First attempt to model numerically seismically-induced soft-sediment deformation structures – a comparison with field examples. Geological Quarterly, 2021, 65: 60, doi: 10.7306/gq.1629

No numerical model has thus far addressed seismites, even though seismites are frequently used for the reconstruction of seismic events in the geological past. This is the more remarkable since the boundary conditions which have to be fulfilled for the development of seismites have also been estimated only empirically. The present contribution is a first attempt to model numerically the soft-sediment deformation structures caused by the passage of S-waves through near-surface sedimentary layers. The simulations are based on the so-called pressure tube model and the iSALE2D program. We modelled a seismic S-wave with six different vertical velocities, ranging from 1.6 to 2.6 m · s^{-1}, passing through sediments with different densities and porosities in a sedimentary succession from the surface down to a depth of 10 m. The modelled soft-sediment deformation structures (load casts, flame structures, injection structures and sedimentary volcanoes) show similar geometries and sizes as those known from laboratory experiments and field studies. The geometry, size and type of these structures depend on the sediment properties and on the initial pressure used as a trigger mechanism, rather than on S-wave velocity. In contrast, the depth of the seismites appears to depend strongly on the S-wave velocity.

Key words: numerical modelling, seismic waves, wave propagation, seismites, soft-sediment deformation structures, load casts, injection structures.

INTRODUCTION

Seismically-induced soft-sediment deformation structures (SSDS) are caused by S-waves travelling through unconsolidated sediments (Rossetti, 1999) and are linked with liquefaction and fluidization processes. The SSDS can originate in water-saturated, unconsolidated sediments if an earthquake has a sufficiently large magnitude to trigger liquefaction (M ≥4.5; Marco and Agnon, 1995; M ≥5.0: Atkinson et al., 1984; Rodríguez-Pascua et al., 2000). Liquefaction reduces the shear strength of the water-saturated sediments, resulting in changing intergranular contacts (Allen, 1982; Obermeier, 1996; Vanneste et al., 1999; Owen and Moretti, 2011), and in plastic behaviour of the sedimentary mass (Van Loon et al., 2020). Liquefaction is restricted to depths of <10 m below the sedimentary surface, commonly <2 m or even a few decimetres.

The passage of a seismic shock wave through a sufficiently susceptible sedimentary layer causes soft-sediment deformation structures (SSDS) throughout the layer as far as the S-wave has not lost too much energy. The deformed layer is called a "seismite" (Seilacher, 1969). Seismites have commonly a lateral extent up to 40 km from the epicentre (Galli, 2000), though this distance depends on the properties of the affected sediments and of the magnitude of the triggering earthquake. It is widely accepted that seismites can be easily formed in almost cohesion-less sands with a relatively high silt content (e.g., Moretti et al., 1999), for instance in lacustrine, marine, and fine-grained fluvial sediments (Alfaro et al., 1997; Hoffmann and Reicherter, 2012; Van Loon and Pisarska-Jamroży, 2014; Pisarska-Jamroży et al., 2018, 2019a, b).

A problem with the recognition of seismites is that strongly deformed layers intercalated between non-deformed layers can also have another origin (e.g., slumping). Among the various criteria that have been proposed for the recognition of seismites (Obermeier et al., 1990; Obermeier, 1996, 2009; Rossetti, 1999; Wheeler, 2002; Hilbert-Wolf et al., 2009; Owen and Moretti, 2011; Van Loon et al., 2016, 2020; Pisarska-Jamroży and Woźniak, 2019), the most commonly adhered to nowadays (Van Loon et al., 2016) is the presence of a combination of at least several of the following characteristics:

- alternating deformed and undeformed layers;
- lateral continuity of SSDS within the deformed layers;
- a wide variety of chaotically-distributed SSDS within the deformed layers;
- the lack of indications for other deformational mechanisms;
- a morphology of the SSDS that is consistent with those in undisputed seismites and in experimentally produced "seismites";

* Corresponding author, e-mail: malgorzata.bronikowska@amu.edu.pl

Received: August 19, 2021; accepted: November 22, 2021; first published online: December 30, 2021

– a clear spatial association with features that may cause seismic S-waves (e.g., faults or active volcanoes).

Among the wide variety of SSDS within seismites, examples representing plastic and brittle behaviour (commonly accompanied by structures indicating fluidisation) occur that developed during the same deformational event (Rossetti et al., 2011; Pisarska-Jamroży and Woźniak, 2019). The presence of fluidised features (escape structures, clastic dykes, sand or silt volcanoes, pillar and vein structures, dish structures) indicates overpressure in the sediment (Doughty et al., 2014). Brittle deformations such as broken-up layers result from a sudden increase of the pore-water pressure. The development of structures indicating loading in a plastic state such as load casts, pseudonodules and flame structures reflects instable density gradients within the sediment, but loading also requires liquefaction and/or fluidisation of the underlying layer (Moretti and Ronchi, 2011; Belzyt et al., 2021).

The main objective of the present contribution is to present a relatively simple method for the numerical modelling of seismites, which model is validated by comparison with field observations. The results can increase the insight into the reconstruction of the sediment properties and earthquake characteristics.

METHODS

The present contribution presents a numerical model that helps understand the genesis of seismites. Each numerical model has some limitations; those of our model are detailed in Section: *Methodical approach – limitations* before the description of the model (Section: *A new approach – model description*) in order to make the various chosen steps understandable. Subsequently, the setup of the simulations is detailed (Section: *Setup of the simulations*).

METHODICAL APPROACH – LIMITATIONS

Numerical modelling of the origination of seismites poses a significant technical challenge for several reasons. First, all field observations suggest their occurrence at some distance from the epicentre of an earthquake (Galli, 2000), but the epicentre can, as a rule, not easily be located in the case of ancient seismites. Moreover, the S-wave velocity and the specific sediment properties at the time of the formation of an ancient seismite are not known, which largely increases the number and size of possible numerical errors. In addition, almost all widely used numerical models are based on the wave equation for a non-disturbed medium, due to some mathematically impossible calculations of wave motion in a disturbed sediment (e.g., Meada et al., 2017; Peng and Wang, 2019; Li et al., 2020), while those which address the irregularities in media (Jefeeris and Been, 2015; Boulanger and Ziotopoulou, 2017) do not include the development of SSDS in the final result, because of the enormous complexity of such numerical solutions. The main focus of such studies addresses the S-wave front velocity, neglecting the effect of the interaction of the seismic wave with the sediment below. Such models can well predict the effects of an earthquake, but they are useless for seismite modelling.

Another obvious problem in the numerical modelling of seismically-induced SSDS is the change in size and complexity of these deformations with increasing distance from the epicentre. Actual or experimentally produced SSDS tend to be relatively small (commonly millimetres to several decimetres: e.g., Owen, 1996; Moretti et al., 1999; Moretti and Sabato, 2007), partly because they are mostly located several kilometres away from the related earthquake epicentre (see Galli, 2000). Consequently, the resolution of modelled seismites has to be very high, which is not feasible at such a large distance. The computational cost of a model with a sufficiently high resolution would certainly be unreasonably high, while the numerical error would still be too large. The only solution for this problem is using a model that deals with a limited areal extent of the sediment, with initial conditions that can be computed with programs addressing the propagation of the seismic wave, and that are specific for a given distance from the epicentre.

Last but not least, the key processes and main agents during seismite formation are liquefaction and fluidisation of the sediment. Liquefaction occurs when the sediment strength is significantly reduced by the shear stress induced by a seismic wave. The cohesionless sediment gains mobility, and in consequence starts to move in the direction of least resistance. Such a movement causes an upward pressure, which sets the sediment in motion (Seed and Idriss, 1971). However, many issues related to liquefaction, such as the water content and the properties of the sediment during deformation are still unknown. Fluidisation can severely damage buildings and even result in collapse. Therefore, it is not surprising that the main focus in liquefaction/fluidisation research thus far was on sand behaviour during and immediately after these processes, rather than on the influence of this mechanism on the formation of SSDS (e.g., Vaid and Thomas, 1995; Andrus and Stokoe, 1997; Youd and Idriss 2001; Rahman and Lo, 2014; Rahman et al., 2020).

Although empirical functions and numerical modelling addressing the sediment liquefaction potential are very accurate and validated against abundant field and experimental data, numerous cases are known which are inconsistent with the above empirical laws. An accurate description of the liquefaction mechanism is, however, beyond the scope of the present contribution, and the above considerations are therefore meant only to inform the reader that the lack of exact theoretical models of this process should be taken into account where the possibilities of seismite modelling are discussed.

A NEW APPROACH – MODEL DESCRIPTION

Accurate seismite modelling requires a new approach avoiding all difficulties mentioned above. Our new model does so: it focuses primarily on the seismites themselves, while the sediment properties, the S-wave velocity and the shear stress required for sediment motion are assumed to be known. The model setup is designated to meet the liquefaction criteria so that the liquefaction process can be addressed, while the simulated sediments are chosen in such a way that they have the properties that best fit liquefaction. Because a high resolution is required, we simulate the passage of the vertical velocity component of the S-wave through a narrow (0.6 m) section of sediment (called “tube” in the following) from the surface down to a depth of 10 m. Such a setting of the model pretends that the simulated seismites develop where the vertical wave velocity is much higher than the horizontal one, which is assumed in our model to be negligible. These assumptions are easily validated because seismically-induced SSDS form due to shear stresses related to a vertical pressure (Seed and Idriss, 1971). The imaginary sediments used for the simulations have a strength that equals the strength of water-saturated sand, with a water content of 25%, and porosities of 15, 20, and 25%; further details are provided in Section: *Setup of the simulations*.

The simulations are conducted using the iSALE2D shock physics hydrocode (Wünnemann et al., 2006), which was origi-

nally designated to study an impact-related phenomenon (see Section: Setup of the simulations). The ISALE2D code allows simulating a water-saturated medium only by adding water to the analytical equation of state (ANEOS) table, which excludes any changes during the program run. In other words, the water content in the sediments remains constant during the entire simulation procedure, and is fixed in the computational material matrix.

This disadvantage of the model is not exceptional: a situation during which all water is expelled from the water-saturated sediment must be very rare: no seismites are known that show clear evidence of such a process. Moreover, it is the water content that significantly influences the strength of sediment. This holds for both actual and simulated seismites, which implies that this highly important aspect is addressed by our model in an adequate way.

It is worth noticing that the artificial numerical sediments that we use for our simulations are not only uniform, but are also assumed to give an ideal response of the sediment to the vertical pressure related to the S-wave velocity. Actual sediments often contain a discrete lamination, or other forms of discontinuity and density differences, which make them far less predictable. Consequently, naturally formed SSDS may differ from the modelled ones. This limitation, which is inherent to every numerical model, does not really influence the results presented here. The energy of the S-wave velocity is so high that the influence of discrete discontinuities in the medium on the final shape and size of the SSDS can be neglected. During the very short time interval, during which the S-wave with its typical velocity erases most of the discrete density differences, the vertical energy (and pressure) can be considered as constantly very high. In consequence, the wave does not "react" to discrete laminations or other irregularities while it passes a narrow sediment section (the tube).

SETUP OF THE SIMULATIONS

All simulations have been conducted using the iSALE2D code, which is based on a hydrocode solution algorithm (Amsden et al., 1980). It was originally developed for studies on hypervelocity impact cratering (Collins et al., 2004; Wünneman et al., 2006), but it can be applied to our study because it includes an elasto-plastic constitutive model, fragmentation models, various equations of state, a strength model and a porosity-compaction model. It has been benchmarked against other hydrocodes (Pierazzo et al., 2008) and validated against experimental data (Pierazzo et al., 2008; Davison et al., 2011; Miljković et al., 2012).

As the material (= sediment) for our simulations, we used an imaginary wet sand described by an analytical equation of state (ANEOS) as a mixture of quartz sand (75%) and water (25%) (yellowish in Figs. 1 and 2) and dry sand (brownish in Figs. 1 and 2) described by ANEOS as quartz. It is worth noticing that this choice of materials and their sedimentary succession was made mainly to address the density and small strength differences of successive layers, which are crucial for liquefaction. The simulated dry sand has a lower density and higher strength, which allows the passing S-wave to disperse during the contact with the less dense wet layer (see Fig. 3).

Two layers of sediment with the same physical properties cannot visibly interact with each other: only the discontinuity at the contact zone between two different layers can cause wave dispersion and, in consequence, the development of deformation structures. Numerous trial simulations have confirmed that the differences in the response of these two materials to high pressure caused by a propagating shock wave are insignificant. However, differences in densities and strength between successive layers must be addressed in the model setup in order to develop seismites.

In our simulation, an S-wave passes a sedimentary column (the 10-m deep tube) with an initial setup reflecting an ideal succession of alternating wet and dry sands. The porosity and density of the sediment are constant and do not vary with depth. This can be considered as valid for depths to some 12 m. The shear strength and other parameters influencing the response of the sediment to high pressure changes for wet/dry sand vary with depth due to the overburden weight. These changes are, however, very small and can be considered as negligible.

The reaction of both the wet and dry sands to a high pressure is described by a strength model that has proven accurate for unconsolidated sediments and that is widely used in studies and laboratory impact experiments (Wünneman et al., 2006). The mixture of water and quartz sand grains, as well as dry sand contains randomly distributed pores which are assumed to constitute 15, 20 and 25% by volume, respectively (see Figs. 1 and 2). These pores become reduced in size during the passage of an S-wave (due to resulting compaction) but the pores (and consequently also the reduction in their sizes) are too small to be visible in Figures 1 and 2.

The resolution of each simulation is 3 cm, while the high-resolution grid consists of 200 horizontal and 4000 vertical cells. The combined grid of high-resolution cells forms a 10 m high and 0.6 m wide sedimentary succession (the above-mentioned "tube", which is connected with a vertical plane ending above the surface and which is used as the trigger mechanism for the pressure related to the vertical component of the S-wave velocity: see Fig. 1). This vertical plane has, in the various simulations, an initial velocity of 1.6, 1.8, 2.0, 2.2, 2.4 and 2.6 $m \cdot s^{-1}$, which corresponds to the surface acceleration commonly determined for modern earthquakes. The simulation run begins when the sediment above the surface starts to move with the given velocity, starting a shock wave which travels down through the sediment tube.

In our model, the main focus is on developing SSDS. Therefore we simulate only a very narrow (0.6 m) section (the "tube") in which the S-wave interacts with the sediment.

RESULTS

A higher S-wave velocity (the modelled velocities range from 1.6 to 2.6 $m \cdot s^{-1}$) is found to cause more compaction of the modelled sedimentary succession (black in Fig. 1). The compaction related to the propagation of the S-waves depends on the type of sediment but not on the S-wave velocity. In dry sands (yellowish in Fig. 1), compaction is almost constant (~10%); it is neither related to the S-wave velocity nor to the initial porosity (i.e., 15, 20 or 25%). Compaction in the water-saturated sands (brownish in Fig. 1) after the passage of the shock wave reaches 40%; it is not related to the S-wave velocity but increases (from 33 to 45%) with an increase of porosity from 15 to 25%. No clear relationship has been found between the compaction and the depth of the sand.

It is worth noticing that all used simulations end when the S-wave reaches a depth of 10 m, so as to avoid numerical errors related to wave reflection. During actual seismic events, when an S-wave travels through a porous medium, the pores become pressed or even disappear, and the sediments become compacted by the stress related to the shock-induced pressure. Almost immediately afterwards, however, the sediment undergoes relaxation, rising again after the short phase of compaction, due to its plasticity. In the simulations presented

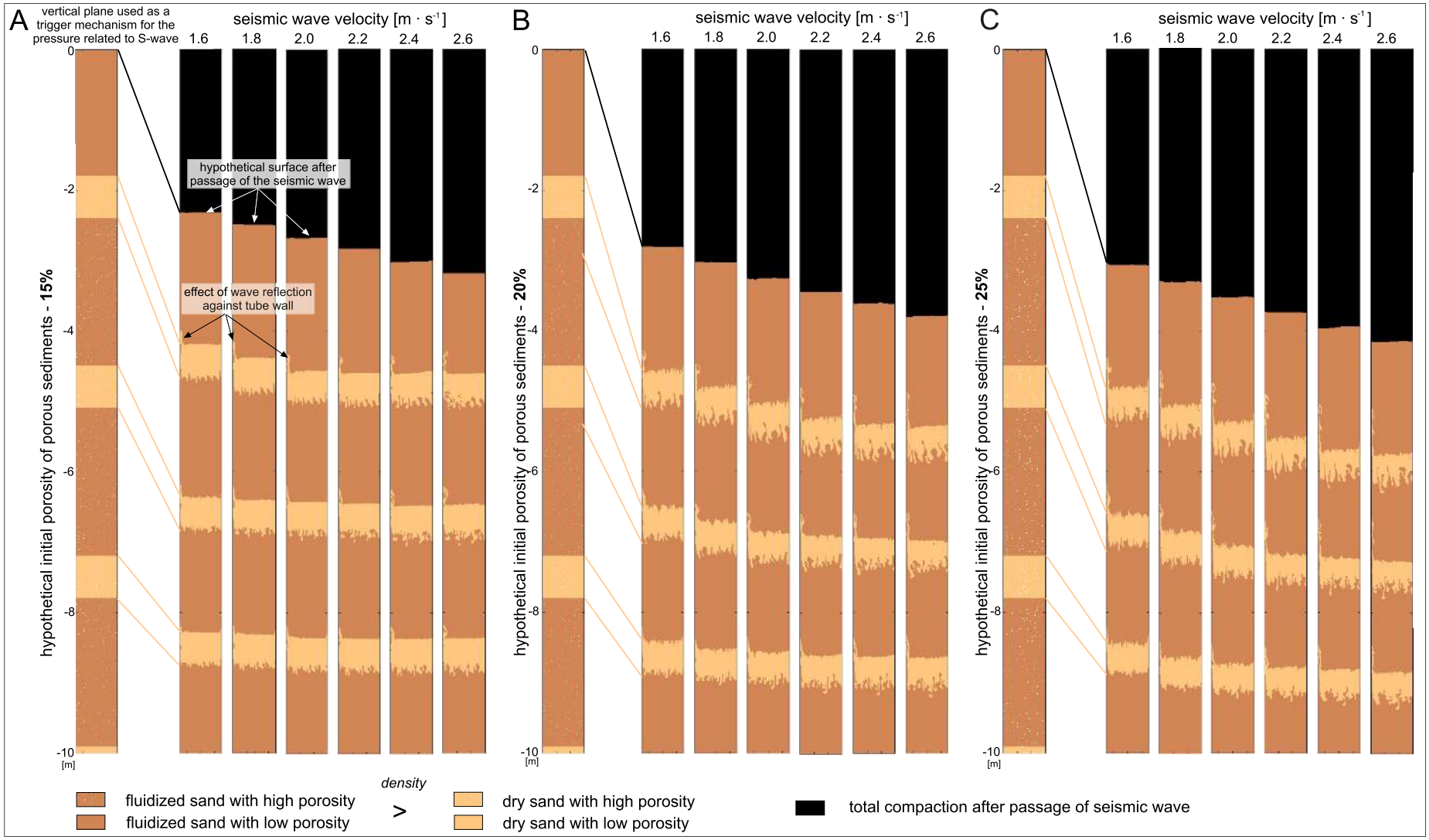

Fig. 1. Hypothetical sedimentary succession in a tube of 10 m deep and 0.6 m wide, with sediments of different porosities (A – 15%, B – 20%, C – 25%)

The model indicates that the passage of an S-wave results in compaction and the development of soft-sediment deformation structures (SSDS); the total compaction depends mainly on the velocity of the S-wave, whereas the size of the SSDS depends mainly on the original porosity of the sediment; note that the imaginary wall of the tube causes reflections of the S-wave, which results in the model in small disturbations close to this wall, which will not occur under actual conditions

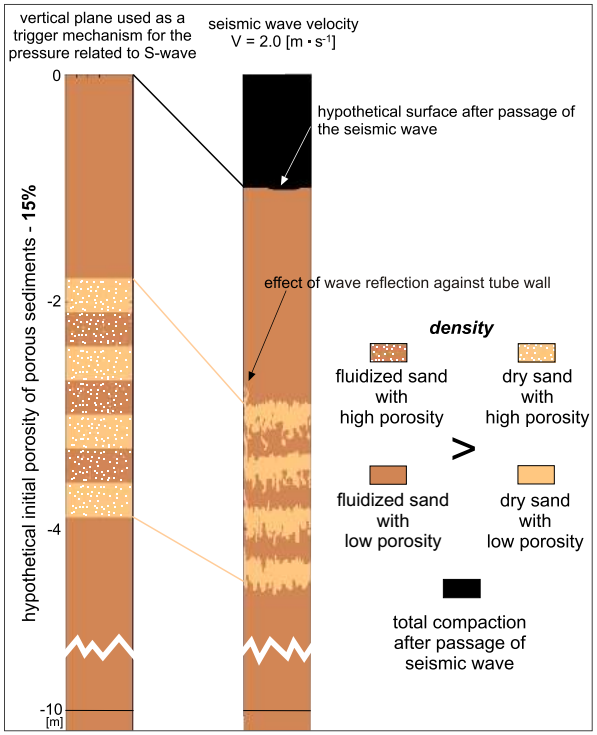

Fig. 2. Simulation of the upper part of a hypothetical sedimentary succession of 10 m thick, consisting of stratified sands with a porosity of 15%, affected by an S-wave that passed with a velocity of 2 m · s^{-1}

Compaction occurred and SSDS developed; similar simulations were carried out for all initial porosities of the sediment and for all wave velocities indicated in Figure 1

here, this relaxation does not occur: the setup does not allow relaxation of the sediments after they have been exposed to the high vertical pressure, which definitely overestimates the compaction values found. Although the relationship between the wave velocity, sediment properties and compaction values are valid, the compaction values presented here should be considered as the maximum ones that may be reached. Also the deformed surface in Figure 2 should be interpreted with caution. The upper surface of the sediment is in our simulations located in the area of the computational grid, where the numerical errors are highest. It is probably true that some of the features located there result from interaction of the S-wave with the empty computational cells; this cannot be considered as a proper physical situation.

The size and shape of seismically-induced SSDS hardly depend on the S-wave velocity. On the other hand, the depth at which SSDS originate depends strongly on it: this depth increases with increasing S-wave velocity, which is particularly clear for relatively porous sands (compare the SSDS in Fig. 1 between sub-figures A, B and C). It appears also that the SSDS in seismites at comparable depths are more complex and more chaotically distributed in more porous sands than in less porous sands (Fig. 1). The reason is that a higher wave velocity causes more mobilization of the particles in liquefied sands (brownish in Fig. 1) and that, consequently, the developing SSDS move farther downwards. This finding is of great importance because it allows the reconstruction of the propagation direction of the seismic S-wave: a distinct downward shift of the SSDS in a lateral direction always roughly indicates the resultant of the maxima of the wave energy (which can be expressed in terms of velocity), whereas an upward shift indicates the minima of the wave energy (Figs. 1 and 2).

The size of the SSDS depends only slightly on the S-wave velocity in sands with a low (15%) porosity, although the sands

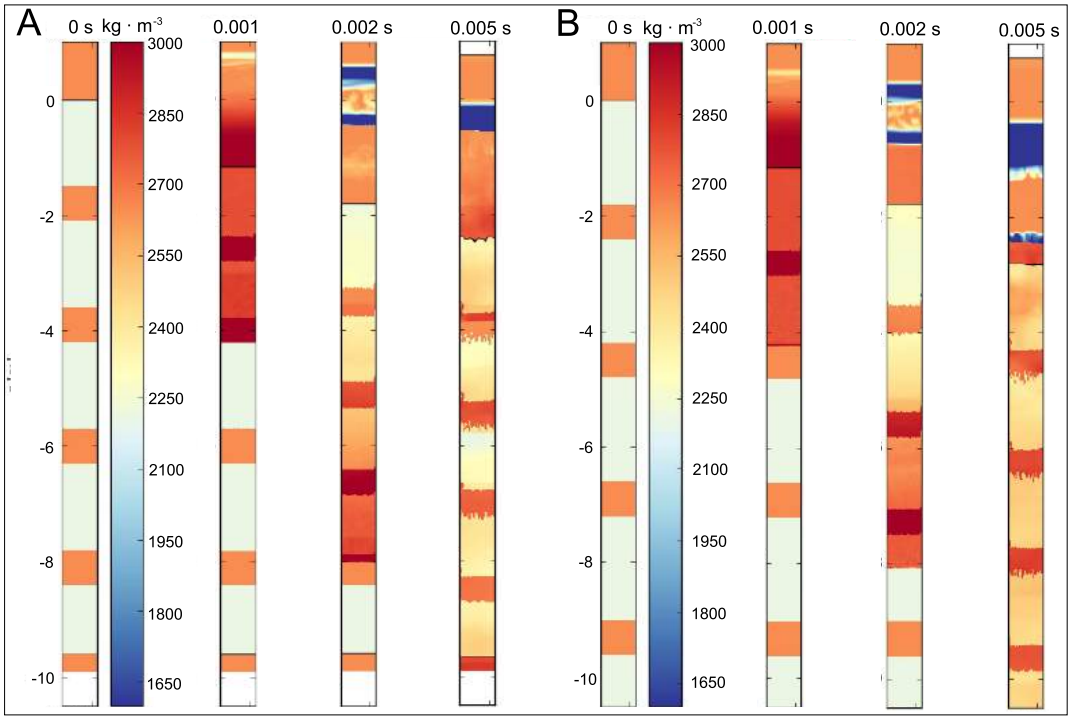

Fig. 3. Simulation of the effect of a passing S-wave with a velocity of 2 m · s^{-1} on two sedimentary successions with different initial vertical density distributions (A and B) before passage (first tube) and after 0.1, 0.2, and 0.5 s

that are least susceptible to compaction develop larger and more pronounced SSDS with increasing S-wave velocity. This is probably because a low porosity results in a less diminishing pressure. When an S-wave travels through the sands, it loses energy each time that it passes and reduces the size of a pore. The lateral differences in the energy of a wave (which is related to its velocity) at the given depth are therefore larger for low-porosity sands (due to less dispersion) than for high-porosity ones. This energy loss is proportional to the initial velocity, so that a higher initial energy of a wave will result in more dispersion.

The geometry and size of the modelled SSDS are consistent with actual seismically-induced SSDS (Fig. 4). The size of the modelled SSDS varies from a few up to 25 cm. Simulations of the S-wave passage through a relatively thin succession of alternating dry and liquefied sands show therefore in our model alternating deformed and undeformed layers (Figs. 2 and 5A).

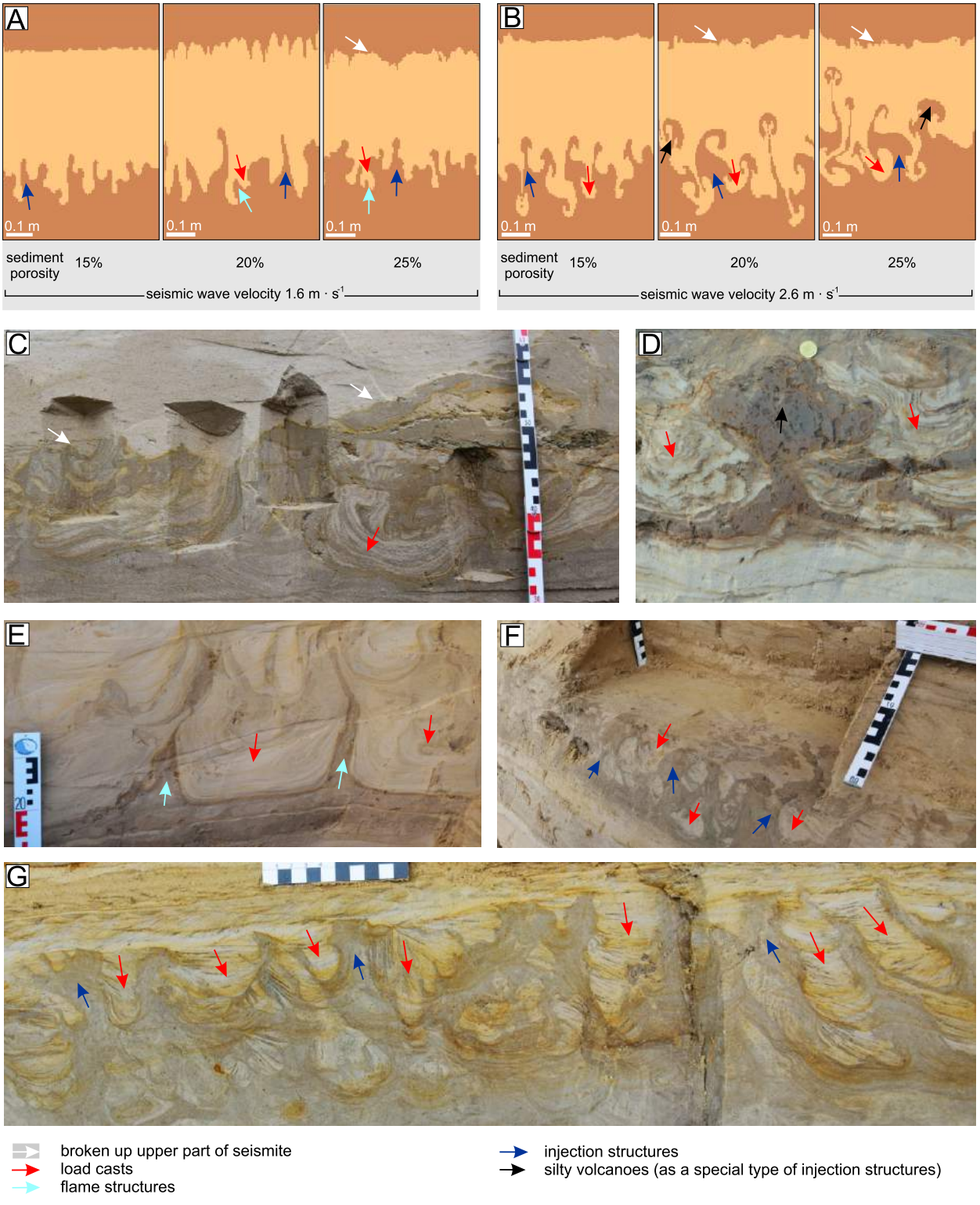

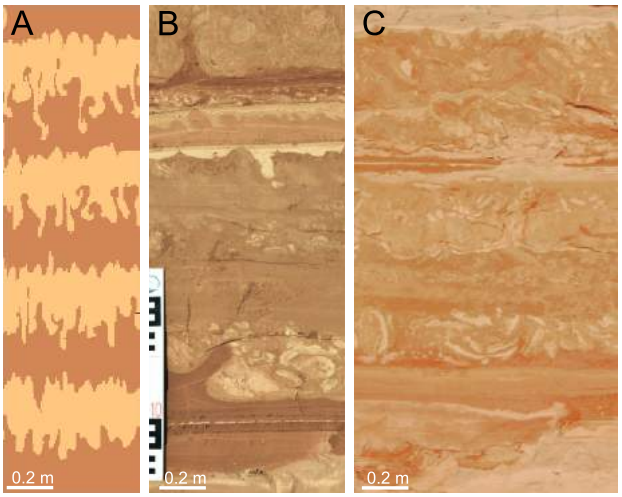

Fig. 5. Comparison of modelled SSDS (A) with actual field examples (B, C)

A – SSDS resulting, following the numerical modelling, from the passage of a seismic S-wave with a velocity of 2.0 m · s^{-1} through a sedimentary succession with 2 m thick stratified porous (15%) sands; **B, C** – seismites at the Rakuti site (SE Latvia) represented by chaotically-deformed layers with numerous small deformations like load casts, pseudonodules, and fragments of broken-up laminae, separated by undeformed layers; this must be ascribed to repeated phases of deformation caused by liquefaction; for details, see Van Loon et al. (2016)

DISCUSSION

Two main issues need some discussion. One is the model itself, together with its relationship with field and experimental data and its potential to predict SSDS development. The second issue concerns the size, geometry and type of the SSDS if a seismically-induced S-wave with a given velocity passes through a sedimentary succession with specific properties.

LIMITATIONS AND ADVANTAGES OF THE MODEL

Although we are aware that the model presented here is relatively simple and cannot be considered as fully developed, we also believe that it provides an interesting insight into the question how seismic S-waves produce SSDS, because all simplifications used for this study can be justified. As mentioned before, the main disadvantage of the modelling procedure presented here is that it addresses only one (vertical) component of only one seismic S-wave (among many). Even though this was our intention, the triggering mechanism for the modelled SSDS can be interpreted in different ways because it can be the resultant vertical velocity of numerous interacting waves. In other words, the velocity used in the model may be considered both as the vertical component of a specific S-wave, as well as the sum of the vertical components of a large number of S-waves. The presented model is therefore specific in that it addresses only a very narrow vertical succession (the "tube") where S-waves interact with the sediment, while it does not specify its exact distance from the epicentre. Consequently, it is reasonable to assume that the initial conditions assumed in the model are met at some point. Because our main focus is only on the development of SSDS, this assumption is feasible.

The model presented here seems to differ significantly regarding its prediction potential from models that focus at the propagation of seismic waves, or at the processes of liquefaction and fluidisation. Although our model should not be considered as complete or even nearly complete, it is well applicable concerning its main objective to allow the reconstruction of past seismic events; the prediction of the effects of modern seismic events is much less the objective of our model. Due to the reasons listed in the methods section, none of the existing models can be used for this purpose. The urgent need for a numerical method of seismite modelling can be fulfilled by the new approach presented here.

CHARACTERISTICS OF THE SSDS

The geometry of the modelled SSDS is consistent with that of actual seismically-induced and experimentally produced load casts, flame structures, injection structures and

Fig. 4. Comparison of modelled SSDS (A and B) with actual field examples (C–G)

A – SSDS developed after ~0.01 s following the numerical model when the seismic wave has a velocity of 1.6 m · s^{-1} ; **B** – idem, when the seismic wave velocity has a velocity of 2.6 m · s^{-1}; **C** – seismite at the Dyburiai site (Lithuania) with strongly deformed load casts of variable size (resulting from different stages of loading), and fragments of broken-up clay laminae (in the uppermost part of the seismite) derived from thin clay laminae affected by liquefaction; for details, see Belzyt et al. (2021); **D** – mushroom-shaped injection structure in a seismite at the Dwasieden site (Rügen Island, NE Germany); for details, see Pisarska-Jamroży et al. (2018); **E** – load casts and flame structures in seismites at the Valmiera site (NE Latvia). The load casts themselves are also deformed, indicating successive phases of deformational activity. Because there are no lithological differences between the sediments within the load casts, the various loading stages must be ascribed to repeated moments of liquefaction. The underlying silty/clayey layer (darker brown) was pressed upwards between the load casts and now forms flame structures. The flame structures still show their original internal lamination and commonly do not intrude the overlying layer with load structures; for details, see Van Loon et al. (2016); **F** – 3D view of deformation structures in a seismite at the Baltmuiza site. The deformed layer contains irregularly-shaped injection structures of sandy silt between load casts and pseudonodules of silty sand that show a wide variety of shapes. The pseudonodules are shown in 3D to have evolved from load casts which sunk into the underlying sandy silt after having become detached from the parent layer; for details, see Woźniak et al. (2021); **G** – seismite with silty injection structures and sandy load casts at the Slinkis site (W Lithuania). The upwards directed injection structures intruded ripple cross-laminated sandy layers, causing the material un between to form load casts. The sharp tops of the injection structures must be described to erosion by the current that resulted in the overlying ripple cross-laminated sand; for details, see Pisarska-Jamroży et al. (2019a)

clastic volcanoes. Load casts consist of what have been called “dry sands” in our model (yellowish in Figs. 1–3A, B and 4A), and they are surrounded by denser sands (brownish in Figs. 1–3A, B and 4A) which became liquefied during the modelled earthquake. Field examples of load casts usually contain sands, silty sands or sandy silts (Fig. 3C, E–G; e.g., Oliveira et al., 2011; Van Loon et al., 2016; Brandes et al., 2018; Belzyt et al., 2021). Flame structures, injection structures and clastic volcanoes, contain fluidised, denser sands (brownish in Figs. 1–3A, B and 4A). However, surprising this result may seem, it can be easily justified. During the passage of the S-wave through the sediment column, the wave causes intensive interaction between two layers with different densities, causing dispersal at their mutual boundary plane. This dispersal causes not only reduction of the wave energy, but also a reflection, after which a new, upward-directed wave with some energy appears. This new wave causes the upward movement of the sediment and consequently, the injection of more dense sediment into the lower dense one. Field examples of these SSDS usually show less dense sediments than the sediments that build load casts (e.g., Oliveira et al., 2011; Van Loon et al., 2016; Belzyt et al., 2021). The origin of injection structures such as sand or silt volcanoes is linked to overpressure in the sediment (cf. Van Loon, 2010; Van Loon and Maulik, 2011; Doughty et al., 2014). Such overpressure conditions can be expressed in the shift of seismite depths related to the maxima and minima of the responsible S-waves.

The sizes of the seismically-induced SSDS in our simulations are comparable with those of actual and experimental ones (e.g., Owen, 1996; Moretti et al., 1999; Moretti and Sabato, 2007). Their shape and geometry show a satisfactory similarity with field observations. The SSDS formed in our simulations are of the same type and have the same random distribution as actual seismites. The modelled SSDS do not show any features which are not present in modern and ancient seismites. The depth of their occurrence and the thickness of the deformed layer are consistent with field observations. The numerically simulated SSDS resulting from the model can consequently be considered as very accurate. Moreover, the numerical simulations show the stacks of deformed and undeformed layers (Fig. 2), as well as the wide range of chaotically-distributed SSDS that are well known from field investigations.

CONCLUSIONS

The following five conclusions can be drawn from our numerical modelling of seismites.

- 2D numerical simulations of seismically-induced SSDS results in structures that are similar to actual ones in seismites, which strongly suggests that the main feature responsible for the origination of seismically-induced SSDS is the shear strength related to the vertical velocity component of the seismic wave.
- The sediment compaction is related to initial sediment properties (particularly porosity) and the pressure exerted by the trigger mechanism, described in terms of the velocity of the seismic wave. The more pore water is present in the modelled sediment, the more susceptible to mobilization – and thus to more compaction – it becomes during propagation of the S-wave. With increasing porosity, the size of the developing SSDS increases. The higher the porosity of sediments is, the more complex the geometry of the SSDS becomes.
- The modelled size, geometry and type of the SSDS are linked only slightly to the velocity of the S-wave. However, the S-wave velocity influences the depth at which the seismite originates: the higher the wave velocity is, the deeper the resulting seismite can occur. The geometry and size of the modelled SSDS are consistent with actual and experimentally-produced seismic SSDS such as load casts, flame structures, injection structures and clastic volcanoes.
- The modelled shift in seismite depth can be related to the S-wave maxima and minima, and therefore to the propagation direction of the wave. These shifts also express overpressure conditions in the sediment.
- All results are consistent with previous studies addressing the liquefaction process. In combination with the compliance of the modelled seismites with field data, this strongly suggests that our model is accurate and can serve as a basis for the further development of more worked out models for the recognition of the various characteristics of ancient seismic events.

Acknowledgements. The study was supported by grants from the Polish National Science Center (no. 2015/19/B/ST10/00661 (GREBAL project) and 2019/33/N/ST10/00095). Helpful remarks on the first version by an Anonymous Reviewer and M. Moretti are appreciated.

REFERENCES

Alfaro, P., Moretti, M., Soria, J.M., 1997. Soft-sediment deformation structures induced by earthquakes (seismites) in Pliocene lacustrine deposits (Guadix-Baza Basin, central Betic Cordillera). Eclogae Geologicae Helvetiae, **90**: 531–540.

Allen, J.R.L., 1982. Sedimentary structures: their character and physical basis. Developments in Sedimentology, **30B**.

Amsden, A., Ruppel, H., Hirt, C., 1980. SALE: A simplified ALE computer program for fluid flow at all speeds. Los Almos National Laboratories Report, LA-8095.

Andrus, R.D., Stokoe K.H., 1997. Liquefaction resistance based on shear wave velocity. National Center for Earthquake Engineering Research (Salt Lake City) Report, 0022.

Atkinson, G.M., Eeri, M., Liam, Finn, W.D., Charlwood, R.G., 1984. Simple computation of liquefaction probability for seismic hazard applications. Earthquake Spectra, **1**: 107–123.

Belzyt, S., Pisarska-Jamroży, M., Bitinas, A., Woronko, B., Phillips, E.R., Piotrowski, J.A., Jusienė, A., 2021. Repetitive soft-sediment deformation by seismicity-induced liquefaction in north-western Lithuania. Sedimentology, **68**: 3033–3056.

Brandes, Ch., Steffen, H., Sandersen, P.B.E., Wu, P., Winsemann, J., 2018. Glacially induced faulting along the NW segment of the Sorgenfrei-Tornquist Zone, northern Denmark: implications for neotectonics and lateglacial fault-bound basin formation. Quaternary Science Reviews, **189**: 149–168.

Boulanger, R., Ziotopoulou, K., 2017. PM4sand version 3.1: a sand plasticity model for earthquake engineering applications. Report UC Davis Center for Geotechnical Modeling Report, UCD/CGM-17/01.

Collins, G.S., Melosh, H.J., Ivanov, B.A., 2004. Modeling damage and deformation in impact simulations. Meteoritics & Planetary Science, **39**: 217–231.

Davison, T.M., Collins, G.S., Elbeshausen, D., Wünnemann, K., Kearley, A., 2011. Numerical modeling of oblique hypervelocity impacts on strong ductile targets. Meteoritics & Planetary Science, **46**: 1510–1524.

Doughty, M., Eyles, N., Eyles, C.H., Wallace, K., Boyce, J.I., 2014. Lake sediments as natural seismographs: earthquake-related deformations (seismites) in central Canadian lakes. Sedimentary Geology, **313**: 45–67.

Galli, P., 2000. New empirical relationships between magnitude and distance for liquefaction. Tectonophysics, **324**: 169–187.

Hilbert-Wolf, H.L., Simpson, E.L., Simpson, W.S., Tindall, S.E., Wizevich, M.C., 2009. Insights into syndepositional fault movement in a foreland basin; trends in seismites of Upper Cretaceous Wahweap Formation, Kaiparowits Basin, Utah, U.S.A. Basin Research, **21**: 856–871.

Hoffman, G., Reicherter, K., 2012. Soft-sediment deformation of Late Pleistocene sediments along the southwestern coast of the Baltic Sea (NE Germany). International Journal of Earth Sciences, **101**: 351–363.

Jeffeeris, M., Been, K., 2015. Soil Liquefaction – a Critical State Approach. CRC Press.

Li, C., Liu, J., Sun, Y., 2020. Optimal third-order sympletic integration modeling of seismic acoustic wave propagation. Bulletin of the Seismological Society of America, **110**: 754–762.

Marco, S., Agnon, A., 1995. High-resolution stratigraphy reveals repeated earthquake faulting in the Masada Fault Zone, Dead Sea Transform. Tectonophysics, **408**: 101–112.

Meada, T., Takemura, S., Furumura, T., 2017. OpenSWPC: an open source integrated parallel simulation code for modeling seismic wave propagation in 3D heterogenous viscoelastic media. Earth, Planets and Space, **69**: 1–20.

Miljković, K., Collins, G.S., Patel, M.R., Chapman, D., Proud, W., 2012. High-velocity impacts in porous solar system materials. AIP Conference Proceedings, **1426**: 871–874.

Moretti, M., Sabato, L., 2007. Recognition of trigger mechanisms for soft-sediment deformation in the Pleistocene lacustrine deposits of the Santı Arcangelo Basin (Southern Italy): Seismic shock vs. overloading. Sedimentary Geology, **196**: 31–45.

Moretti, M., Ronchi, A., 2011. Liquefaction features interpreted as seismites in the Pleistocene fluvio-lacustrine deposits of the Neuquén Basin (Northern Patagonia). Sedimentary Geology, **235**: 200–209.

Moretti, M., Alfaro, P., Caselles, O., Canas, J.A., 1999. Modelling seismites with a digital shaking table. Tectonophysics, **304**: 369–383.

Obermeier, S.F., 1996. Use of liquefaction-induced features for paleoseismic analysis – an overview of how seismic liquefaction features can be distinguished from other features and how their regional distribution and properties of source sediment can be used to infer the location and strength of Holocene paleo- earthquakes. Engineering Geology, **44**: 1–76.

Obermeier, S.F., 2009. Using liquefaction-induced and other soft-sediment features for paleoseismic analysis. In: Paleoseismology (ed. J.P. McCalpin): 487–564. Elsevier, New York.

Obermeier, S.F., Jacobson, R.B., Smoot, J.P., Weems, R.E., Gohn, G.S., Monroe, J.E., Powars, D.S., 1990. Earthquake-induced liquefaction features in the coastal setting of South Carolina and in the fluvial setting of the New Madrid seismic zone. U.S.G.S. Professional Paper, **1504**.

Oliveira, C.M.M., Hodgson, D.M., Flint, S.S., 2011. Distribution of soft-sediment deformation structures in clinoform successions of the Permian Ecca Group, Karoo Basin, South Africa. Sedimentary Geology, **235**: 314–330.

Owen, G., 1996. Experimental soft-sediment deformation: structures formed by the liquefaction of unconsolidated sands and some ancient examples. Sedimentology, **43**: 279–293.

Owen, G., Moretti, M., 2011. Identifying triggers for liquefaction-induced soft-sediment deformation in sands. Sedimentary Geology, **235**: 141–147.

Peng, P., Wang, L., 2019. 3DMRT: a computer package for 3D model-based seismic wave propagation. Seismological Research Letters, **90**: 2039–2045.

Pierazzo, E., Artemieva, N., Asphaug, N., Baldwin, E., Cazamias, E.C., Coker, R., Collins, G.S., Crawford, D.A., Davison, T., Elbeshauen, D., Holsapple, K.A., Housen, K.R., Korycansky, D.G., Wünnemann, K., 2008. Validation of numerical codes for impact and explosion cratering: Impacts on strengthless and metal targets. Meteoritics & Planetary Science, **43**: 1917–1938.

Pisarska-Jamroży, M., Woźniak, P.P., 2019. Debris flow and glacioisostatic-induced soft-sediment deformation structures in a Pleistocene glaciolacustrine fan: the southern Baltic Sea coast, Poland. Geomorphology, **326**: 225–238.

Pisarska-Jamroży, M., Belzyt, S., Börner, A., Hoffmann, G., Hüneke, H., Kenzler, M., Obst, K., Rother, H., Van Loon, A.J., 2018. Evidence from seismites for glacio-isostatically induced crustal faulting in front of an advancing land-ice mass (Rügen Island, SW Baltic Sea). Tectonophysics, **745**: 338–348.

Pisarska-Jamroży, M., Belzyt, S., Bitinas, A., Jusienė, A., Woronko, B., 2019a. Seismic shocks, periglacial conditions and glacitectonics as causes of the deformation of a Pleistocene meandering river succession in central Lithuania. Baltica, **32**: 63–77.

Pisarska-Jamroży, M., Van Loon, A.J., Mleczak, M., Roman, M., 2019b. Enigmatic gravity-flow deposits at Ujście (western Poland), triggered by earthquakes (as evidenced by seismites) caused by Saalian glacioisostatic crustal rebound. Geomorphology, **326**: 239–251.

Pisarska-Jamroży, M., Woronko, B., Bujak, Ł., Bitinas, A., Belzyt, S., Mleczak, M., 2019c. Large-scale deformation structures characterize glaciolacustrine kame sediments – a new kame-investigation approach. Abstract book INQUA Congress 2019 (Dublin) O-1128.

Rahman, M., Lo, S., 2014. Undrained behavior of sand-fines mixtures and their state parameters. Journal of Geotechnical and Geoenvironmental Engineering, **140**: 04014036.

Rahman, M., Asce, M., Nguyen, H.B.K., Fourie, A.B., Kuhn, M.R., 2020. Critical state soil mechanics for cyclic liquefaction and postliquefaction behavior: DEM study. Journal of Geotechnical and Geoenvironmental Engineering, **147**: 04020166.

Rodríguez-Pascua, M.A., Calvo, J.P., De Vicente, G., Gomez Gras, D., 2000. Seismites in lacustrine sediments of the Prebetic Zone, SE Spain, and their use as indicators of earthquake magnitudes during the late Miocene. Sedimentary Geology, **135**: 117–135.

Rossetti, D.F., 1999. Soft-sediment deformation structures in late Albian to Cenomanian deposits, Sao Luis Basin, northern Brasil: evidence for palaeoseismicity. Sedimentology, **46**: 1065–1081.

Rossetti, D.F., Bezerra, F.H.R., Goes, A.N., Neves, B.B.B., 2011. Sediment deformation in Miocene and post-Miocene strata, Northeastern Brazil: Evidence for paleoseismicity in a passive margin. Sedimentary Geology, **235**: 172–187.

Seed, H.B., Idris, I.M., 1971. Simplified procedure for evaluating soil liquefaction potential. Journal of Soil Mechanics and Foundations Division, **97**: 1249–1273.

Seilacher, A., 1969. Fault-graded beds interpreted as seismites. Sedimentology, **13**: 15–159.

Vaid, Y.P., Thomas, J., 1995. Liquefaction and postliquefaction behavior of sand. Journal of Geotechnical Engineering, **121**: 1321–1337.

Van Loon, A.J., 2010. Sedimentary volcanoes: overview and implications for the definition of a “volcano” on Earth. GSA Special Paper, **470**: 31–41.

Van Loon, A.J., Maulik, P., 2011. Abraded sand volcanoes as a tool for recognizing paleo-earthquakes, with examples from the Cisuralian Talchir Formation near Angul (Orissa, eastern India). Sedimentary Geology, **238**: 145–155.

Van Loon, A.J., Pisarska-Jamroży, M., 2014. Sedimentological evidence of Pleistocene earthquakes in NW Poland induced by glacioisostatic rebound. Sedimentary Geology, **300**: 1–10.

Van Loon, A.J., Pisarska-Jamroży, M., Nartišs, M., Krievāns, M., Soms, J., 2016. Seismites resulting from high-frequency, high-magnitude earthquakes in Latvia caused by Late Glacial glacio-isostatic uplift. Journal of Palaeogeography, **5**: 363–380.

Van Loon, A.J., Pisarska-Jamroży, M., Woronko, B., 2020. Sedimentological distinction in glacigenic sediments between load casts induced by periglacial processes from those induced by seismic shocks. Geological Quarterly, **64** (3): 626–640.

Vanneste, K., Meghraoui, M., Camelbeeck, T., 1999. Late Quaternary earthquake-related soft-sediment deformation along the Belgian portion of the Feldbiss Fault, Lower Rhine Graben system. Tectonophysics, **309**: 57–79.

Wheeler, R.L., 2002. Distinguishing seismic from nonseismic soft-sediment structures: criteria from seismic-hazard analysis. GSA Special Paper, **359**: 1–11.

Woźniak, P.P., Belzyt, S., Pisarska-Jamroży, M., Woronko, B., Lamsters, K., Nartišs, M., Bitinas, A. 2021. Liquefaction and re-liquefaction of sediments induced by uneven loading and glacigenic earthquakes: implications of results from the Latvian Baltic Sea coast. Sedimentary Geology, **421***:* 105944.

Wünnemann, K., Colling, G.S., Melosh, H., 2006. A strain-based porosity model for use in hydrocode simulations of impacts and implications for transient crater growth in porous target. Icarus, **180**: 514–527.

Youd, T.L., Idriss, I.M., 2001. Liquefaction resistance of soil: summary report from the 1996 NCEER and 1998 NCEER/NFS workshop on evaluation of liquefaction resistance of soil. Journal of Geotechnical and Geoenvironmental Engineering, **127**: 1275–1285.

Artykuł nr 2
Paper no. 2

Bronikowska, M., Pisarska-Jamroży, M., Van Loon, A.J.

Dropstones deposition – results of numerical modelling of deformation structures, and implications for the reconstruction of the water depth in shallow lacustrine and marine successions

Journal of Sedimentary Research 91, 507-519.

Journal of Sedimentary Research

Journal of Sedimentary Research, 2021, v. 91, 507–519
Research Article
DOI: 10.2110/jsr.2020.111

DROPSTONE DEPOSITION: RESULTS OF NUMERICAL PROCESS MODELING OF DEFORMATION STRUCTURES, AND IMPLICATIONS FOR THE RECONSTRUCTION OF THE WATER DEPTH IN SHALLOW LACUSTRINE AND MARINE SUCCESSIONS

MAŁGORZATA BRONIKOWSKA,[1] MAŁGORZATA PISARSKA-JAMROŻY,[1] AND A.J. (TOM) VAN LOON[2]
[1]*Geological Institute, Adam Mickiewicz University, B. Krygowskiego 12, 61-680 Poznań, Poland*
[2]*College of Earth Science and Engineering, Shandong University of Science and Technology, Qingdao 266590, Shandong, China*
e-mail: malgorzata.bronikowska@amu.edu.pl

ABSTRACT: **Dropstones in lacustrine and marine sediments show a wide range of sizes: from less than a millimeter to many meters. Their size and shape determine the velocity and the acceleration when they settle through the water column, and this, in turn, determines in principle the imprint that they make in the bottom sediment. Although these parameters are crucial for dropstone deposition, the unknown material (sediment) properties (like strength, porosity, pore-water content, viscosity, etc.) of the bottom sediment play a just as important role in this process as the water depth, which can physically be understood as the length of the pathway traveled vertically through a dense medium before the impact. Reconstruction of the principal environmental conditions at the time of dropstone fall and deposition consequently requires considering the variety of factors affecting the final imprint depth of a dropstone, the combination of several numerical methods.**

Here, we show the results of numerical modeling of dropstones with different sizes that settle through water columns with different depths. Our results show how environmental factors control the deformation structures formed at the sedimentary surface during the impact of a dropstone, and how deep the imprint caused by the settling dropstone will be.

INTRODUCTION

Dropstones (also called "lonestones") are extrabasinal clasts of which the diameter is significantly larger than that of the sediments in which they are found. They commonly range in size from pebbles to cobbles, but also smaller particles can be recognized as dropstones if their size is larger than the thickness of the strata in which they are embedded (Haarland et al. 1966; Menzies 2002), which implies that the host sediment must consist predominantly of silt- and/or clay-size particles. Small dropstones cannot always be distinguished from the autochthonous sediments, even in microsedimentological analyses, unless their composition is "exotic."

Dropstones reach the surface of the commonly fine-grained and water-saturated bottom sediments, commonly producing an imprint if their kinetic energy is sufficiently large, or even penetrating the uppermost layer (Haarland et al. 1966; Menzies 2002). Particularly dropstones of pebble size and larger are able to deform, penetrate, and rupture bottom sediments, leaving a clear soft-sediment deformation structure (SSDS). According to our knowledge, no previous study has been devoted to the relationship between dropstone size, water depth, and resulting SSDS. Therefore, we have modeled the process of dropstone settling and the resulting imprints, with the objective to shed a new light on the reconstruction of the water depth during deposition of sediments that contain dropstones. Obviously, the modeling results that we present can be applied to almost all types of lonestone, irrespective of their glacial or non-glacial origin but, as detailed further on, it appears that a relationship between water depth and imprint exists only for shallow (< 10 m) water depths.

Origin of Dropstones

The origin of coarse (pebble-size or larger) clasts in a fine-grained (fine sand or finer) sediment has long puzzled geologists. Diamictites representing glacial tills were recognized fairly soon, but strongly bimodal sediments in other settings (including glaciomarine and glaciolacustrine ones) raised questions about their natural origin in a time span (the first half of the previous century) when sedimentology had not yet developed as an Earth-science discipline (see Van Loon 1970). This is expressed well by a discussion between Hohl (1934), who wondered whether "Gerölltone" (German for "pebbly mudstones") could have a natural origin, and stated that this was impossible. Later researchers put forward some possible genetic processes (gastroliths, transport by seaweed, etc.) that certainly, however, could not explain the widespread occurrence of such types of sediment. An answer came by Ackerman (1949, 1951), who recognized the role of thixotropy in sediment behavior, and who may be considered one of the earliest researchers to recognize mass flows.

Only when sedimentology had started to develop as a geological discipline on its own and the process of sediment gravity flows (then commonly called "mass flows") became understood to a reasonable degree thanks to the benchmark studies of Crowell (1959) and Dott (1963), pebble-rich sediments (referred to in the literature for a long time as "pebbly mudstones") lost their enigmatic character.

It is interesting, however, that numerous studies in the past few decades have made clear that dropstones, indeed, can result from a wide variety of nonglacial processes. They can be transported by other (nonglacial) rafts, by flotation, or through the air (Bennett et al. 1996). Examples of

Published Online: May 2021
 1527-1404/21/091-507

biological "rafts" are marine mammals, reptiles, birds, floating kelp, and tree stumps (e.g., Jolliffe 1989; Woodborne et al. 1989; Jokiel 1990; Bennett et al. 1996). Flotation is almost exclusively restricted to small particles (Syvitski and Van Everdingen 1981) or a specific lithology such as pumice (Osborne et al. 1991) or fragments of dried coral (Kornicker and Squires 1962). Transport through the air can result in dropstones in the form of volcanic ejecta (Sohn and Chough 1989) or meteorites. Pebbles may even be transported by waterspouts or landspouts that pick up boulders on the beach and carry them over the water, where they can eventually be dropped (e.g., de Long et al. 2006; Oard 2008). Bennett et al. (1996) mention also that dropstones can be found in sediments as a result of hominids or other primates that throw stones. Also in these cases, however, it seems hardly possible, if possible at all, that the resulting fine-grained sediments with scattered clasts can be confused with glaciomarine or glaciolacustrine sediments with dropstones.

Confusion about the interpretation of such sediments is particularly unlikely nowadays since research in glacigenic sediments has made much progress, and the feature of isolated clasts in marine and lacustrine sediments has now commonly been accepted to be the result of melting of sediment-laden icebergs and ice rafts. It must be realized, however, that this "discovery" appeared so fascinating that all coarse clasts in a fine-grained marine or lacustrine setting have been interpreted by some researchers as dropstones. This resulted eventually in the hypothesis of Snowball Earth, as clasts were found worldwide in deposits from the Neoproterozoic. It has been shown, however, that many of these Neoproterozoic pebbly mudstones do not result from the release of sedimentary particles from melting icebergs, but rather are debris-flow deposits (e.g., Van Loon 2008). These deposits differ from dropstones, though exceptions exist, in that dropstones tend to occur commonly as isolated clasts, whereas the casts in lithified debris-flow deposits tend to constitute a significant, but hard to determine, percentage by volume.

However, dropstones in a glacigenic setting may also occur in clusters, called "dumpstones" (Thomas and Connell 1985). They are commonly interpreted as a result of dumping events from icebergs or ice rafts (Thomas and Connell 1985; Pisarska-Jamroży et al. 2018a). Icebergs (we will use this term in the following for "icebergs and/or ice rafts") can carry clasts of all sizes dispersed within the ice as well as a considerable volume of particles deposited by a variety of processes during a long time. Such material is called "ice-rafted debris" (IRD; Hoffman and Schrag 2002). Asymmetric thermal subrosion of icebergs can cause instability, so that they tumble over and release their IRD in the form of simultaneously dropped masses of clasts, resulting in stone heaps on the sea or lake floor.

Transport by Icebergs

Icebergs may carry IRD over large distances, depending on their size and the ambient temperature. Under suitable conditions, dropstones left by a passing iceberg can therefore be used for the reconstruction of the route followed by the iceberg. This is well known from, among other features, the Heinrich events that left abundant IRD on the floor of the Atlantic Ocean (Heinrich 1988; Dowdeswell et al. 1995; Eyles et al. 1997; Hesse and Khodabakhsh 2016). Commonly, however, icebergs travel less far, and it is well known from Quaternary research that ice masses frequently became detached from the front of land ice caps and floated away in proglacial lakes, which commonly had a relatively small size (hundreds of square meters to a few tens of square kilometers) because they tended to develop in the valleys or channels formed by meltwater streams. This means that the great majority of such proglacial lakes had, in contrast to the huge lakes that developed, for instance, around the present-day border between the United States and Canada, a depth that was limited by the depth of the meltwater channels, commonly a few meters, occasionally more than 10 m. This is reflected in the finding that ice rafts were commonly grounded in Pleistocene lakes of limited depth (e.g., Thomas and Connell 1985; Dowdeswell et al. 2000; Kalm and Kadastik 2000; Mokhtari Fard and Van Loon 2004; Winsemann et al. 2008; Yorke et al. 2012; Livingstone et al. 2015; Van Loon et al. 2019). Obviously, the marine environments where floating icebergs could drop the clasts that they carried along, was commonly much deeper.

Dropstones in lacustrine and marine sediments have frequently been described, among others by Thomas and Connell (1985), Gilbert (1990), Brodzikowski and Van Loon (1991), Leckie et al. (1995), Bennett et al. (1996), Smith and Andrews (2000), Williams et al. (2008), Le Heron (2015), and Pisarska-Jamroży et al. (2018a).

METHODS

For the numerical reconstruction of the process of dropstone deposition, it is necessary to model both the dropstone's motion in the water column and the mechanical response of the bottom sediments to the pressure caused by the impacting dropstone. Consequently, two separate but complementary numerical methods are combined in the present study.

The velocity calculations were conducted using programs written by the authors in C language. These programs can be obtained from the corresponding author upon request and can be run on any Unix machine. The response of the bottom sediments to the pressure caused by impacting dropstones was simulated by the iSALE2D hydrocode, described in detail in the next sections.

Velocity Calculations

The first method is aimed at calculating the velocity of a dropstone at the moment when it reaches the sea or lake bottom; this is done through basic equations of motion in dense media that are integrated numerically. During its fall through the water column, the dropstone experiences acceleration caused by gravity, deceleration caused by the drag force, and the buoyancy force (which pushes the dropstone up). The equation used for numerical integration of the dropstone motion in the water column contains three parts: the first one describing Newtonian motion in a dense medium, gravity as the second, and a third, addressing the buoyancy force:

$$a_z = \frac{F_d + \mathrm{F}_g + \mathrm{F}_b}{m} \tag{1}$$

$$F_d = -v_z \cdot v_{\mathrm{tot}} \cdot \rho_w \cdot s_c \cdot C_D \tag{2}$$

$$F_b = \rho_w \cdot g \cdot \frac{m}{\rho_c} \tag{3}$$

where v_z is the vertical component of the dropstone's velocity, v_{tot} is the total velocity of the impacting dropstone, ρ_w and ρ_c are, respectively, the water and dropstone densities, s_c denotes the surface area of the spherical dropstone, C_D is a drag coefficient, and g is the acceleration due to gravity.

In this simple model, no other factors that might influence the process of dropstone movement are included. The reason for this simplification is that only the three above-mentioned forces have a significant impact on the final vertical component of the velocity (and eventual deposition) of the dropstone. Many other factors can influence the lateral velocity of the dropstone during its travel through the water (e.g., currents, waves, the shape of the basin floor). All these "disturbing" processes are, however, of only marginal importance for the vertical velocity and consequently for the vertical impact pressure during deposition of the dropstone.

In this model, the dropstone is described by a uniformly dense sphere with a specific diameter between 0.2 and 1.0 m. Obviously, elliptical or irregular particles will result in different final velocities of a dropstone (as like currents or any other features resulting in lateral movement of the water or the dropstone will affect the presented values), but all these parameters influence the final velocity much less than the water depth, so

that it seems unjustified to go into detailed calculations for (almost) each of the (almost) countless variations in parameters. Although the precise parameters that may influence the velocity of settling dropstones under actual sedimentary conditions are very diverse, our simplification of spherical dropstones settling vertically through the water therefore seems reasonable.

The second input parameter is the water depth (i.e., the vertical extent of the water column), which varies in our study between 2 and 10 m; these values were taken because Pleistocene proglacial lakes, just like modern ones, have strongly fluctuating lake levels, and because ongoing sediment supply from the borders causes large parts of these lakes to be less than 10 m deep, although large lakes may be much deeper in their central parts. It should be realized in this context that proglacial areas tend to have an irregular topography (not only during ice retreat as a result of ice scouring but also during ice advance because of the large supply of sediment by irregular braided meltwater streams) and that such a topography favors the development of small and shallow lakes. This is exactly why sedimentological studies of sediments deposited in areas that were covered by Pleistocene ice sheets mention so many glaciolacustrine successions.

It should be noted in this context that, as will be detailed further on, clasts settling in water do not undergo a continuous acceleration, but reach a maximum velocity at a depth of maximally some 10 m deep. This implies that the model that we present here, however applicable in the great majority of glaciolacustrine Pleistocene sediments, cannot be used for reconstruction of the depth of a lake or sea if it exceeds 10 m. This also implies that the model seems less applicable to sediments with dropstones in pre-Quaternary deposits, because the preservation potential of shallow-lacustrine sediments is low, so that most of the ancient deposits with dropstones represent deep-marine or deep-lacustrine settings.

The initial velocity of the settling dropstone is assumed to be zero, which represents the situation during which the dropstone starts sinking from the water surface. Although some processes (e.g., slumping of sediments on ice above the water or iceberg turnover) may result in a non-zero initial velocity of the dropstone, this simplification seems reasonable. A main reason is that a particle that is dropped with non-zero velocity into the water experiences a sudden slowdown caused by the density difference between air and water. Such a deceleration is significant for small particles (which almost lose their initial velocity completely at this point), but it is almost negligible for the biggest ones. In the case of small dropstones, the resulting velocity in the water column diminishes to only a few percent of its above-water velocity, so that this does not influence the final velocity and energy of the impacting particle significantly. In the case of huge boulders, which do not experience this deceleration at all, the situation is essentially similar: the non-zero velocity at the beginning adds only a small percentage of the energy that is added by all other forces like gravity taken away by the dragging. Consequently, the resulting final velocity is also in this case only slightly different from what it would be if the particle would start with zero velocity at the water surface. Constant parameters in this model are the dropstone density (2700 kg/m^3, which is typical of granite and lithified non-porous sandstone/quartzite), a drag coefficient (D_c) of 0.6 (the value commonly used for low-velocity spheres in a dense medium), and the water density (assumed to have a constant value of 1000 kg/m^3). For numerical integration, we use the standard Runge–Kutta–Fehlberg differential equation solver rkf45 (Shampine et al. 1976) with time steps of 0.01 s, which gives a reasonable accuracy while requiring only a short computational time.

Impact on Bottom Sediments

To investigate the response of the bottom sediments to the pressure caused by an impacting dropstone, we use the iSALE2D code (Wünnemann et al. 2006), which is based on a hydrocode solution algorithm (Amsden et al. 1980) and which was originally developed for studies on hypervelocity impact cratering (Collins and Wünnemann 2004; Wünnemann et al. 2006). The iSALE2D code includes an elasto-plastic constitutive model, fragmentation models, various equations of state, a strength model and a porosity-compaction model. It has been benchmarked against other hydrocodes (Pierazzo et al. 2008) and validated against experimental data (Pierazzo et al. 2008; Davison et al. 2011; Miljkovićet al. 2012).

In our models addressing the impact depth of a dropstone, the dropstone is resolved by 20 cells per projectile radius (CPPR). Preliminary resolution studies have shown that this resolution provides sufficient accuracy for good estimation of the impact depth; investigation of the deformations resulting from the dropstone's impact in the bottom sediments requires, however, a higher resolution. For the modeling of such deformations, we consequently applied a higher resolution of 40 CPPR (black contours in Fig. 1), but in the frame of the deposition depth, low-resolution models appear to be just as accurate as high-resolution ones (red contours in Fig. 1). The differences between the results obtained by these two types of simulation are negligible, so that 20-CPPR models must be considered adequate for the calculation of the impact depth of dropstones.

For the material model of the bottom sediments we use an equation of state (EOS) for quartz and the Drucker–Prager strength model with three different sets of parameters representing low-, medium-, and high-strength sediments, respectively (Table 1). The material properties of bottom sediments are still poorly known despite of numerous descriptions. These descriptions are, however, commonly insufficiently accurate for modeling purposes like ours, for several reasons. First, a sediment's strength (like the strength of any other material) strongly depends on the size of the sample, while this dependence is nonlinear and difficult to estimate for water-saturated glacigenic sediments, consequently, numerical modeling is the most commonly applied well-established method for determining unknown sediment properties like porosity, strength, viscosity (and many other properties), and its response to pressure. Also, bottom sediments from cores taken from the sea floor have been subjected to compaction; this makes it practically impossible to determine their mechanical properties at the time of the dropstone's impact precisely.

The application of maximum, moderate, and minimum strength values in the simulations restricts the range of possible scenarios regarding the dropstone's impact by taking into account only three representative, practice-based material models. Because the applied simulations all concern low-velocity impacts, there is no need to simulate additional properties for the description of the response of the sediments to the pressure caused by the impacting dropstone. All processes occurring during dropstone impact can thus be described by simple physics and do not require advanced material modeling.

As input parameters for the iSALE2D simulations, five different sets of velocities were used, each for a different water depth (understood as the height of the water column between the bottom and the water surface at the point from where the particle starts settling); these velocities were calculated by numerical integration of the dropstone movement in water of five different depths, viz. 2, 3, 4, 5, and 10 m (as explained above, the model cannot be applied to deeper water, because the settling velocity does no longer increase beyond this depth; this implies, as stated above, that the model is not easily applicable to deep-marine and deep-lacustrine settings, but is rather aimed at the proglacial lakes of limited size and depth, which represent the great majority of such lakes in areas glaciated during the Pleistocene). The dropstone diameters varied between 0.2 and 1.0 m. All scenarios were carried out for three types of bottom sediments with different material properties.

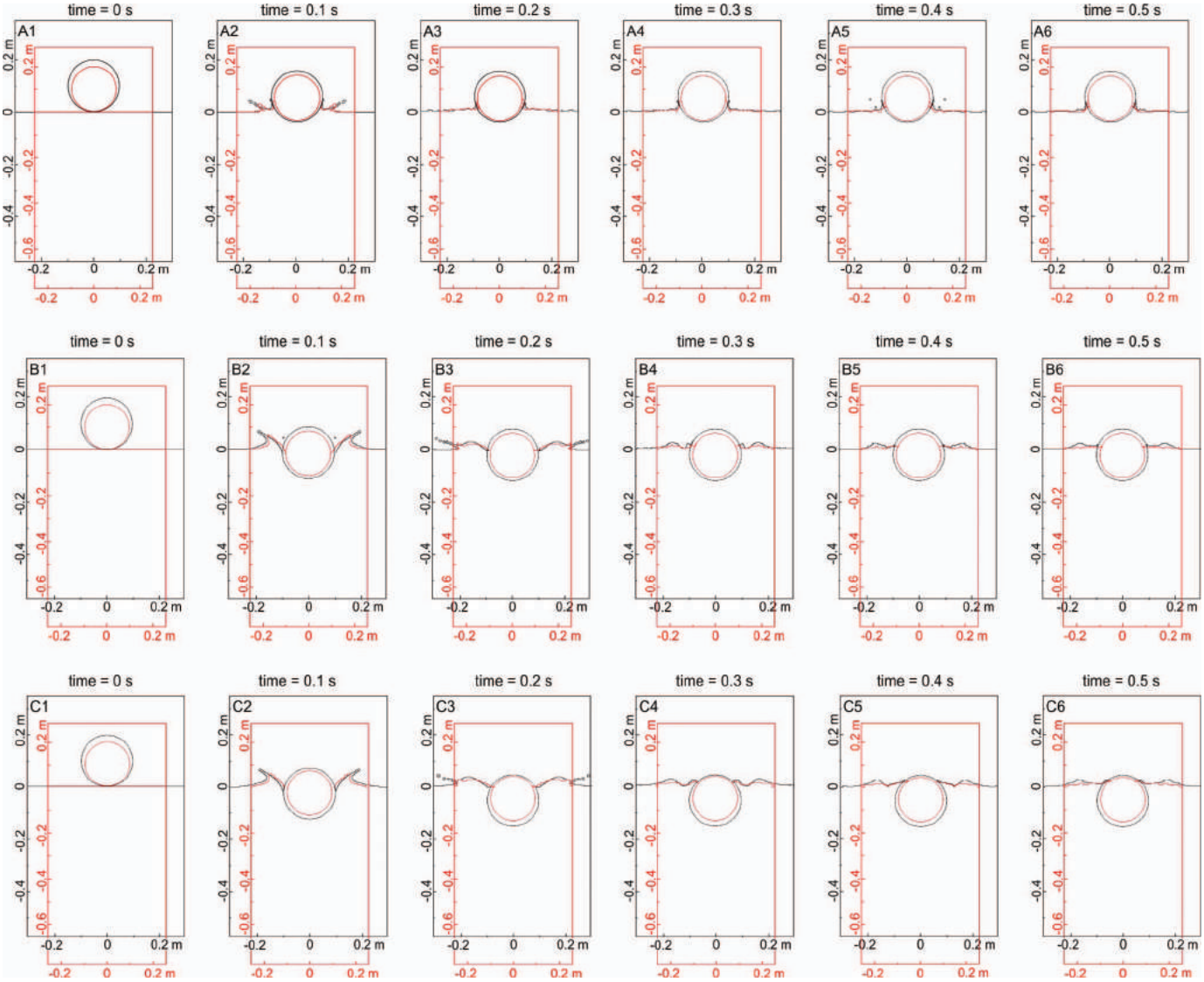

FIG. 1.—Comparison between high-resolution (40 CPPR) models (black contours) and low-resolution (20 CPPR) models (red contours). The modeled dropstone has a diameter of 0.2 m in all three simulations. Successive letters (A–C) are used for models of bottom sediments with different strengths, whereas the successive numbers indicate consecutive time steps of the simulations.

RESULTS

For more clarity, the present section with our results is divided into several parts, each addressing a specific factor that influences the dropstone sinking or impacting process. First, we describe the relationship between the water depth, the grain size and the impact velocity of the dropstone. Subsequently, we discuss the results concerning the influence of the strength of the bottom sediment on the final depth of the imprint made by the dropstone. In the third part, we show how the imprint depth depends

TABLE 1.—*Strength and porosity model parameters used for iSALE2D simulations of the bottom-sediment response to pressure resulting from a dropstone impact.*

Parameter	Low-Strength Sediments	Moderate-Strength Sediments	High-Strength Sediments
YDAM0 (yield strength at zero pressure)	0.1000×10^3	0.1500×10^3	1.0000×10^3
YLIMDAM (limiting strength at high pressure)	1.0000×10^3	1.5000×10^3	10.000×10^3
FRICDAM (coefficient of internal fraction)	0.7000	0.7000	0.7000
ALPHA0 (initial porosity)	1.8000	1.8000	1.8000
EPSE0 (elastic volumetric strain threshold)	0.0000	0.0000	0.0000
ALPHAX (distension at transition from exponential to power-low compaction)	1.2900	1.2900	1.2900
KAPPA (compaction-rate parameter in exponential compaction regime)	0.9880	0.9880	0.9880
CHI (ratio of porous to solid material sound speed at zero pressure)	0.3300	0.3300	0.3300

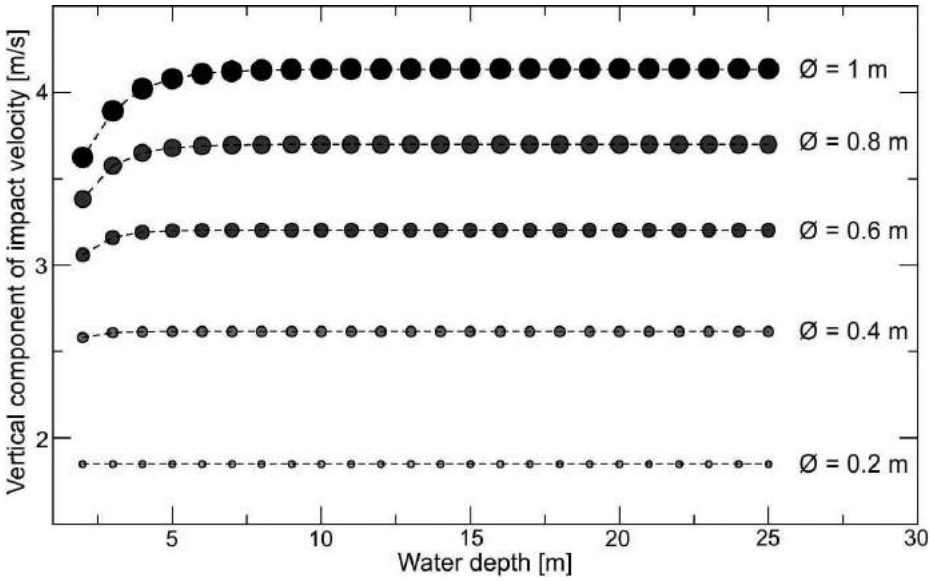

FIG. 2.—Final impact velocity of a dropstone settling through the water column as a function of its diameter (or radius) for different water depths.

on the grain size, and its impact velocity. Finally, we show the results that describe the deformations caused by the impacting dropstone in water-saturated sediments.

Impact Velocity of the Sinking Dropstones

Our numerical investigation indicates a distinct relationship between the impact velocity of free-settling dropstones and the water depth (Fig. 2). This relationship is strong for large dropstones (diameter $>$ 0.6 m) but is negligible for smaller ones (diameter $<$ 0.4 m), but the transition between these two categories is gradual. With increasing water depth, the final (impact) velocity as a function of the dropstone size becomes constant due to the increase in time during which friction acts on the dropstone's surface. Consequently, the impact velocity of a sinking dropstone depends only on the size for depths $<$ 10 m, because the dependence on the water-column length (i.e., the length of the vertical pathway from the water surface to the bottom) becomes negligible beyond this depth. The above results are not truly surprising: dropstones settling in water are accelerated by gravity, while simultaneously decelerated by the drag force acting on their surface area. For relatively large (and consequently relatively heavy) dropstones, the gravity is much stronger than the drag, so that the (vertical) length of the pathway through the water is important for the acceleration. On the other hand, simple Newtonian physics indicates that, after some time of settling, the velocity of the dropstone becomes constant, implying that a long pathway does not result in an increasing velocity after a specific water depth has been reached.

The Influence of the Bottom-Sediment Properties on the Impact

The response of the bottom sediment to the pressure caused by an impacting dropstone depends on its sediment properties, especially strength and viscosity. Due to the fact that these properties are only poorly known for water-saturated sediments at the sedimentary surface, three sets of strength model parameters are used here: the first set corresponds to oversaturated, weak (unconsolidated) sediments (low strength), the second to water-saturated, moderately strong (somewhat consolidated) sediments (medium strength), and the last one to consolidated (somewhat compacted), but still pore-water containing sediment (high strength). The application of these three strength models allows exploration of the most likely (moderate strength) as well as the most extreme (low and high strength) response of sediments to the pressure caused by an impacting dropstone.

The influence of the bottom-sediment strength on the final imprint depth (defined here as the lowermost part of the dropstone in vertical position at the time when it stopped moving) of the dropstone is significant (Fig. 3). The imprint depth of dropstones with a diameter of 0.2 m varies between 0.04 and 0.15 m (see first row in Fig. 3), depending on the sediment strength; for larger clasts, this dependence is even stronger (see second and third rows in Fig. 3).

In the case of high-strength sediments (see column A in Fig. 3), the dropstone does not become completely buried, and this holds for all studied sizes of dropstones. However, such high-strength sediments (corresponding to wet and dry sand) are characteristic of dry environments and cannot be considered as representative for the sediments on which dropstones tend to be deposited. The most appropriate strength model for bottom sediments is moderate strength (see column B in Fig. 3), but also low-strength sediments should be considered as possible (see column C in Fig. 3). However, in the next subsections, only results for the moderate-strength model will be presented, as these are most comparable with actual bottom sediments in proglacial lakes or seas.

The Influence of the Dropstone Size and the Water Depth on the Final Imprint Depth

As mentioned above, two factors influence the final imprint depth of an impacting dropstone almost completely. The first is the dropstone's size, which can be directly translated into the dropstone's mass, which influences both the impact energy and the dropstone's surface area that affects the drag force. The second key factor is the impact velocity, which depends on the dropstone size and the water depth (see Fig. 4). This second, seemingly obvious, relationship creates, however, a more complex and interesting relationship between the water depth, the dropstone diameter, and the final imprint depth of the dropstone.

The water depth can be reconstructed most commonly for depths $<$ 10 m; the relationship between the dropstone's size and its imprint depth becomes constant for both large and small dropstones, i.e., the velocity of the clast with radius $r = 0.1$ m becomes constant for water depths $>$ 3 m, while a constant velocity is reached for water depths $>$ 8 m for clast with $r = 0.3$ m. The water depth corresponding to the constant velocity of the largest studied dropstones ($r = 0.5$ m) is about 15 m.

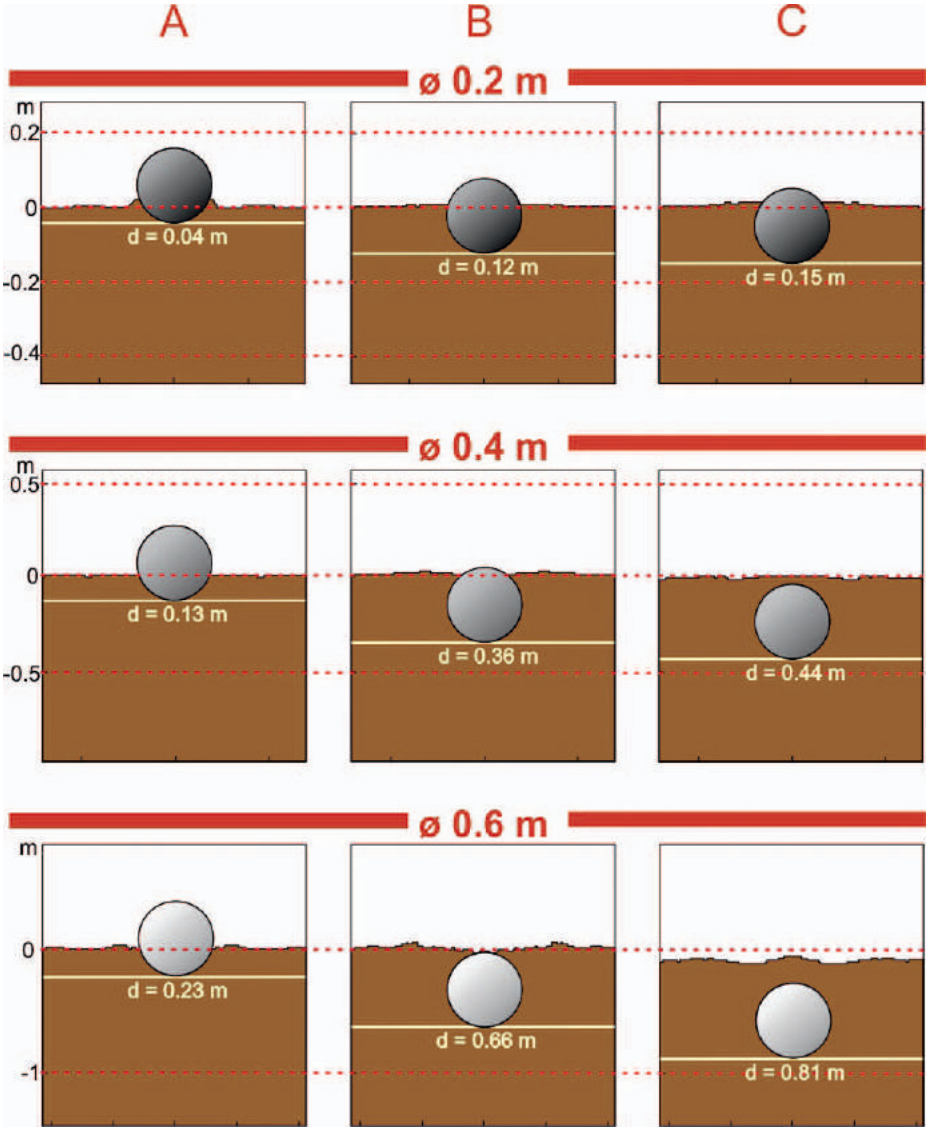

FIG. 3.—Final imprint depth (d) of dropstones with a diameter of 0.2 m (top row), 0.4 m (medium row), and 0.6 m (bottom row) for three sets of strength parameters: **A)** high, **B)** moderate, and **C)** low.

The relationship between the water depth and the final imprint depth of the dropstone therefore is most clear for the biggest dropstones (with a diameter $>$ 0.6 m), whereas it is practically negligible for smaller ones (Fig. 4). The strength of this relationship depends mostly on the dropstone diameter while the transition between strong and negligible influence is smooth. The imprint depth related to the dropstone diameter increases with increasing water depth but becomes constant for depths $>$ 5 m (Fig. 4). It is worth mentioning that the water depth at the time of dropstone deposition cannot be determined unambiguously on the basis of observations of individual small dropstones, but it can be estimated with reasonable accuracy, as will be detailed further on, on the basis of observations of a sufficient number of dropstones in the sediments, or if a sufficiently large dropstone is present.

Deformations Caused by a Dropstone in Laminated Sediments

Simulations show that the intensity and type of deformation structures are related to the diameter of the spherical dropstone (which has a constant and known density) and to the properties of the bottom sediment and to the water depth; the latter two values are commonly not known (Fig. 5). A clear tendency exists indicating that the larger the dropstone is, the deeper its imprint in soft bottom sediments: whereas dropstones with a diameter from 0.4 to 1 m become entirely covered by ejected sediment and are no longer exposed at the surface of the bottom sediments, dropstones with a smaller diameter ($\leq$ 0.2 m) are buried only partially and stick out above the sedimentary surface (Fig. 5). The depth of buried dropstones varies from roughly 5/4 to roughly 4/3 of the dropstone's vertical height (diameter in our model) for dropstones with a diameter of 0.6–1 m, and from roughly 2/3 to roughly 1 for dropstones with a diameter of 0.2–0.4 m. The larger the dropstone, the thicker the deformed sediment above and in the direct vicinity of the dropstone.

All dropstones in the simulation (Fig. 5) penetrate soft-bottom sediments, causing deformations that become not only weaker with increasing lateral distance from the dropstone, which is only logical, but also different in nature. The type and intensity of the deformation

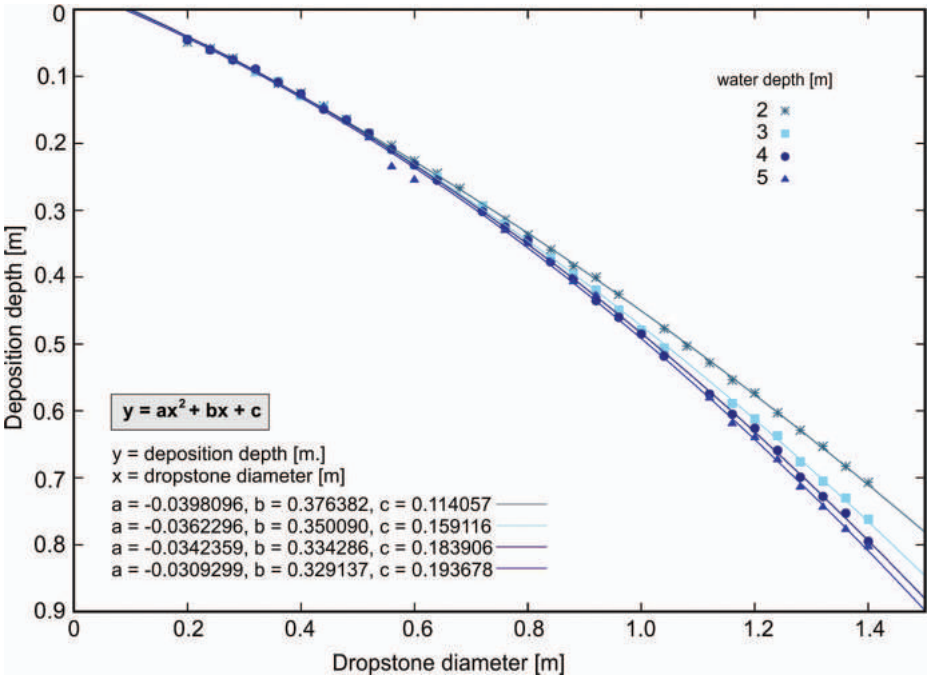

FIG. 4.—Relationship between the dropstone diameter (horizontal axis), water depth (see legend) and final imprint depth (vertical axis). The points in the plot have been obtained by numerical simulations conducted for dropstone with diameters between 0.2 and 1.0 m, whereas the straight lines represent the quadratic regressions of the calculated data. The numerical coefficients for the regression are presented in the legend.

structures caused by the impact of a dropstone depend on the size of the dropstone. In the case of relatively small dropstones (< 0.4 m in diameter), their contact with sediments deposited on top of them will be curved upwards, whereas this will be parallel for dropstones with a diameter > 0.4 m. Penetration into the bottom sediment in combination with "rupturing" of the sediment will result for all sizes of dropstone, but the "ruptured" level of the sediment is, for larger dropstones, thicker than the impact depth (Fig. 5). Furthermore, the lateral displacement of sediments around large dropstones causes the development of bulges against the dropstone. The amplitude of the bulges around the dropstone increases with the dropstone diameter; in sediments with dropstones of 0.2–0.6 m, the bulges look like normal folds, but in the case of the largest dropstones, the bulges resemble overturned folds (Fig. 5).

The morphology of the surface of the soft-sediment bottom is changed by the dropstone impact, i.e., the largest dropstones (with a diameter of 1 m) cause the development of a single bulge and depression around the dropstone (in cross section visible as slightly-marked hummocky like structures at both sides of the dropstone). The impact of smaller dropstones causes a more complex morphology of the bottom surface, with a series of bulges and depressions; the smaller the dropstone, the narrower the bulges. The morphology is changed also because of the amount of sediment ejected by the dropstone. The larger the dropstone, the higher the bottom sediment is ejected: the height of the ejected sediment ranges from roughly 1/5 to roughly 5/3 of the dropstone size for dropstones with a diameter of 0.4–1 m, but smaller dropstones do not eject sediment.

DISCUSSION

The present study shows that sedimentary analysis of the features related to dropstones (depth of imprint, SSDS) can shed some light on the depositional environment, but the link between the imprint depth and the depositional conditions is not simple. Numerous factors influence the final effects of the dropstone impact. Its size (which is taken here spherical, and which can thus be translated into its mass and surface area) is crucial for the drag force causing deceleration when it is falling through the water column. It also influences its kinetic energy and consequently the pressure exerted by the dropstone on the bottom sediments. Next, the water depth has a significant impact on the final velocity (the velocity at the moment when the dropstone reaches the bottom sediments) of the dropstone (see Fig. 2), and hence on its imprint depth.

The simple model shows that the water depth plays a significant role in the dropstone deposition process only for some limit value depending on the dropstone size (see Fig. 2). When the water depth reaches this limit, the impact velocity of the dropstone becomes constant. Also, the sediment properties such as the strength and viscosity of the bottom sediments are crucial for the final effect of the dropstone's impact. In low-strength sediments, the dropstone can become buried completely, causing deformations of the sediment reaching distances of several dropstone radii, whereas high-strength sediments make the dropstone settle on their surface without causing SSDS.

It remains difficult, however, to distinguish between the influences on the final effect of the dropstone impact as resulting from the individual parameters. The reconstruction of the dropstone's depositional process should, consequently, include the whole range of possible scenarios. For example, different imprint depths of dropstones with the same diameter can, obviously, be caused by different water depths, but also by differences in sediment properties. This complexity might raise the idea that the results of the present study are some kind of sophisticated theory rather than a practical tool for field studies. Such an idea would, however, not be justified. Our results suggest that the dropstone deposition process can be unraveled if all parameters are given due attention. Although sediment properties can, as a rule, not be determined from the imprint depth, they can be estimated from the extent and type of deformations caused by the impacting dropstone.

The resulting soft-sediment deformation structures are found in numerous proglacial lacustrine and marine successions (Figs. 6, 7). Our result of the modeling of the impact depth and possible burial by ejected sediment caused by the impact of dropstones with a diameter of 0.2 m (Fig. 6A) is consistent with the observations by Thomas and Connell (1985) for much smaller dropstones (with diameters of 0.05–0.2 m), which became embedded in the sediment for 1/3 up to 2/3 of their height, and from our

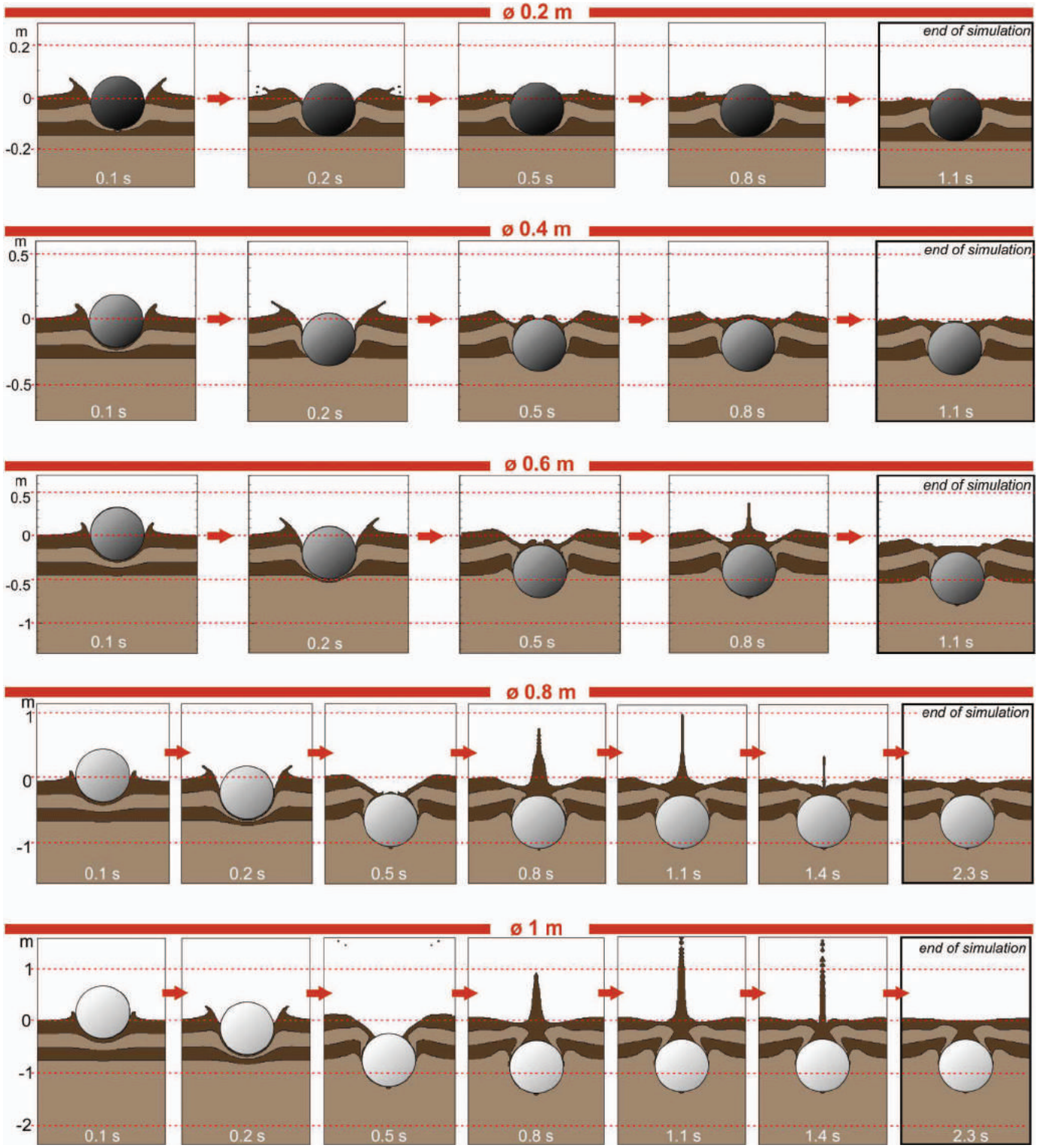

FIG. 5.—Simulation of falling dropstones with diameters of 0.2 m (first row), 0.4 m (second row), 0.6 m (third row), 0.8 m (fourth row), and 1 m (fifth row), calculated in steps of tenth of a second through 2 m deep water after reaching soft bottom sediments, up to the moment that the dropstone stops moving farther downwards.

own field observations (Fig. 6B–F). The modeled curved contact (for dropstones with diameter $\leq$ 0.4 m) with overlying sediments is well known and described as "bending" and "on-lap" structures of dropstones (cf. Thomas and Connell 1985).

The simulated penetration of, as well as the rupturing by, a dropstone is better developed in the case of larger dropstones (Fig. 7A–D), which is consistent field observations (Fig. 7E–G). One should also take into account that erosional processes can erase previously formed structures.

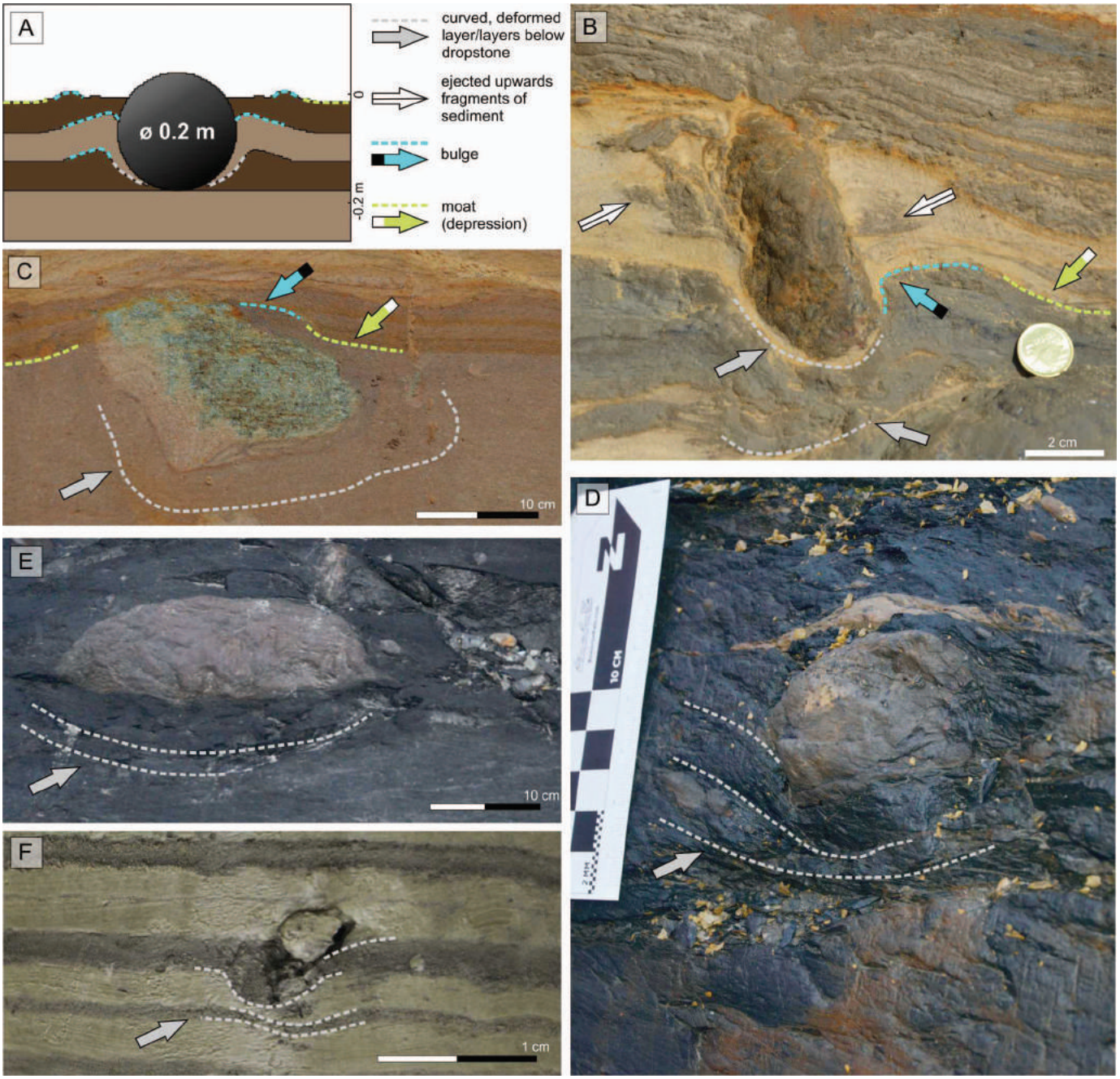

FIG. 6.—Dropstones with diameter smaller than 0.2 m. **A)** Result of simulation with dropstone of diameter 0.2 m falling through 2 m deep water, reaching soft bottom sediments (see Fig. 5). **B)** Dropstone in glaciolacustrine sediments at the Dwasieden site on Rügen island in NE Germany (Pisarska-Jamroży et al. 2018a, 2018b). **C)** Weathered dropstone in lacustrine sediments at the Valmiera site in NE Latvia (Van Loon et al. 2016). **D**, **E)** Dropstones in marine sediments from Treskelen on Svalbard. **F)** Dropstone in varved clay from Onega Lake in Russia (photo by courtesy of Tiit Hang).

Furthermore, the simulated depressions and moat around dropstones have been recognized in the field (Fig. 6, 7). The bulges that can be observed in the field are similar to normal or overturned folds (Fig. 6E, 7E–G). SSDS around dropstones (cf. Thomas and Connell 1985) can, however, also be caused by falling volcanic lapilli (Fig. 8), as found on Cheju Island in South Korea (Sohn and Chough 1989), but the imprinting process of lapilli may be more severe, as the lapilli do not start with a zero velocity at the water surface, but with a higher velocity due to their traveling through the air.

The methods presented in the present study can be implemented successfully in practice. They allow modeling the depositional conditions of the analyzed dropstones by numerical experiments by investigating all possible parameters. Our results provide a reliable tool for future field analyses, considering the consistency between the results of our model and earlier field analyses regarding the depositional conditions of dropstones; it thus provides a useful tool for the reconstruction of the water depth in basins where dropstones were deposited on soft bottom sediments (Fig. 9).

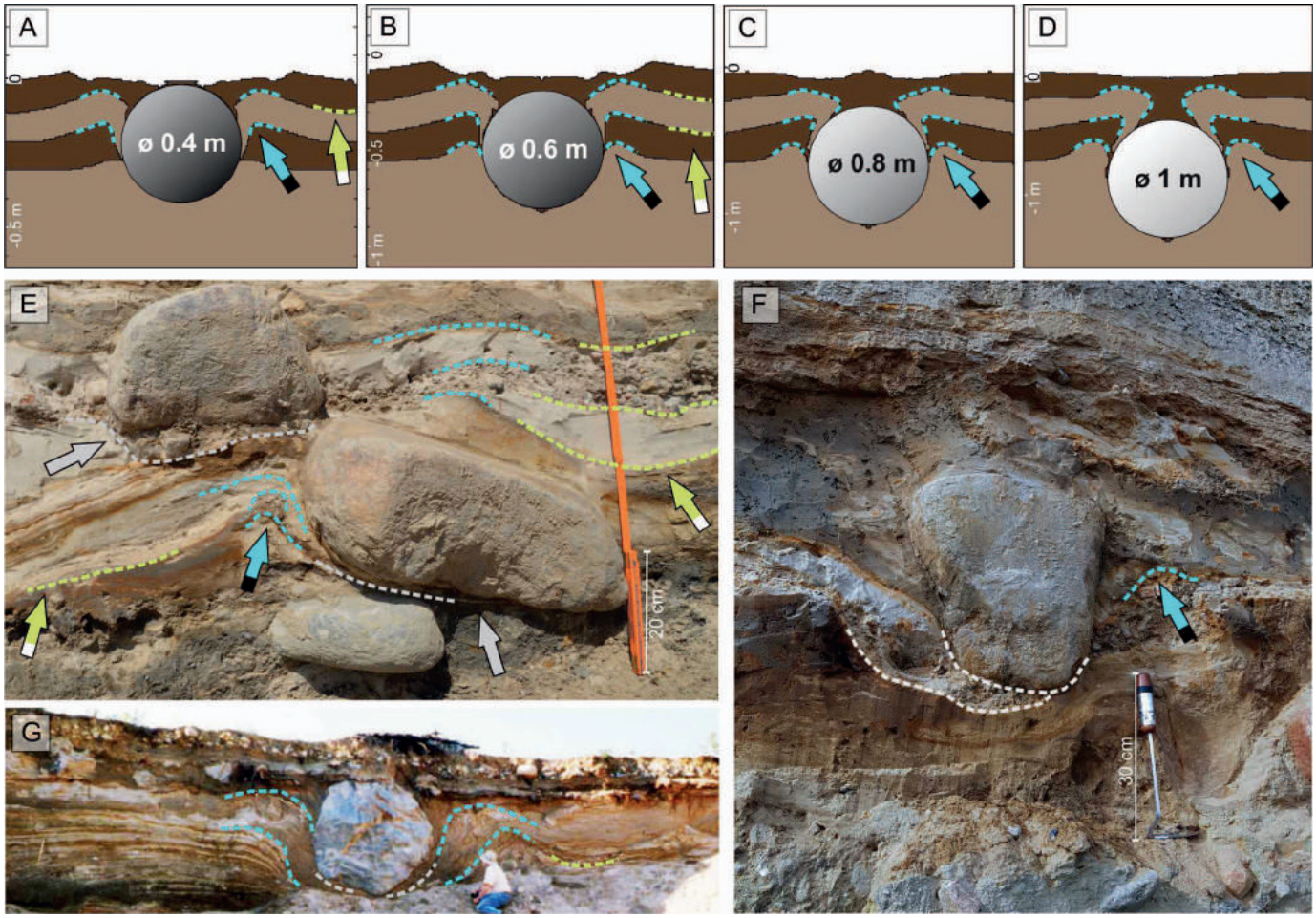

FIG. 7.—Dropstones with diameters larger than 0.2 m. **A–D)** Result of simulation with dropstones with diameters of 0.4, 0.6, 0.8, and 1 m falling through 2-m-deep water after reaching soft bottom sediments (see Fig. 5). For details see Figure 5. **E)** Concentration of dropstones (representing dumpstones) in glaciolacustrine sediments from Dwasieden on Rügen island in NE Germany (Pisarska-Jamroży et al. 2018a, 2018b). **F)** Dropstone from Dwasieden on Rügen island in NE Germany (Pisarska-Jamroży et al. 2018a, 2018b). **G)** Dropstone in glaciolacustrine sediments Nykavarn in SE Sweden (Mokhtari Fard and Van Loon 2004).

Although the whole range of possible parameters are not investigated in the present study, the presented scenarios include at least the most likely ones for the impact of dropstones in lacustrine or marine bottom sediments. The depth of the imprints and the nature of the SSDS in the direct vicinity of dropstones can be used for the reconstruction of the time during which a dropstone settled from a floating iceberg; the same model can, obviously, be applied to lonestones dropped by marine or fresh-water creatures, birds, floating seaweed, or tree stumps.

CONCLUSIONS

The study has resulted in the following conclusions.

1. The presented model allows the reconstruction of the impacting of dropstones (which have been modeled in the present study to be spherical and homogeneous), but the model has several restrictions, which can be summarized as follows:
   (a) the (commonly unknown) material properties of the bottom sediments control the final imprint depth of the dropstone and must be determined as accurately as possible if the water depth at the time of the dropstone impact is to be reconstructed, but practice shows that the assumption of medium strength of the bottom sediment is commonly realistic.
   (b) There is a water depth that limits further increase of the settling velocity of a dropstone (and thus of its impact velocity); the velocity becomes constant after reaching this depth, which depends only on the dropstone size (see Fig. 2). For dropstones in basins that are deeper than the velocity-limiting depth, the reconstruction of the water depth is no longer possible. For basins with depths < 10 m, the relationship between the dropstone's size and its imprint depth becomes constant for both large and small dropstones, i.e., the velocity of a clast with radius $r = 0.1$ m becomes constant for water depths > 3 m, while a constant velocity is reached for water depths > 8 m for clasts with $r = 0.3$ m. The water depth corresponding to the constant velocity of the largest studied dropstones ($r = 0.5$ m) is about 15 m.
2. For reconstruction in the field of the dropstone's impact, the following steps are suggested:
   (a) the properties of the bottom sediment should be determined using the imprint depth of at least three dropstones at the same level in a specific sediment (see Fig. 9);

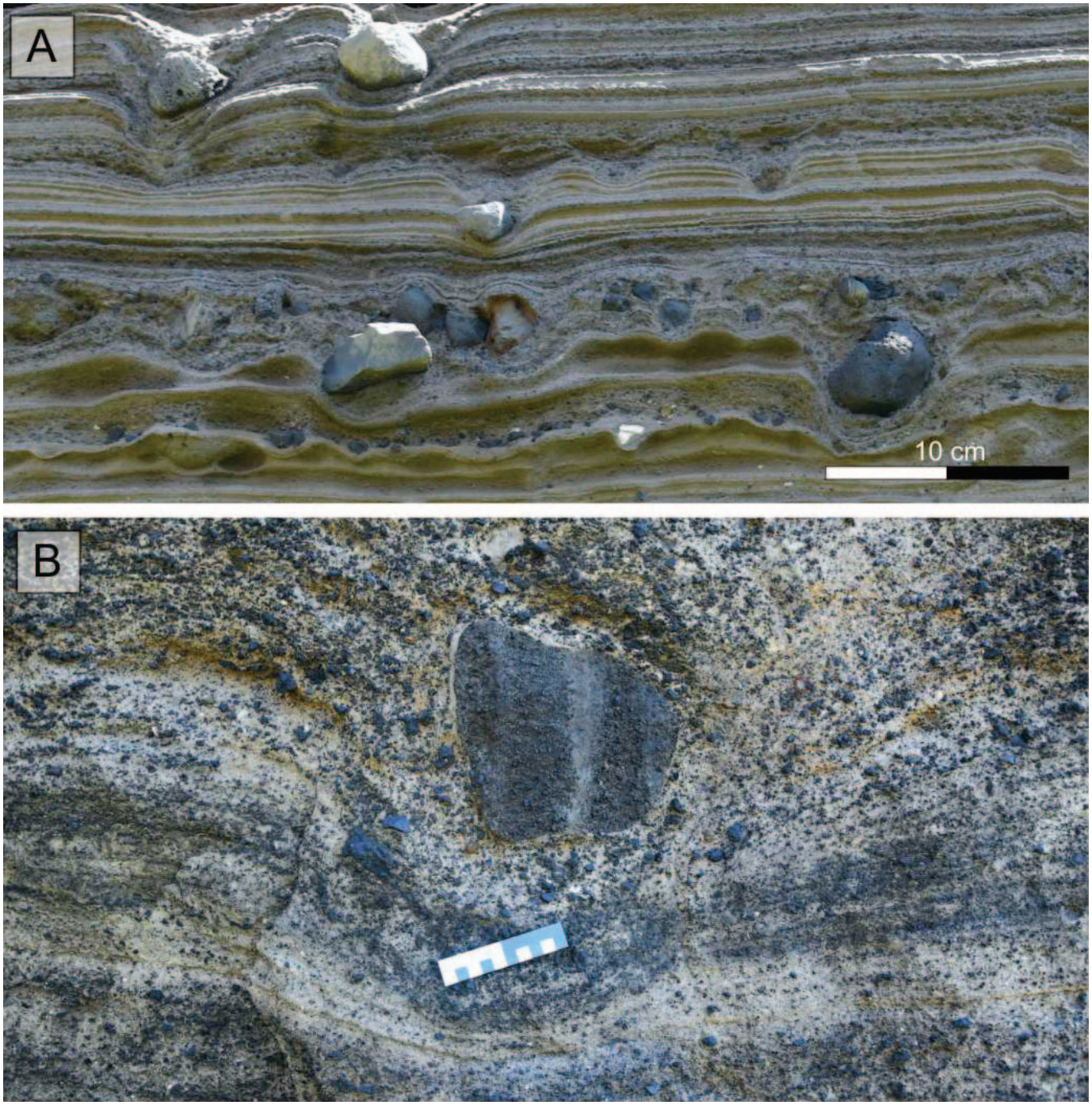

FIG. 8.—**A**, **B)** Soft-sediment deformation structures caused by oversized clasts (lapilli) from the Suwolbong tuff ring on Cheju Island in South Korea (photo by courtesy of Szymon Belzyt).

(b) the water depth at the time of impact should be determined by comparison of the observed imprint depth with the functions provided in Figure 4;

(c) the deformations surrounding the dropstone should be analyzed in order to verify the reconstructed scenario.

3. The deformations caused by the impacting dropstone strongly depend on its diameter; the exact measurements of these soft-sediment deformation structures can also provide information about the impact scenario.

ACKNOWLEDGMENTS

The study was supported by two National Science Center (Poland) grants 2015/19/B/ST10/00661 (GREBAL project) and 2019/33/N/ST10/00095. We acknowledge the developers of iSALE for their priceless work on the iSALE

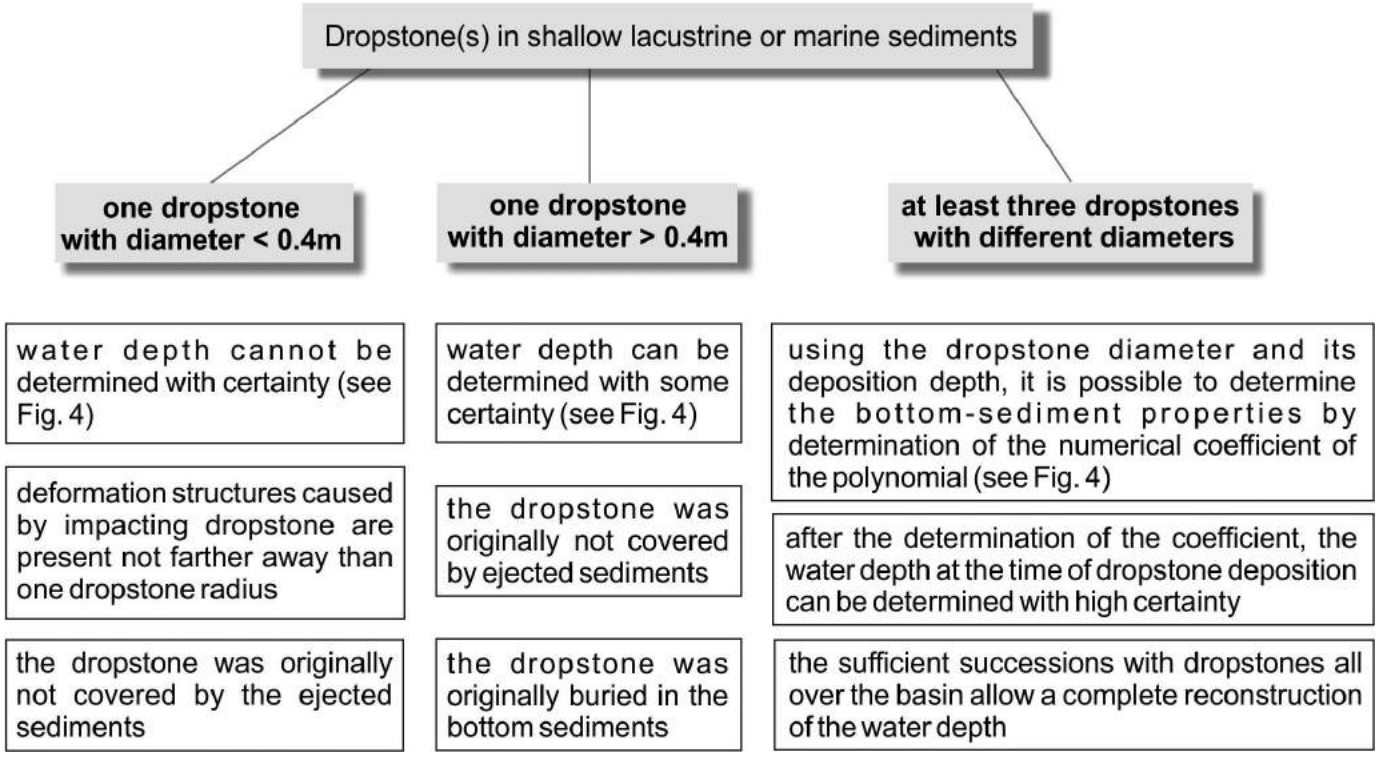

FIG. 9.—Possible applications of the model.

code, three anonymous reviewers and the editor whose comments have improved the manuscript.

REFERENCES

ACKERMANN, E., 1949, Thixitropie bei Umlagerungen feinkörniger Sedimente: Geologische Rundschau, v. 37, p. 100–101.

ACKERMANN, E., 1951, Geröllton!: Geologische Rundschau, v. 39, p. 237–239.

AMSDEN, A., RUPPEL, H., AND HIRT, C., 1980, SALE: a simplified ALE computer program for fluid flow at all speeds: Los Alamos National Laboratories, Report LA-8095.

BENNETT, M.R., DOYLE, P., AND MATHER, A.E., 1996, Dropstones: their origin and significance: Palaeogeography, Palaeoclimatology, Palaeoecology. v. 121, p. 331–339.

BRODZIKOWSKI, K., AND VAN LOON, A.J., 1991, Glacigenic Sediments: Amsterdam, Elsevier, Developments in Sedimentology 49, 664 p.

COLLINS, G.S., AND WÜNNEMANN, K., 2007, Numerical modeling of impact ejection processes in porous targets [Abstract]: 38th Lunar and Planetary Science Conference, Abstract 1338.

CROWELL, J.C., 1959, Origin of pebbly mudstones: Geological Society of America, Bulletin, v. 68, p. 993–1009.

DAVISON, T.M., COLLINS, G.S., ELBESHAUSEN, D., WÜNNEMANN, K., AND KEARLEY, A., 2011, Numerical modeling of oblique hypervelocity impacts on strong ductile targets: Meteoritics & Planetary Science, v. 46, p. 1510–1524.

DE LONG, W.P., DE LANGE, P.J., AND MOON, V.G., 2006, Boulder transport by waterspouts: an example from Aorangi Island, New Zealand: Marine Geology, v. 230, p. 115–125.

DOTT, R.H., JR., 1963, Dynamics of subaqueous gravity depositional processes: American Association of Petroleum Geologists, Bulletin, v. 47, p. 104–128.

DOWDESWELL, J.A., MASLIN, M.A., ANDREWS, J.T., AND MCCAVE, I.N., 1995, Iceberg production, debris rafting, and the extent and thickness of Heinrich layers (H-1, H-2) in North Atlantic sediments: Geology, v. 23, p. 301–304.

DOWDESWELL, J.A., WHITTINGTON, R.J., JENNINGS, A.E., ANDREWS, J.T., MACKENSEN, A., AND MARIENFELD, P., 2000, An origin for laminated glacimarine sediments through sea-ice build-up and suppressed iceberg rafting: Sedimentology, v. 47, p. 557–576.

EYLES, N., EYLES, C.H., AND GOSTIN, V.A., 1997, Iceberg rafting and scouring in the Early Permian Shoalhaven Group of New South Wales, Australia: evidence of Heinrich-like events: Palaeogeography, Palaeoclimatology, Palaeoecology, v. 136, p. 1–17.

GILBERT, R., 1990, Rafting in glacimarine environments: Geological Society of London, Special Publication 53, p. 105–120.

HAARLAND, W.B., HEROD, K.N., AND KRINSLEY, D.H., 1966, The definition and identification of tills and tillites: Earth-Science Reviews, v. 2, p. 225–256.

HEINRICH, H., 1988, Origin and consequences of cyclic ice rafting in the northeast Atlantic Ocean during the past 130,000 years: Quaternary Research, v. 29, p. 142–152.

HESSE, R., AND KHDABAKHSH, S., 2016, Anatomy of Labrador Sea Heinrich layers: Marine Geology, v. 380, p. 44–66.

HOFFMAN, P.F., AND SCHRAG, D.P., 2002, The snowball Earth hypothesis: testing the limits of global change: Terra Nova, v. 14, p. 129–155.

HOHL, R., 1934, Zur Frage der Gerölltone: Zentralblatt für Mineralogie, Geologie und Paläeontologie, Abteilung B: Geologie und Paläotologie, 1934, p. 226–229.

JOKIEL, P.L., 1990, Long-distance dispersal by rafting: re-emergence of an old hypothesis: Endeavour, v. 14, p. 66–73.

JOLLIFFE, I.P., 1989, The rafting of shingle under the agency of seaweeds: Progress in Underwater Science, v. 13, p. 65–78.

KALM, V., AND KADASTIK, E., 2000, Waterlain glacial diamicton along the Palivere ice-marginal zone on the west Estonia Archipelago, eastern Baltic Sea: Estonian Academy of Sciences, Proceedings, v. 50, p. 114–127.

KORNICKER, L.S., AND SQUIRES, D.F., 1962, Floating corals: a possible source of erroneous distribution data: Limnology and Oceanography, v. 7, p. 447–452.

LECKIE, D.A., MORGANS, H., WILSON, G.J., AND EDWARDS, A.R., 1995, Mid-Paleocene dropstones in the Whangai Formation, New Zealand: evidence of mid-Paleocene cold climate?: Sedimentary Geology, v. 97, p. 119–129.

LE HERON, D.P., 2015, The significance of ice-rafted debris in Sturtian glacial successions: Sedimentary Geology, v. 322, p. 19–33.

LIVINGSTONE, S.J., PIOTROWSKI, J.A., BATEMAN, M.D., AND ELY, J.C., 2015, Discriminating between subglacial and proglacial lake sediments: an example from the Dänischer Wohld Peninsula, northern Germany: Quaternary Science Reviews, v. 112, p. 86–108.

MENZIES, J., 2002, Modern and Past Glacial Environments: Elsevier, 576 p.

MILJKOVIĆ, K., COLLINS, G.S., PATEL, M.R., CHAPMAN, D., AND PROUD, W., 2012, High-velocity impacts in porous solar system materials: American Institute of Physics, Conference Proceedings, v. 1426, p. 871–874.

MOKHTARI FARD, A., AND VAN LOON, A.J., 2004, Deformation of an early Preboreal deposit at Nykvarn (SE Sweden) as a result of the bulldozing effect of a grounding iceberg: Sedimentary Geology, v. 165, p. 355–369.

OARD, M.J., 2008, What is the meaning of dropstones in the rock record?: Journal of Creation, v. 22, p. 3–5.

OSBORNE N.M., ENRIGHT, N.J., AND PARNELL, K.E., 1991, The age and stratigraphic significance of sea-rafted Loisels Pumice in northern New Zealand: Royal Society of New Zealand, Journal, v. 21, p. 357–371.

PIERAZZO, E., ARTEMIEVA, N., ASPHAUG, N., BALDWIN, E., CAZAMIAS, E.C., COKER, R., COLLINS, G.S., CRAWFORD, D.A., DAVISON, T., ELBESHAUSEN, D., HOLSAPPLE, K.A., HOUSEN, K.R., KORYCANSKY, D.G., AND WÜNNEMANN, K., 2008, Validation of numerical codes for

impact and explosion cratering: impacts on strengthless and metal targets: Meteoritics & Planetary Science, v. 43, p. 1917–1938.

Pisarska-Jamroży, M., Van Loon, A.J., and Bronikowska, M., 2018a, Dumpstones and dropstones as records of overturning ice rafts in a Weichselian proglacial lake (Rügen Island, NE Germany): Geological Quarterly, v. 62, p. 917–924.

Pisarska-Jamroży, M., Belzyt, S., Börner, A., Hoffmann, G., Hüneke, H., Kenzler, M., Obst, K., Rother, H., and Van Loon, A.J., 2018b, Evidence from seismites for glacio-isostatically induced crustal faulting in front of an advancing land-ice mass (Rügen Island, SW Baltic Sea): Tectonophysics, v. 745, p. 338–348.

Shampine, L., Watts, H., and Davenport, S., 1976, Solving non-stiff ordinary differential equations: the state of the art: SIAM Review, v. 18, p. 376–411.

Smith, L.M., and Andrews, J.T., 2000, Sediment characteristics in iceberg dominated fjords, Kangerlussuaq region, East Greenland: Sedimentary Geology, v. 130, p. 11–25.

Sohn, Y.K., and Chough, S.K., 1989, Depositional processes of the Suwolbong tuff ring, Cheju Island (Korea): Sedimentology, v. 36, p. 837–855.

Syvitski, J.P.M., and Van Everdingen, D.A., 1981, A re-evaluation of the geological phenomenon of sand floatation: a field experimental approach: Journal of Sedimentary Petrology, v. 51, p. 1315–1322.

Thomas, G.S., and Connell, R.J., 1985, Iceberg drop, dump, and grounding structures from Pleistocene glacio-lacustrine sediments: Journal of Sedimentary Petrology, v. 55, p. 243–249.

Van Loon, A.J., 1970, Grading of matrix and pebble characteristics in syntectonic pebbly mudstones and associated conglomerates, with examples from the Carboniferous of northern Spain: Geologie en Mijnbouw, v. 49, p. 41–55.

Van Loon, A.J., 2008, Could "Snowball Earth" have left thick glaciomarine deposits?, *in* Maruyama, S., and Santosh, M., eds., Snowball Earth to Cambrian Explosion: Gondwana Research, v. 14, p. 73–81.

Van Loon, A.J., Pisarska-Jamroży, M., Nartišs, M., and Krievâns, M., 2016, An erratic dropstone of granodiotite with a water-escape structure from a Weichselian terrace along the River Gauja (NE Latvia): Catena, v. 140, p. 140–144.

Van Loon, A.J., Soms, J., Nartišs, M., Krievāns, M., and Pisarska-Jamroży, M., 2019, Sedimentological traces of ice-raft grounding in a Weichselian glacial lake near Dukuli (NE Latvia): Baltica, v. 32, p. 170–181.

Williams, G.E., Gostin, V.A., McKirdy, D.M., and Preiss, W.V., 2008, The Elatina glaciation, late Cryogenian (Marinoan epoch), South Australia: sedimentary facies and palaeoenvironments: Precambrian Research, v. 163, p. 307–331.

Winsemann, J., Asprion, U., Meyer, T., Schultz, H., and Victor, P., 2008, Evidence of iceberg-ploughing in a subaqueous ice-contact fan, glacial Lake Rinteln, NW Germany: Boreas, v. 32, p. 386–398.

Woodborne, M.W., Rogers, J., and Jarman, N., 1989, The geological significance of kelp-rafted rock along the West Coast of South Africa: Geo-Marine Letters, v. 9, p. 109–118.

Wünnemann, K., Collins, G., and Melosh, H., 2006, A strain-based porosity model for use in hydrocode simulations of impacts and implications for transient crater growth in porous targets: Icarus, v. 180, p. 514–527.

Yorke, L., Rumsby, B.T., and Chiverrell, R.C., 2012, Depositional history of the Tyne valley associated with retreat and stagnation of Late Devensian ice streams: Proceedings of the Geologists' Association, v. 123, p. 608–625.

Received 12 July 2020; accepted 4 February 2021.

Artykuł nr 3
Paper no. 3

Pisarska-Jamroży, M., Van Loon, A.J., **Bronikowska, M.**

Dumpstones and dropstones as records of overturning ice rafts in a Weichselian proglacial lake (Rügen Island, NE Germany)

Geological Quarterly 62, 917-924.

Geological Quarterly, 2018, **62** (4): 917–924
DOI: http://dx.doi.org/10.7306/gq.1448

Dumpstones as records of overturning ice rafts in a Weichselian proglacial lake (Rügen Island, NE Germany)

Małgorzata PISARSKA-JAMROŻY[1, *], A.J. (Tom) VAN LOON[2, 3] and Małgorzata BRONIKOWSKA[1]

[1] Adam Mickiewicz University, Geological Institute, Krygowskiego 12, 61-680 Poznań, Poland

[2] Shandong University of Science and Technology, College of Earth Science and Engineering, Qingdao 266590, Shandong, China

[3] Geocom Consulting, Valle del Portet 17, 03726 Benitachell, Spain

Pisarska-Jamroży, M., Van Loon, A.J., Bronikowska, M., 2018. Dumpstones as records of overturning ice rafts in a Weichselian proglacial lake (Rügen Island, NE Germany). Geological Quarterly, **62** (4): 917–924, doi: 10.7306/gq.1448

Associate editor: Wojciech Granoszewski

Dumpstones and dropstones up to 0.8 m in size occur in a silty/sandy Weichselian glaciolacustrine succession near Dwasieden on Rügen Island in the SW Baltic Sea (NE Germany). The deposits are exceptional because two levels of dumpstones and dropstones are present, suggesting two dumping phases interrupting characteristic fine-grained glaciolacustrine sedimentation. Plastic downwarping of sediments below the dumpstones and dropstones result in soft-sediment deformation structures. The distribution and orientation of the long axes of the clasts are useful tools for the reconstruction of the state of the lake bottom, as well as for the water depth. The horizontal position of the gravels and boulders (parallel to the bedding) suggests deposition in relatively shallow-water. The dumping events are linked to iceberg rafting in a glacial lake during the Weichselian Glaciation (MIS 2).

Key words: dumpstones, dropstones, ice-rafted debris, Weichselian, glaciolacustrine sediments.

INTRODUCTION

Icebergs and ice rafts are free to float in lakes and seas under the influence of the wind and/or currents. Iceberg rafting is a common process in contemporary polar regions (Cowan et al., 1997; Smith and Andrews, 2000; Dowdeswell et al., 2000; Hass, 2002; Menzies, 2002) and was common also during the Pleistocene glaciations (Dowdeswell et al., 2000; Kalm and Kadastik, 2000; Menzies, 2002; Błaszkiewicz and Gruszka, 2005; Williams et al., 2008; Ampaiwan et al., 2009; Yorke et al., 2012; Le Heron, 2015; Livingstone et al., 2015).

Single large icebergs can carry many thousands of particles of all sizes; these are dispersed within the ice and are jointly called “ice-rafted debris” (IRD) (Hoffman and Schrag, 2002). These particles are released when the ice melts. Most IRD released from icebergs is sand-sized, but often there are also larger particles (Hass, 2002).

ICE-RAFTED DEBRIS

Melting of the subaqueous part of a floating ice mass results in the release of sedimentary particles that are embedded in the ice. They sink through the water column and accumulate on the surface of the sea or lake bottom, which most commonly consists of fine-grained sediments. The main process involved in the release of IRD is melting of the ice. Most melting occurs subaqueously, due to thermal subrosion caused by the above-zero temperature of the ambient water. Subaerial melting results in a concentration of IRD on the – commonly irregular – surface of the iceberg.

The grain size distribution of IRD within a sediment depends on the properties of the source material, but the characteristics of deposited IRD also depend on depositional processes such as sorting during settling and winnowing, for instance by wave action and currents, within the water column and at the bottom (e.g., Anderson et al., 1980).

DEPOSITS WITH IRD

IRD can be set free from icebergs or ice rafts in different ways, and there are consequently also different depositional processes involved. The result is that different types of deposits, consisting either exclusively of IRD or of dispersed IRD in autochthonous sediments, can originate.

* Corresponding author, e-mail: pisanka@amu.edu.pl

Received: May 17, 2018; accepted: September 21, 2018; first published online: December 21, 2018

The released clasts that sink through the water column can, if large enough, easily deform the water-saturated fine-grained sediments that commonly are present at the bottom of an ocean or lake. They can partly or completely penetrate, and occasionally even rupture, the bottom sediments. When a mass of particles is jointly released from an iceberg as a result of overturning or a gravity flow, a chaotic (sometimes large) dump structure is formed (Miller, 1996).

The deposits that consist of – or contain – IRD have been studied by researchers in different disciplines (e.g., Quaternary geologists, marine geologists, climatologists, sedimentologists). The result is that different terms have been used for the various types of such deposits, which has occasionally led to confusion. We therefore indicate in the following two subsections which terms are applied to indicate the dropstone and dumpstone deposits under study here.

DROPSTONES

Dropstones have been described frequently from both glaciolacustrine and marine deposits (e.g., Leckie et al., 1995; Bennett et al., 1996; Smith and Andrews, 2000; Van Loon et al., 2016). They are formed when particles (commonly pebble-sized or larger, as smaller particles cannot always be distinguished from the autochthonous sediments) are released from the subaqueous part of an iceberg by thermal subrosion.

Commonly floating icebergs move so fast, under the influence of currents, that only scattered dropstones occur in the autochthonous sediment. Yet, the total amount of dropstones left by a passing iceberg can be so large that the pathway followed by the iceberg can be traced. This is well-known from, among other features, the Heinrich events that left abundant IRD on the floor of the Atlantic Ocean (Heinrich, 1988; Dowdeswell et al., 1995; Eyles et al., 1997; Hesse and Khodabakhsh, 2016).

Pebble-sized and larger IRD can commonly be recognized as dropstones if they deform underlying laminae. Granules are also called dropstones when their size is larger than the thickness of the strata in which they are embedded (Haarland et al., 1966; Menzies, 2002).

The dropstones found in the glaciolacustrine deposits under study here are described in a following section.

DUMPSTONES

A special situation exists when an iceberg or ice raft becomes unstable because of asymmetrical thermal subrosion of the subaqueous part or – less commonly – by continuous melting of one side of the subaerial part under the influence of solar irradiation. In such a case, the iceberg can suddenly tumble over. The particles set free on the irregular ice surface then are jointly released, which may result in uncommonly high concentrations of IRD – occasionally even in the form of stone heaps – on the lake or sea-floor.

The thus-formed clusters of IRD create lens-shaped beds of coarse deposits and have been called “berg dumps” and “dumpstones” (Thomas and Connell, 1985). They have also been described as “iceberg overturn deposits” (see Gilbert, 1990; Woodworth-Lynas and Dowdeswell, 1994; Cowan et al., 1997; Dowdeswell et al., 2000), “palimpsest lags” (Powell, 1984), “gravel pods” (Yorke et al., 2012), “iceberg dump tills” (if the coarser particles are deposited together with melt-out diamictons), “rain-out diamicts” (Brodzikowski and Van Loon, 1991), “dropstone diamictons” and “dropstone mud” (Benn and Evans, 1998). Dumpstones have only fairly rarely been described, among others by Woodworth-Lynas and Dowdeswell (1994), Bennett et al. (1996), Mokhtari Fard and Van Loon (2004), and Ampaiwan et al. (2009). Descriptions of dumpstones that originated in a glaciolacustrine setting are even rarer; they are commonly considered as an important indicator of an ice-contact calving margin (e.g., Cowan et al., 1997; Yorke et al., 2012), and are typical of ice-contact lakes (Brodzikowski and Van Loon, 1991).

The process responsible for the deposition of such sediments is commonly called a “dumping event” (Dowdeswell and Murray, 1990). Following this usage, we adopt the term “dumpstones” to indicate such types of deposits. They form the main subject of the present contribution and will be described and analysed in a following section.

SEDIMENTARY AND STRATIGRAPHICAL CONTEXT

The glaciolacustrine deposits under study are exposed in a coastal cliff near Dwasieden (Germany), on Rügen, an island in the southwestern part of the Baltic Sea (Fig. 1). The deposits form part of a Saalian and Weichselian succession; the deposits on which we focus here have been dated by OSL as Weichselian (Steinich, 1992; Krbetschek, 1995; Ludwig, 2006; Ludwig and Panzig, 2010).

The Weichselian Glaciation in Northern Germany is divided into three main phases (Liedtke, 1981), viz. (1) the Brandenburgian Phase, between 24 and 20 ka (Heine et al., 2009; Kenzler et al., 2015, 2017), (2) the Pomeranian Phase,

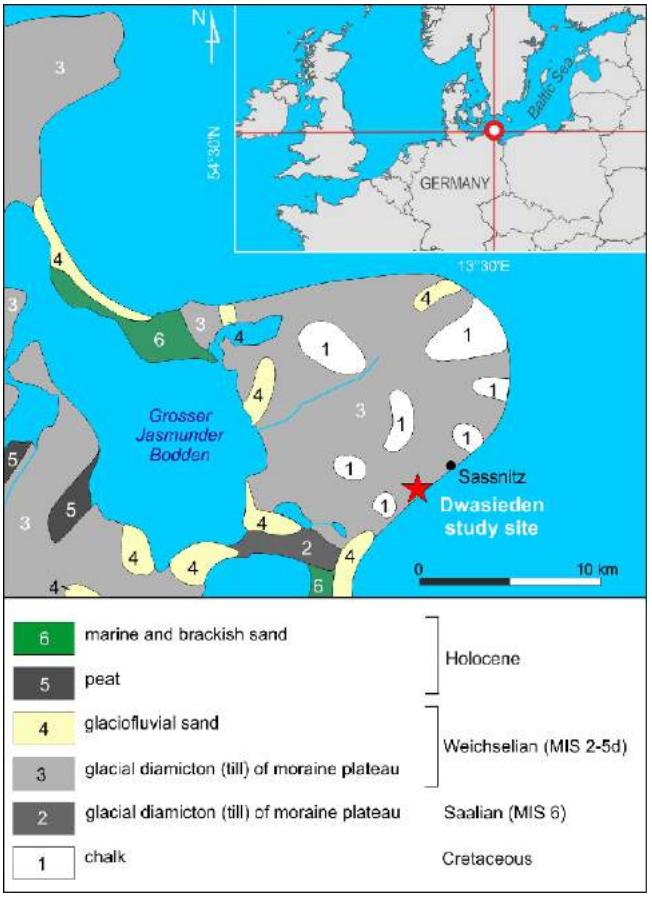

Fig. 1. The study site at Dwasieden in its geological setting

between 20 and 16 ka (Litt et al., 2007; Heine et al., 2009; Lüthgens and Böse, 2011; Lüthgens et al., 2011; Rinterknecht et al., 2014), and (3) the Mecklenburgian Phase, approx. 16–15 ka (Kaiser et al., 2009; Küster and Preusser, 2009; Rinterknecht et al., 2014) or up to 14–12 ka in the case of the Angermünde-Chojna subphase of the Mecklenburgian Phase (Pisarska-Jamroży, 2013).

The lowermost diamicton in the cliff section, directly below the glaciolacustrine sediments under study, was deposited during the Saalian Glaciation (MIS 6), whereas the overlying diamicton, directly above the glaciolacustrine deposits, represents the Brandenburgian Phase of the Weichselian Glaciation (MIS 2; cf. Kenzler et al., 2015, 2017; Pisarska-Jamroży et al., 2018).

METHODS

The various deposits of the section under study have been investigated sedimentologically, distinguishing a number of lithofacies that have been coded following Miall's (1978) classification, with a slight modification introduced by Zieliński and Pisarska-Jamroży (2012). All lithofacies symbols are explained in the figure captions.

The grain size of the deposits is indicated according to the Udden-Wentworth scale (Udden, 1914; Wentworth, 1922). Despite the fact that the IRD include the full spectrum of grain sizes, we focused in the field on macroscopically recognizable IRD. The orientation of the long axes of elongated gravels and boulders as well as the orientation of striae on pebble-sized clasts have been measured.

THE DUMPSTONES AND DROPSTONES

As far as we are aware, no dumpstone deposits suggesting two phases of dumping have been described before from a Weichselian proglacial lake. Here, we describe some characteristic examples of dumpstones and dropstones from the cliff section at Dwasieden.

DESCRIPTION

The Weichselian glaciolacustrine deposits in the cliff section contain significant quantities of outsized clasts in the form of dumpstones and dropstones at several locations and at different levels (Fig. 2). The glaciolacustrine succession overlies a glacial diamicton (till) and is also overlain by a glacial diamicton (lithofacies Dm in Figs. 3 and 4); the lower diamicton is 1–1.5 m thick and was deposited as a subglacial traction till during the Saalian Glaciation, whereas the upper one is up to 2 m thick and also represents a subglacial traction till, which was, however, formed during the Brandenburgian Phase of the Weichselian Glaciation (cf. Kenzler et al., 2015, 2017).

The clasts representing IRD in the glaciolacustrine deposits are up to 0.8 m in size and consist predominantly of Scandinavian granitoids (Fig. 3). Moreover, two clasts with glacial striae on some of their surfaces (Fig. 3E) are clear evidence of a glacigenic origin. Due to the random occurrence of the clasts, the orientation of the glacial striae on the two clasts does not provide any reliable information about the direction of the source area, the transport direction of the ice, or the depositional process. The hosting glaciolacustrine deposits are 1.5 m thick and consist of deformed and horizontally-laminated silts and fine sands (Fig. 2). The coarser clasts are irregularly distributed in a 20 m long and commonly some 10 cm thick lenticular layer; they form occasionally clusters of boulder-sized

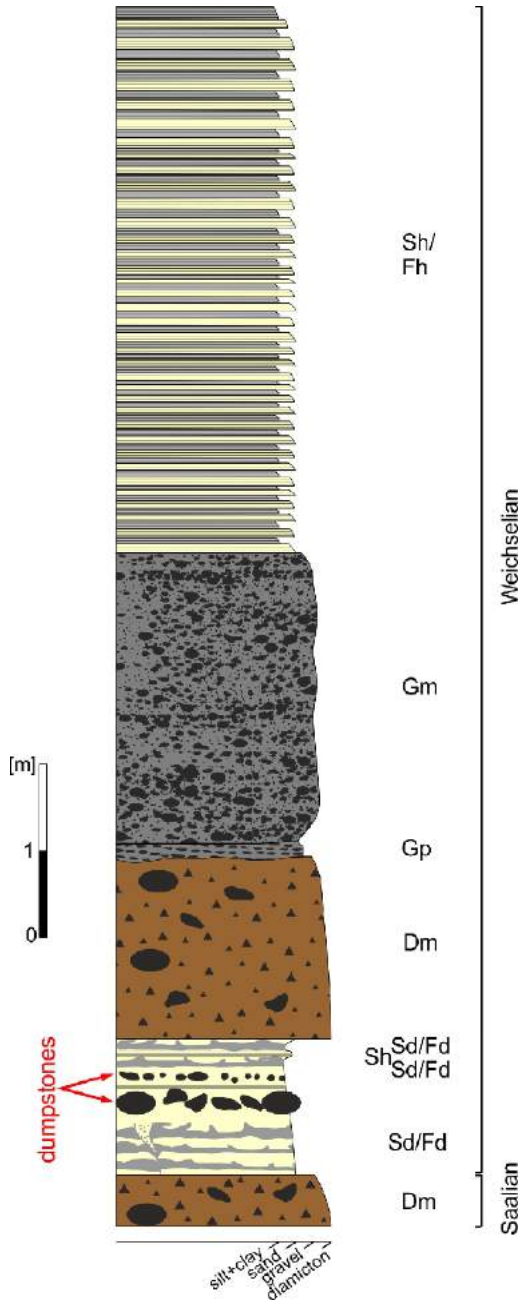

Fig. 2. The succession in the cliff section in Dwasieden on Rügen Island, showing the position of dumpstone deposits within glaciolacustrine sediments

Dm – massive diamicton, Fd – deformed fines, Fh – horizontally-laminated fines (silt + clay), Gm – massive gravel, Gp – planar cross-stratified gravel, Sd – deformed sand, Sh – horizontally-laminated sand

and smaller particles within this layer, and are occasionally covered by a thin drape, in such a way that the hosting layer has locally an exceptional thickness that is roughly equal to the visible vertical size of the boulders (Fig. 3).

In addition to the clusters, some boulders occur as isolated outsized clasts (Fig. 3C – see the clasts on the left side of the photo). These are present below the above-mentioned lenticular layer with boulder clusters but still within glaciolacustrine deposits. Also in this lower level, however, some clusters of outsized clasts are present, forming lenses that are up to 1.5 m long; the clasts concentrated in these clusters show

Fig. 3. Boulder-sized dumpstones in the Dwasieden glaciolacustrine deposits

A–**D** – horizons of large dumpstones; **E** – glacial striae on the surface of some gravel-sized dumpstones; explanations as on Figure 2

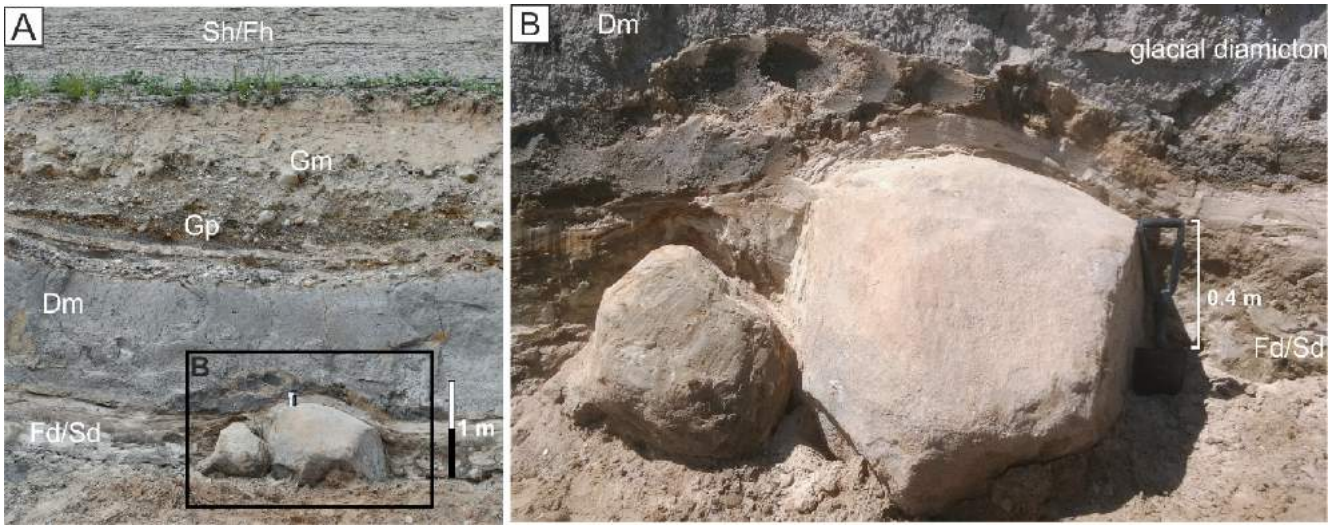

Fig. 4. Dumpstones within fine-grained sandy, thin, curved layer draped by sandy sediments

Explanations as on Figure 2

grain-to-grain contacts (Figs. 3A–D and 4). The long axes of most of these clasts are oriented parallel or semi-parallel (Fig. 3C) to the lamination but some elongate clasts (with length/width ratios ranging from about 1.5 to about 2) are positioned almost perpendicular to the lamination (Fig. 5A, B).

The larger clasts penetrate and deform (locally in a fairly chaotic way) the underlying silty and sandy laminae; in particular in the direct vicinity of the largest clasts, the laminae are strongly deformed (Figs. 4 and 5). The laminations immediately below the grains are down-warped, and the laminae are laterally truncated (Figs. 3C and 5). In contrast, laminae overlying the clasts are gently curved, draping them, commonly with some deflection (Fig. 4B). This type of boundary contact between IRD and the host sediment has been called “bedding contact” by Thomas and Connell (1985).

INTERPRETATION

The glaciolacustrine silty and sandy sediments in the lower part of the Dwasieden cliff were deposited in a lake at the front of the ice. The different grain sizes must be ascribed to the settling of silt with an admixture of clay particles that were widely dispersed via interflows and underflows, in combination with sands that were probably derived from inflowing meltwater from the nearby ice sheet (cf. Smith and Ashley, 1985; Best et al., 2005; Pisarska-Jamroży, 2013).

The occurrence of particles with strongly different (much larger) sizes than the lacustrine host sediments indicates a completely different depositional mechanism. The only feasible interpretation of the local deposits with boulders is that these were formed as dumpstones, derived from ice rafts that tumbled over and released all particles that had been set free on their surface due to melting. This interpretation is supported by the fact that the laminae above the pebbles and boulders are thinner than the laminae at their sides: the autochthonous sedimentation was less on top of the clasts that stuck out above the sedimentary surface of the lake. The same is visible for the outsized clasts that are present at a lower level, and that show a similar thinning of the drapes that cover them (cf. Thomas and Connell, 1985). There is no evidence of plough marks and squeezing-up (sediment prows) around the clasts that might suggest subglacial traction or melting-out processes (cf. Jørgensen and Piotrowski, 2003). Most of the boulder-sized, rounded and subrounded dumpstones were deposited parallel or semi-parallel to the bedding. This suggests that they were not re-oriented in the water column, in contrast to the smaller (pebble-sized) clasts, at least as far as they are elongated, showing a relatively high length/width ratio of at least approx. 2 (Figs. 5 and 6).

The dumping of clasts from ice rafts in the proglacial lake at Dwasieden apparently took place in at least two phases, as can be deduced from the two exposed levels that contain dumpstones and dropstones. These two levels are separated by silty and sandy sediments without large clasts, pointing at a break in the deposition of IRD.

DISCUSSION

Four main processes are commonly held responsible for the formation of dropstones and/or dumpstones: (1) biological rafting, (2) ice rafting, (3) flotation, and (4) projectiles (see Bennett et al., 1996). Biological rafting can be excluded for the Dwasieden deposits because of the climate during the Weichselian Glaciation. Flotation can also be excluded, as only small grains (up to 25 mm) can float on water due to surface tension (Syvitski and Van Everdingen, 1981). Projectiles are almost exclusively linked to volcanic activity (volcanic bombs) or astronomical processes (meteorites), and the composition of the clasts at Dwasieden does exclude such an origin. It can thus be stated with certainty that the dumpstones and dropstones at Dwasieden were released from melting ice rafts. According to Houmark-Nielsen and Kjær (2003), the study area was covered by a glaciolacustrine basin between 33–23 ka; this seems consistent with the palaeogeographical study by Anjar et al. (2012). This lake could be reached occasionally by ice rafts carrying IRD (see Hambrey, 1994).

The presence of at least two levels of dumpstones and dropstones suggests that the clasts in the lower level (which contains significantly less IRD than the upper level) were deposited during one phase of iceberg melting, followed by “normal” glaciolacustrine sedimentation; the same or another ice

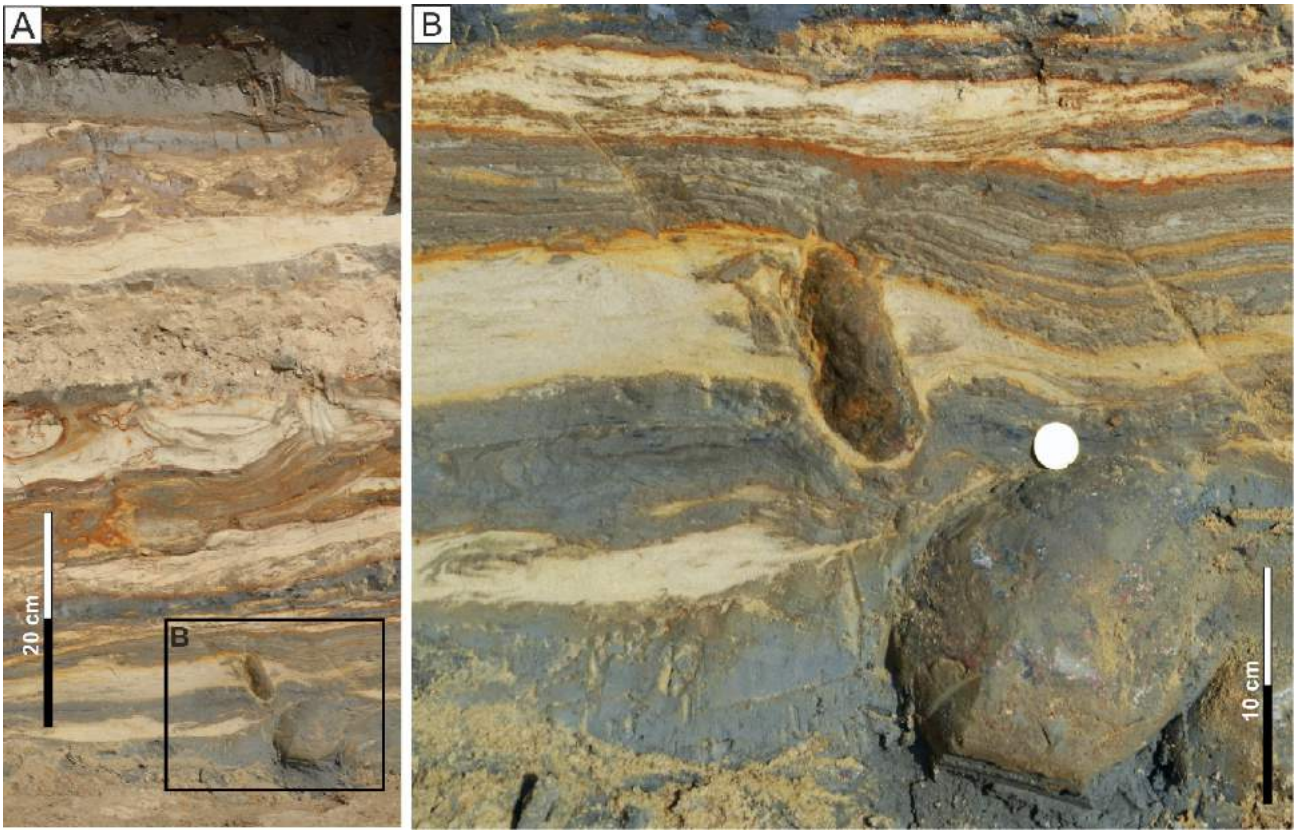

Fig. 5. Dropstones in the glaciolacustrine deposits

A – two dropstones, the lower one quasi-isometric and the upper one elongated;
B – dropstones separated by deformed sandy and silty deposits

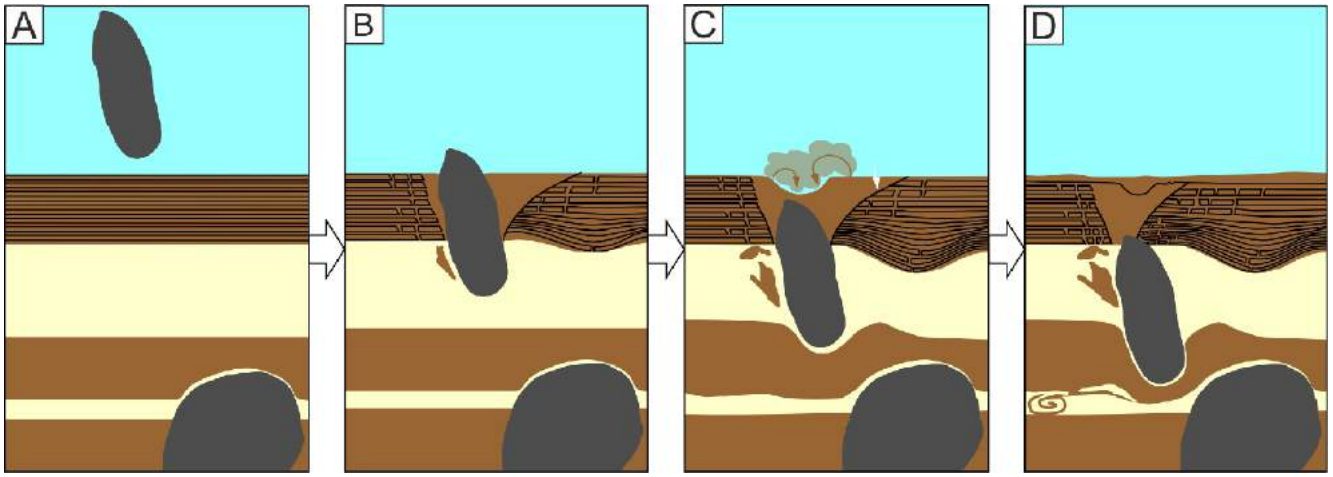

Fig. 6. Schematic model of a dropstone falling through the water column (A), the dropstone penetrates and deforms the bottom sediment (B), causes resuspension of sediments (C), and development of soft-sediment deformation structures (D)

Compare with Figure 5

raft subsequently probably gradually became unstable, eventually tumbling over and dumping its sediment load as dumpstones in a stratigraphically higher layer (Fig. 3C).

Most cobble- and boulder-sized clasts are aligned more or less parallel to the laminae of the host sediment, which suggests according to Benn and Evans (1998) that the bottom sediment was soft and mostly unable to hold the falling elongated clasts in the vertical position that they might have taken during their fall through the water column. Some examples of vertically positioned clasts are, however, present (Fig. 5). On the other hand, no deformation structures have been found, indicating that clasts hitting the bottom fell over, or that they followed a somewhat tortuous pathway during their fall (as do leaves falling from a tree) and hit the bottom at an angle. It thus must be deduced that the clasts that were not exceptionally flattened most likely had insufficient time during their fall through the water column to obtain the vertical position that would have given the least resistance. This, in turn, might indicate that the lake was relatively shallow (probably a few to maximally about ten meters), which would explain why only one ice raft (possibly two) could reach the Dwasieden site, melt, and drop their sediment load.

The sedimentary surface hit by the settling clasts must have been water-saturated and still unconsolidated, because water-escape structures are absent in the sediments below and immediately beside the large stones; such structures would certainly have originated in compacted sediments after a large clast had fallen on the bottom, considering the sudden increase in pore-water pressure that the falling clast would have caused (cf. Domack and Lawson, 1985; Knudsen and Marren, 2002).

CONCLUSIONS

The following conclusions can be drawn from this study.

1. The Dwasieden area was covered by a lake during MIS 2; boulder- sand cobble-sized IRD released from ice rafts in this lake, occasionally in the form of dumpstones, are embedded in the fine-grained glaciolacustrine deposits.

2. Lack of escape structures below and alongside large dropstones or dumpstones indicates a non-consolidated state of the bottom sediments when the dropstones or dumpstones were deposited.

3. A bed-parallel position of flattened and/or elongated clasts suggests a relatively shallow depositional environment.

Acknowledgements. We thank M. Kenzler and W. Wysota, for valuable suggestions that improved the quality of our contribution. The study has been financially supported by a grant for the GREBAL project (No. 2015/19/B/ST10/00661) from the National Science Centre Poland.

REFERENCES

Ampaiwan, T., Hisada, K.-I., Charusiri, P., 2009. Lower Permian glacially influenced deposits in Phuket and adjacent islands, peninsular Thailand. Island Arc, **18**: 52–68.

Anderson, J.B., Kurtz, D.D., Domack, E.W., Blashaw, K.M., 1980. Glacial and glacial marine sediments of the Antarctic continental shelf. The Journal of Geology, **88**: 399–414.

Anjar, J., Adrielsson, L., Bennike, O., Björck, S., Filipsson, H.L., Groeneveld, J., Knudsen, K.L., Larsen, N.K., Möller, P., 2012. Palaeoenvironments in the southern Baltic Sea Basin during Marine Isotope Stage 3: a multi-proxy reconstruction. Quaternary Science Reviews, **34**: 81–92.

Benn, D.I., Evans, D.J.A., 1998. Glaciers and Glaciation. Arnold, London.

Bennett, M.R., Doyle, P., Mather, A.E., 1996. Dropstones: their origin and significance. Palaeogeography, Palaeoclimatology, Palaeoecology, **121**: 31–339.

Best, J.L., Kostaschuk, R.A., Peakall, J., Villard, P.V., Franklin, M., 2005. Whole flow field dynamics and velocity pulsing within natural sediment-laden underflows. Geology, **33**: 765–768.

Błaszkiewicz, M., Gruszka, B., 2005. Development and infill of Vistulian glacial Lake Gniew (N Poland): a sedimentological analysis. Geological Quarterly, **49** (4): 449–462.

Brodzikowski, K., Van Loon, A.J., 1991. Glacigenic sediments. Developments in Sedimentology, **49**.

Cowan, E.A., Cai, J., Powell, R.D., Clark, J.D., Pitcher, J.N., 1997. Temperate glacimarine varves: an example from Disenchantment Bay, southern Alaska. Journal of Sedimentary Research, **67**: 536–549.

Domack, E.Q., Lawson, D.E., 1985. Pebbles fabric in an ice-rafted diamictons. Journal of Geology, **93**: 577–591.

Dowdeswell, J.A., Murray, T., 1990. Modelling rates of sedimentation from icebergs. Geological Society London Special Publications, **53**: 121–137.

Dowdeswell, J.A., Maslin, M.A., Andrews, J.T., McCave, I.N., 1995. Iceberg production, debris rafting, and the extent and thickness of Heinrich layers (H-1, H-2) in North Atlantic sediments. Geology, **23**: 301–304.

Dowdeswell, J.A., Whittington, R.J., Jennings, A.E., Andrews, J.T., Mackensen, A., Marienfeld, P., 2000. An origin for laminated glacimarine sediments through sea-ice build-up and suppressed iceberg rafting. Sedimentology, **47**: 557–576.

Eyles, N., Eyles, C.H., Gostin, V.A., 1997. Iceberg rafting and scouring in the Early Permian Shoalhaven Group of New South Wales, Australia: evidence of Heinrich-like events. Palaeogeography, Palaeoclimatology, Palaeoecology, **136**: 1–17.

Gilbert, R., 1990. Rafting in glacimarine environments. Geological Society London Special Publications, **53**: 105–120.

Haarland, W.B., Herod, K.N., Krinsley, D.H., 1966. The definition and identification of tills and tillites. Earth-Science Reviews, **2**: 225–256.

Hambrey, M.J., 1994. Glacial Environments. UCL Press, London.

Hass, H.Ch., 2002. A method to reduce the influence of ice-rafted debris on a grain size record from northern Fram Strait, Arctic Ocean. Polar Research, **21**: 299–306.

Heine, K., Reuther, A.U., Thieke, H.U., Schulz, R., Schlaak, N., Kubik, P.W., 2009. Timing of Weichselian ice marginal positions in Brandenburg (northeastern Germany) using cosmogenic in situ Be-10. Zeitschrift für Geomorphologie N.F., **53**: 433–454.

Heinrich, H., 1988. Origin and consequences of cyclic ice rafting in the northeast Atlantic Ocean during the past 130,000 years. Quaternary Research, **29**: 142–152.

Hesse, R., Khdabakhsh, S., 2016. Anatomy of Labrador Sea Heinrich layers. Marine Geology, **380**: 44–66.

Hoffman, P.F., Schrag, D.P., 2002. The snowball Earth hypothesis: testing the limits of global change. Terra Nova, **14**: 129–155.

Houmark-Nielsen, M., Kjær, K.H., 2003. Southwest Scandinavia, 40–15 kyr BP: palaeogeography and environmental change. Journal of Quaternary Science,**18**: 769–786.

Jørgensen, F., Piotrowski, J.A., 2003. Signature of the Baltic Ice Stream on Funen Island, Denmark during the Weichselian glaciation. Boreas, **32***:* 242–256.

Kaiser, K., Hilgers, A., Schlaak, N., Jankowski, M., Kühn, P., Bussemer, S., Przegiętka, K., 2009. Palaeopedological marker horizons in northern central Europe: characteristics of Late Glacial Usselo and Finow soils. Boreas, **38**: 591–609.

Kalm, V., Kadastik, E., 2000. Waterlain glacial diamicton along the Palivere ice-marginal zone on the west Estonia Archipelago, eastern Baltic Sea. Proceedings of the Estonian Academy of Sciences, **50**: 114–127.

Kenzler, M., Tsukamoto, S., Meng, S., Thiel, C., Frechen, M., Hüneke, H., 2015. Luminescence dating of Weichselian interstadial sediments from the German Baltic Sea coast. Quaternary Geochronology, **30**: 215–256.

Kenzler, M., Tsukamoto, S., Meng, S., Frechen, M., Hüneke, H., 2017. New age constraints from the SW Baltic Sea area – implications for Scandinavian Ice Sheet dynamics and palaeo-environmental conditions during MIS 3 and early MIS 2. Boreas, **46**: 34–52.

Knudsen, O., Marren, P., 2002. Sedimentation in a volcanically dammed valley, Brùarjökull, northeast Iceland. Quaternary Science Reviews, **21**: 1677–1692.

Krbetschek, M.R., 1995. Lumineszenz-Datierungen quartärer Sedimente Mittel-, Ost- und Nordostdeutschlands. Unpublished Ph.D. thesis, TU Bergakademie, Freiberg.

Küster, M., Preusser, F., 2009. Late Glacial and Holocene aeolian sands and soil formation from the Pomeranian outwash plain (Mecklenburg, NE-Germany). Eiszeitalter und Gegenwart (Quaternary Science Journal), **58**: 156–163.

Le Heron, D.P., 2015. The significance of ice-rafted debris in Sturtian glacial successions. Sedimentary Geology, **322**: 19–33.

Leckie, D.A., Morgans, H., Wilson, G.J., Edwards, A.R., 1995. Mid-Paleocene dropstones in the Whangai Formation, New Zealand: evidence of mid-Paleocene cold climate? Sedimentary Geology, **97**: 119–129.

Liedtke, H., 1981. Die nordischen Vereisungen in Mitteleuropa. Forschungen zur deutschen Landeskunde 204.

Litt, T., Behre, K.-E., Meyer, K.-D., Stephan, H.-J., Wansa, S., 2007. Stratigraphical terms for the Quaternary of the north German glaciation area. Eiszeitalter und Gegenwart (Quaternary Science Journal), **56**: 7–66.

Livingstone, S.J., Piotrowski, J.A., Bateman, M.D., Ely, J.C., 2015. Discriminating between subglacial and proglacial lake sediments: an example from the Dänischer Wohld Peninsula, northern Germany. Quaternary Science Reviews, **112**: 86–108.

Ludwig, A.O., 2006. Cyprina-clay and I1 beds in the Pleistocene sequence in North-east Rügen and the island Hiddensee (south-western Baltic sea). Zeitschrift für geologische Wissenschaften, **34**: 349–377.

Ludwig, A.O., Panzig, W.-A., 2010. Das Pleistozän südlich Sassnitz – Fazies und Lagerung glazilimnischer/-fluviatiler Sedimente am Kliff bei Dwasieden [Pleistocene outcrops south of Sassnitz – facies and stratgraphy of glaciolimnic/fluvial sediments in the cliff near Dwasieden]. Exkursionsführer zur 35. Hauptversammlung der Deutschen Quartärvereinigung DEUQUA e.V. und der 12. Jahrestagung der INQUA PeriBaltic Working Group in Greifswald/Mecklenburg-Vorpommern: 68–69.

Lüthgens, Ch., Böse, M., 2011. Chronology of Weichselian main ice marginal positions in north-eastern Germany. Quaternary Science Journal, **60**: 236–247.

Lüthgens, C., Böse, M., Preusser, F., 2011. Age of the Pomeranian ice-marginal position in northeastern Germany determined by Optically Stimulated Luminescence (OSL) dating of glaciofluvial sediments. Boreas, **40**: 598–615.

Menzies, J., 2002. Modern and Past Glacial Environments. Butterworth-Heinemann.

Miall, A.D., 1978. Lithofacies types and vertical profile models in braided river deposits: a summary. Canadian Society of Petroleum Geologists Memoir, **5**: 597–604.

Miller, J.M.G., 1996. Glacial sediments. In: Sedimentary Processes; Stratigraphy, Facies and Environment (ed. H.G. Reading): 454–483. Blackwell Science, Cambridge.

Mokhtari Fard, A., Van Loon, A.J., 2004. Deformation of an early Preboreal deposit at Nykvarn (SE Sweden) as a result of the bulldozing effect of a grounding iceberg. Sedimentary Geology, **165**: 355–369.

Pisarska-Jamroży, M., 2013. Varves and megavarves of the Eberswalde Valley (NE Germany) – a key for the interpretation of glaciolimnic processes. Sedimentary Geology, **291**: 84–96.

Pisarska-Jamroży, M., Belzyt, S., Börner, A., Hoffmann, G., Hüneke, H., Kenzler, M., Obst, K., Rother, H., Van Loon, A.J., 2018. Evidence from seismites for glacio-isostatically induced crustal faulting in front of an advancing land-ice mass (Rügen Island, SW Baltic Sea). Tectonophysics, **745**: 338–348.

Powell, R.D., 1984. Glacimarine processes and inductive lithofacies modelling of ice shelf and tidewater glacier sediments based on Quaternary examples. Marine Geology, **57**: 1–52.

Rinterknecht, V., Börner, A., Bourlès, D., Braucher, R., 2014. Cosmogenic ^{10}Be dating of ice sheet marginal belts in Mecklenburg-Vorpommern, western Pomerania (northeast Germany). Quaternary Geochronology, **19**: 42–51.

Smith, L.M., Andrews, J.T., 2000. Sediment characteristics in iceberg dominated fjords, Kangerlussuaq region, East Greenland. Sedimentary Geology, **130**: 11–25.

Smith, N.D., Ashley, G., 1985. Proglacial lacustrine environments. In: Glacial Sedimentary Environments (eds. G. Ashley, J. Shaw and N.D. Smith): 135–216. Society of Economic Paleontologists and Mineralogists Short Course 16.

Steinich, G., 1992. Die stratigraphische Einordnung der Rügen-Warmzeit. Zeitschrift für geologische Wissenschaften, **20**: 125–154.

Syvitski, J.P.M., Van Everdingen, D.A., 1981. A re-evaluation of the geological phenomenon of sand floatation: a field experimental approach. Journal of Sedimentary Petrology, **51**: 1315–1322.

Thomas, G.S., Connell, R.J., 1985. Iceberg drop, dup and grounding structures from Pleistocene glacio-lacustrine sediments. Journal of Sedimentary Petrology, **55**: 243–249.

Udden, J.A., 1914. Mechanical composition of clastic sediments. Geological Society of America Bulletin, **25**: 655–744.

Van Loon, A.J., Pisarska-Jamroży, M., Nartišs, M., Krievāns, M., Soms, J., 2016. Seismites resulting from high-frequency, high-magnitude earthquakes in Latvia caused by Late Glacial glacio-isostatic uplift. Journal of Palaeogeography, **5**: 363–380.

Wentworth, C.K.A., 1922. A scale of grade and class terms for clastic sediments. Journal of Geology, **30**: 377–392.

Williams, G.E., Gostin, V.A., McKirdy, D.M., Preiss, W.V., 2008. The Elatina glaciation, late Cryogenian (Marinoan epoch), South Australia: sedimentary facies and palaeoenvironments. Precambrian Research, **163**: 307–331.

Woodworth-Lynas, C.M.T., Dowdeswell, J.A., 1994. Soft sediment striated surfaces and massive diamicton facies produced by floating ice. In: Earth's Glacial Record(eds. M. Deynoux, J.M.G. Miller, E.W. Domack, N. Eyles, I.J. Fairchild and G.M. Young): 241–259. Cambridge University Press, Cambridge.

Yorke, L.., Rumsby, B.T., Chiverrell, R.C., 2012. Depositional history of the Tyne valley associated with retreat and stagnation of Late Devensian Ice Streams. Proceedings of the Geologists' Association, **123**: 608–625.

Zieliński, T., Pisarska-Jamroży, M., 2012. Which features of deposits should be included in a code and which not? (in Polish with English summary). Przegląd Geologiczny, **60**: 387–397.